Effect of purine nucleosides in renal ischemic cellular injury

PhD dissertation

Petra Szoleczky

Doctoral School of Basic Medicine

Semmelweis University

Supervisor: Gábor Kökény M.D., Ph.D.

Official reviewers: Tibor Kovács M.D., DSc.
Barna Vásárhelyi M.D., DSc.

Head of the Final Examination Committee:
Emil Monos, PhD, DSc, professor emeritus

Members of the Final Examination Committee:
Lilla Reiniger M.D., Ph.D.
Zoltán Lengyel M.D., Ph.D.

Budapest
2017

TABLE OF CONTENT

THE LIST OF ABBREVIATIONS

A1: adenosine A1 receptor

A2a: adenosine A2a receptor

A2b: adenosine A2b receptor

A3: adenosine A3 receptor

ABT 702: [4-amino-5-(3-bromophenyl)-7-(6-morpholino-pyridin-3-yl)pyrido(2,3-d)pyrimidine

Ac-DEVD-AMC: fluoro-chrome-7-amino-4-methyl-coumarin

Acetyl-CoA: acetyl coenzyme A

ADA: adenosine deaminase

ADE: adenosine

ADP: adenosine diphosphate

AIF: mitochondrial-associated apoptosis-inducing factor

AK: adenosine kinase

AKI: acute kidney injury

AMP: adenosine monophosphate

AP-1: activator protein-1

APAF1: apoptotic protease activating factor 1

ATP: adenosine triphosphate

ATN: acute tubular necrosis

CTL: control

CHOP: C/EBP homologous protein

CYPD: cyclophilin D

DISC: death-inducing signaling complex

ECAR: extracellular acidification rate

EGFR: epithelial growth factor receptor

Egr-1: early growth response factor-1

EHNA: erytro-9-(2-hydroxy-3-nonyl)adenine hydrochloride

ER: endoplasmic reticulum

FADD: Fas-associated death domain

FCCP: oligomycin, carbonyl cyanide p-trifluoromethoxyphenylhydrazone

GD: glucose deprivation

GFR: glomerular filtration rate

GPX4: glutathione peroxidase 4

GTP: Guanosine triphosphate

HIF-1: hypoxia inducible factor-1α

HTS: High-throughput screening

IL-6: interleukin 6

IL-1β: interleukin-1beta

IL-18: interleukin-18

INO: inosine

INT: 2-(4-Iodophenyl)-3-(4-nitrophenyl)-5-phenyl-2H-tetrazolium chloride

IRI: ischemic reperfusion injury

LDH: lactate dehydrogenase

LOPAC1280: library of 1280 pharmacologically active compounds

MLKL: mixed lineage kinase domain-like pseudokinase

MPTP: mitochondrial membrane permeability transition pores

MTT: 3-(4,5-dimethyl-2-thiazolyl)-2,5-diphenyl-2H-tetrazolium bromide

NAD^+: Nicotinamide adenine dinucleotide

NEC: necrostatin-1

NO: nitric oxide

NOS: nitric oxide synthase

OCR: oxygen consumption rate

OD; oxygen depletion

OGD: oxygen-glucose deprivation

PAMP: pathogen associated molecular patterns

PARP-1: poly-(ADP-ribose) polymerase family-1

PDE: phosphodiesterase

PMS: N-methylphenazonium methyl sulfate

PPR: proton production rate

PRE: pre-treatment

RIP1/RIP3: receptor-interacting protein

RFU: relative fluorescent unit

RNOS: Reactive Nitrogen Oxide Species

ROS: reactive oxygen species

SAR: structure-activity relationship

TGF-ß: transforming growth factor-ß

TRAIL: TNF-related apoptosis-inducing ligand

Z-VAD-fmk: carbobenzoxy-valyl-alanyl-aspartyl-[O-methyl]-fluoromethylketone

1. INTRODUCTION

The kidney is an admirable organ; it has an ability to repair after significant injury. However, this capacity is limited and in elderly patients are at high risk for further reduced kidney function. Moreover, no effective therapy exists yet to treat an established acute kidney injury (AKI) alone. Therefore, there is a high clinical priority to nourish the endogenous repair processes and retard associated fibrosis. (1) Despite of a lot of progress have been achieved in the fields of intensive care medicine and dialysis treatment, and despite the effort to identify new therapeutic strategies, AKI still remains a factor that dramatically increases the mortality of hospitalized patients. In the last decade, we observed a three-fold increase in the number of patients with severe AKI. The most frequent causes of AKI are secondary, such as sepsis, nephrotoxic medication, and ischemia, each causing acute tubular necrosis (ATN) which leads to almost 50% mortality or chronic renal failure in 10% of the cases, in need of dialysis treatment. (2)

1.1 Acute tubular necrosis (ATN):

In the kidney, the primary targets for ischemic and toxic injury are the proximal tubule cells; these cells often undergo injury due to ischemia because of the local tissue oxygen demand and accumulation of metabolic waste products. During ischemia, the cells lose their functional integrity; loss of cell polarity, cytoskeleton disorganization or cell-matrix adhesion loss leads to cell death by apoptosis and necrosis. (3) During the ischemic injury, damaged tubular cells release “cellular debris” into the tubular lumen as damaged cells peel off from the basement membrane. This leads to obstruction of the tubular lumen and consecutive increase of the tubular pressure while reducing glomerular filtration rate (GFR). Some effects extend beyond the ischemic injury to cause further tubular cell damage. In the outer medulla, swelling of the tubular cells create mechanical blockade and decrease the medullary blood flow. These latter changes establish a positive-feedback process and extend the injury even further. Therefore, cell culture experiments using renal tubular cells represent a model system allowing better understanding of pathophysiological processes during ischemia, which might help to develop new treatment modalities.

1.2 Ischemia/reperfusion

Ischemic injury is the most common clinical feature of cell injury caused by oxygen deprivation and is present in several clinical processes including stroke, cardiac infarct, acute kidney injury and organ transplantation. Ischemia/reperfusion injury (IRI) of the kidney is a major cause of ATN leading to acute kidney injury (AKI). Clinical symptoms are initially often indirect, which makes difficult to recognize the beginning of the ischemia. In case the diagnosis of ischemia is made within 24 hours after the onset of clinical symptoms, and an aggressive treatment is immediately established, the survival rate could be 20% higher as compared to the cases of delayed diagnosis (4).

Tissue injury, however, occurs in two phases due to an ischemic insult. The first phase of cellular damage is a direct consequence of oxygen and energy deprivation, while the tissue injury extends further during reperfusion phase (Figure 1).

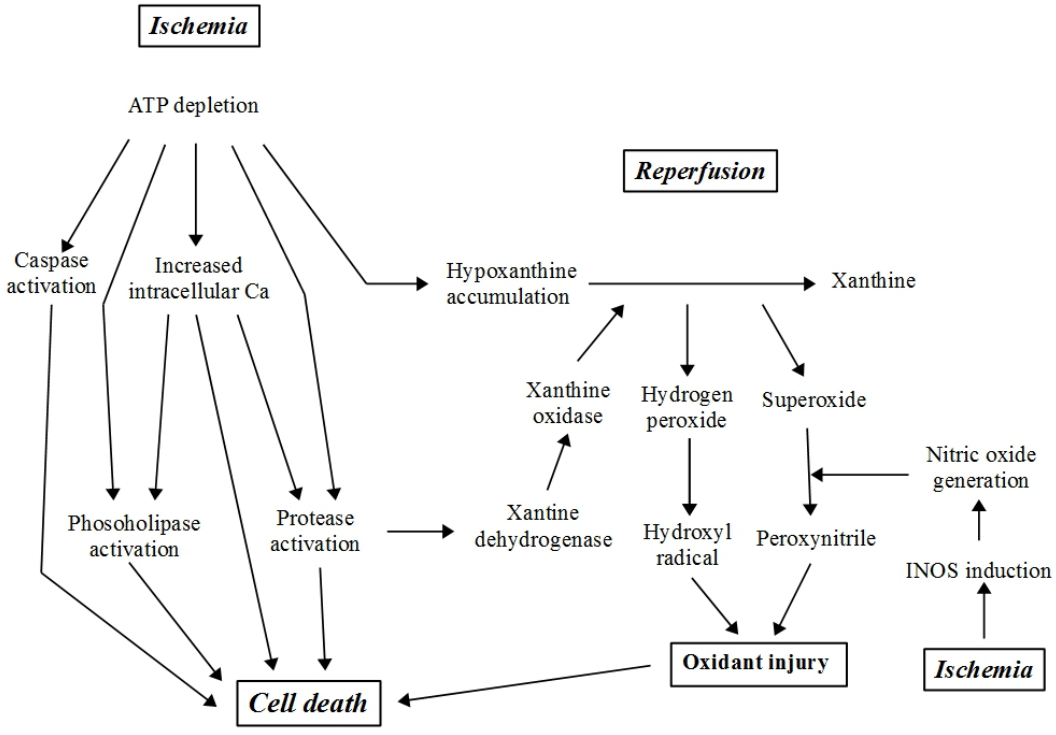

Figure 1. Prospective therapeutic approaches to acute kidney injury

1.2.1 Cellular events of renal ischemic injury

Renal ischemia induces a broad range of cellular and molecular responses, which are complex and not fully understood. During ischemia, the damaged tissue produces extreme amounts of reactive oxygen species (ROS) due to oxygen depletion, which causes deprived oxidative phosphorylation and disorder in ATP synthesis (5). The cellular ATP levels fall rapidly, ATP is degraded to ADP and AMP. AMP is metabolized further to adenine nucleotides and to hypoxanthine. Nucleotides are nearly impermeable to cells, but nucleosides (adenosine and inosine) can pass through the cell membrane, which further cuts down the potential "energy supply". With all these mechanisms of ATP depletion, the cell cannot get rid of excess intracellular calcium via the Ca^{2+}-ATPases, which leads to increased intracellular calcium levels. The activity of plasma membrane Na^{+}-K^{+} ATPase channels also decrease in parallel with the fall of intracellular ATP levels, leading to increased intracellular Na^{+} concentration. Therefore, the trans-membrane Na^{+} concentration gradient decreases, which facilitates more Ca^{2+} to enter the cell via Na^{+}-Ca^{2+} exchanger (6). Accumulated calcium can be taken up into both non-mitochondrial compartments and mitochondria, but increased amounts of Ca^{2+} uptake causes mitochondrial swelling. However, at this point, all of these disorders are reversible in case of a restored oxygen supply.

Irreversible injury occurs when the above cellular changes lead to disruption of the cell membrane. The intracellular calcium overload stimulates both plasma and endoplasmic/sarcoplasmic reticulum Ca^{2+}-ATPases, resulting in further exacerbation of the existing energy depletion. Furthermore, the increased cytosolic Ca^{2+} concentration activates the Ca^{2+}-dependent proteases and phospholipases, and it may lead to proteolysis and membrane alterations. However, elevated Ca^{2+} levels can also lead to cytoskeletal degradation (7). Additionally, hypoxanthine accumulates in the cell, because the oxidation of hypoxanthine is disrupted during an ischemic condition. As a consequence of the ischemia induced cellular calcium overload, Ca^{2+}-dependent proteases convert xanthine dehydrogenase to xanthine oxidase (8).

1.2.2 Cellular events after reperfusion

A significant part of the IRI might occur after the reperfusion. Reversibly injured cells may recover after restoration of the blood flow, but those cells that suffered irreversible damage will not recover despite of the reperfusion. Reperfusion, moreover, might lead to severe damage of even reversibly injured cells. There is increasing evidence that the mechanisms of this post-ischemic damage, referred as reperfusion injury, includes complex regulatory networks, which are not understood yet.

Inflammation

During the ischemic insult, renal tubular epithelial cells start to produce different chemokines, which regulate the expression of proinflammatory cytokines and cell adhesion molecules. These chemokines and cytokines are key factors, as they activate leukocytes and promote endothelial cell injury through intracellular cascades and endothelial injury. Consequently, the activated leukocyte-endothelial interactions may physically disturb blood flow (9). For instance, interleukin 6 (IL-6) and TNFα play a major role in the renal dysfunction after I/R. (10, 11) Cytokine-like caspases are a novel group of cysteine proteases, known as major mediators of cell death and inflammation. Increases of both caspase-1 and caspase-3 have been reported in ischemic injury. Caspase-1 mediates inflammation through the activation of interleukin-1beta (IL-1β) and interleukin-18 (IL-18). Inhibition of caspase-1 protects against ischemic injury in brain, heart and kidney models of ischemia (12).

Oxydative and nitrosative stress

Oxygen free radicals play an important role in renal ischemia and upcoming AKI. Oxidative stress has three major components: 1) indirect effect of the oxidant; 2) regulatory effect on cell signaling; 3) direct damage by RNOS (Reactive Nitrogen Oxide Species). There are several sources of reactive oxygen species (ROS) during reperfusion. Oxygen deprived mitochondria provide high amount of ROS and when blood supply is restored during reperfusion, as free electrons can increase superoxide production (5). Next source is xanthine oxidase. Xanthine oxidase levels increase by xanthine dehydrogenase conversion under hypoxic conditions; however Ca^{2+}-dependent proteases convert xanthine dehydrogenase to xanthine oxidase during the ischemic phase as well. In the presence of O_2 xanthine dehydrogenase oxidizes hypoxanthine and

xanthine to uric acid and produce ROS (13). Another source of free radicals in post-ischemic tissue is a consequence of inflammation during reperfusion, neutrophil infiltration and respiratory burst. Neutrophil activation produces superoxide by NADPH oxidase enzyme activation. ROS can cause lipid peroxidation of membrane phospholipids, and increase membrane permeability (14). Nitrosative stress also has an effect in renal damage. The reaction between superoxide ion and nitric oxide (NO) results peroxynitrite, which is a cytotoxic metabolite and can cause lipid peroxidation and DNA damage (15).

1.2.3 Cell death

After ischemic renal injury, the type of cell death depends primarily on the duration and extent of the ischemic insult, and the resistance of the cell type. However, cell death is more likely to be a series of interrelated events.

Apoptosis

Apoptosis may occur due to less severe injury, and is characterized by cytoplasmic and nuclear shrinkage, DNA fragmentation, and breakdown of the cell into membrane bound apoptotic bodies that are rapidly cleared by phagocytosis.

Caspase activation is common in apoptosis (although caspase-independent apoptosis exist also). The apoptotic caspases are generally divided into two classes: the initiator caspases, which include caspase-2, -8, -9 and -10 and the effector caspases, which include caspases-3, -6 and -7. The apoptotic response can be activated by intrinsic or extrinsic pathway. The intrinsic pathway is mediated by mitochondria; among the several released proteins, cytochrome C has the most stimulating pro-apoptotic activity. Cytochrome C binds to and activates the cytoplasmic APAF1 (apoptotic protease activating factor 1) protein. This apoptosome complex binds dATP and activates caspase-9, thus triggers a caspase cascade. The extrinsic pathway can be activated by an extracellular death ligand. The death ligands binding to their receptors and create a homotrimeric ligand-receptor complex, which forms an oligomeric death-inducing signaling complex (DISC) with cytosolic factors. DISC activates the initiator caspase-8, which cleaves and activates the effector caspase-3 (16) and ensures crosstalk between extrinsic and intrinsic pathways and the release of mitochondrial proteins. (17)

Necrosis

Historically, necrosis has been deemed to be an accidental cell death without determined pathways or cellular regulation. Necrosis was defined by an increase in cell volume, swelling of organelles, plasma membrane rupture and eventual leakage of intracellular components.

Recent studies have identified several pathways of genetically determined and regulated non-apoptotic forms of cell death, also known as regulated necrosis. Eventually, the outcome of this genetically controlled cell death process is the same as the formerly defined necrosis. It is characterized by cellular leakage and by cytoplasmic granulation, as well as organelle and/or cellular swelling. The emerging pathways are ferroptosis (iron-dependent necrosis), oxytosis (oxidative stress-induced programmed cell death), NETosis (type of neutrophil death, with the formation of extracellular traps against invading bacteria), ETosis (death with release of extracellular traps), cyclophilin D (CYPD)-mediated regulated necrosis, parthanatos (poly-(ADP-ribose) polymerase family-1 (PARP-1) dependent cell death), pyroptosis (proinflammatory programmed cell death) and pyronecrosis (ASC and cathepsin B dependent cell death but is independent of caspase-1 and -11). There are four separate pathways, which might lead to organ damage in renal ischaemia/reperfusion injury (I/R): 1) RIPK1/RIPK3-dependent necroptosis; 2) CYPD-mediated regulated necrosis; 3) pyroptosis; 4) ferroptosis.

Necroptosis

Necroptosis is a receptor mediated protein kinase-based necrotic cell death; so far, it is the most studied and the best characterized pathway of regulated necrosis (18). Necroptosis and apoptosis have several common upstream signaling elements, such as TNFα, which can trigger both. However, caspase-8 has to be inhibited or disrupted to initiate necroptosis, which can be induced also by other death receptors (19). Several intracellular triggers have also been identified. For instance, interferons induce RIP1/RIP3 (receptor-interacting protein) kinase mediated cell death in case the Fas-associated death domain (FADD) is lost or disabled or caspase-8 is inactivated (20). In addition, several other triggers have been identified so far to induce necroptosis, such as CD95L (Fas ligand) (19), TRAIL (TNF-related apoptosis-inducing ligand) (19), genotoxic stress (21), T cell receptor, virus-mediated activation of DNA-dependent

activator of IFN-regulatory factors (DAI) (22), anticancer drugs (23, 24), pathogen associated molecular patterns (PAMPs) (25), and finally, interferons (20). However, regardless of the trigger, the common and important criterion is that, in the absence of active caspase-8, RIP1 interacts with RIP3 to form an amyloid-like fibrillar complex, the necrosome. The necrosome is a multimolecular complex, which includes mixed lineage kinase domain-like pseudokinase (MLKL), RIPK3 and in some cases RIPK1 as well. MLKL is then translocated to the plasma membrane and induces its rupture (26).

CYPD-dependent regulated necrosis

During the renal ischemic injury, the increased intracellular calcium level leads to mitochondrial overload with calcium. Consequently, mitochondrial membrane permeability transition pores (MPTP) open in the inner membrane and leads to subsequent necrotic cell death. The mitochondrial permeability transition (MPT) allows solutes to enter the mitochondrial matrix with 1.5 kDa or smaller molecular mass, which leads to the loss of inner mitochondrial membrane potential and matrix swelling. This process critically depends on CypD. CypD can associate with the inner mitochondrial membrane proteins and promote mitochondrial permeability transition (27).

Pyroptosis

Pyroptosis was first described in macrophages during infection with *Salmonella enterica* subsp. *Typhimurium* (28). Pyroptosis is initiated by nonapoptotic caspases that activate proinflamatory cytokines. Caspase-11 directly cleaves the key molecule caspase-1, also known as interleukin (IL)-1-beta-converting enzyme (29). In macrophages, pyroptosis is characterized by membrane permeabilization, DNA damage and inflammatory cytokine release. However, the role of pyroptosis in renal ischemia-reperfusion is currently unclear and the mechanism how pyroptosis could participate in the development of AKI needs further studies. An *in vivo* study has shown that the expression of pyroptosis-related proteins (caspase-1, caspase-11 and IL- 1β) increased significantly at 6h after renal IRI with a peak at 12h. In vitro, hypoxia-reoxygenation injury induced pyroptosis characterized by increased pore formation, elevated LDH release, and upregulation of endoplasmic reticulum (ER) stress biomarkers such as glucose-regulated protein-78 and C/EBP homologous protein (CHOP). ER stress is present during ischemic injury, mostly as a self-defense system. However, over

activated ER stress might lead to cell death via activation of CHOP and other signaling pathways (such as cJun N-terminal kinase /JNK/) (30).

Parthanatos

The PARP family consist of 18 members (31). PARP-1 is an important enzyme that regulates poly(ADP-ribosyl)ation and gene expression in the nucleus. PARP-1 catalyzes the transfer of ADP-ribose from NAD^+, activation of PARP-1 is required for DNA repair (32, 33) and PARP-1 activation occurs when DNA breaks are present. It has been demonstrated that PARP-1 inhibition or gene deletion protects against ischemia-reperfusion. (34, 35) Parthanatos is one of the several mechanisms where PARP-1 mediated cell death occurs. It is a unique cell death, a result of over activation of the nuclear PARP-1 enzyme without the need of caspase activation, but needing the nuclear translocation of the mitochondrial-associated apoptosis-inducing factor (AIF). Under physiological conditions, PARP-1 maintains nuclear homeostasis, regulates gene expression and amplification, cell differentiation, participates in cell division, DNA replication, mitochondrial function, malignant transformation, and cell death (36). When the cells are exposed to toxic stimulus with significant DNA damage, PAR polymer is generated by over activation of the PARP-1 enzyme. The physical interaction between PAR and AIF induces AIF release from the mitochondria and its translocation to the nucleus. (37) This leads to mitochondrial membrane depolarization and DNA fragmentation. (38)

Ferroptosis

Ferroptosis is a programmed cell death characterized by the accumulation of cellular reactive oxygen species in an iron-dependent manner. (39) Morphologically, ferroptosis is characterized by mitochondria reduced in size with condensed membrane densities, accumulation of intracellular ROS and inhibition of cellular iron uptake. (40) Ferroptosis can be induced by the inhibition of system x_c^- , like Erastin, and direct inhibition of GPX4 (glutathione peroxidase 4). System x_c^- inhibition results in intracellular cysteine pool depletion, leading to reduced glutathione levels, as cysteine is a precursor of glutathione synthesis. Direct inhibition of GPX4 enzyme activity causes elevated lipid ROS levels and glutathione depletion. As glutathione is an essential cofactor of GPX4, system x_c^- inhibition mediated glutathione depletion indirectly

inhibits the GPX4 enzyme as well. (41) At present, it is still unclear how these cell death pathways are linked to each other, but targeting more than one pathway might be the key for future therapies.

In summary, understanding more details of cellular processes during ischemia and reperfusion might result in more targeted therapies in the future, which could effectively prevent injury and accelerate tissue repair, and therefore ameliorate chronic progressive kidney diseases.

1.3 Design of an in vitro renal ischemia model

Renal IRI has a very complex pathological mechanism, with further insults such as nutrient deprivation, cellular waste accumulation and hypercapnia. Therefore, it is challenging to design and set up an *in vitro* model of renal ischemia-reperfusion. It is never possible to reproduce the exact i*n vivo* environment, but *in vitro* models provide a possibility to investigate isolated specific stimuli and test their contribution to physiological or pathological events, and can give direction for future development of *in vivo* studies. During assay design, the specific cell type should be chosen carefully, ensuring appropriate response to isolated ischemic stimuli and to provide valuable information (knowledge) for development of future *in vivo* studies.

Tubular epithelial cells consume a lot of energy due to their high metabolic activity; therefore, these cells are very sensitive for rapid energy depletion. This explains the fact that proximal tubule is the primary target of ischemic injury, and that tubular epithelial cells are the most relevant for hypoxic studies. Several morphological and functional changes occur in proximal tubular cells following I/R, such as change in epithelial polarity, disruption of intercellular junctions and intracellular cytoskeleton, and cell death via complex pathways (42). To present, the porcine proximal tubular epithelial immortalized cell line (LLC-PK) has been widely used as a model to study the effects of hypoxia, because the structure and function of porcine kidney is similar to the human kidney (43).

In order to design an appropriate *in vitro* ischemia/reperfusion model, one has to consider a few experimental parameters, such as oxygen deprivation, carbon dioxide elevation, limited nutrient availability and waste removal. Researchers use various

techniques to mimic ischemia *in vitro;* however, there is no standard method yet. There are two ways to induce ischemic response *in vitro*: by the ischemic microenvironment, that mimics oxygen and nutrient deprivation or by several chemical agents such as cyanide, azide, rotenone and antimicyn, A. The use of chemical agents have several limitations. These chemical agents are not endogenous molecules thus they do not characterize entirely the ischemic pathologies and their effects are usually irreversible therefore making it difficult to study the reperfusion phase. Moreover, cellular responses are different when hypoxia is induced by chemical agents or by oxygen deprivation (44). There is another, yet more complex way to induce hypoxia, where ischemia and reperfusion are present at the same time. Ischemia can be achieved by full or partial oxygen deprivation with or without nutrient depletion, whereas reperfusion can be modeled by providing glucose and oxygen to the cells. Researchers usually use less than 1% O_2, however, it is not possible to obtain true anoxia *in vitro* because removal of all residual oxygen from the medium is challenging. Oxygen levels above the cell culture media can be manipulated by using pre-mixed gas tanks, and sealed chambers commonly used for hypoxic studies. However, controlling the dissolved gas is complex and several parameters might influence the gas equilibration. For example, surface area, diffusion distance (media height), and saline content of the media (45). The media volume can dramatically affect gaseous diffusion, nutrition supply and waste accumulation; volume reduction decreases diffusion distance, thus enhances equilibration. Unfortunately, there is no agreement on the optimal volume to surface area ratio; the recommended ratio is between 100 ul/cm2 (46) and 200 ul/cm2 (47). Beside oxygen concentration, the media composition is also a critical parameter to set up an *in vitro* ischemia model. Media formulations have been designed to maintain normal cell morphology, promote growth and provide excellent cell viability. The crucial parameters of media are glucose concentration, serum content and alternative glycolytic substrates such as sodium pyruvate. Moreover, sodium pyruvate may act as an antioxidant agent; it protects cells from injury by preventing reactive oxygen species formation (47). Amino acids and proteins may moderate the injury by reducing the number of oxygen species (48) and can serve as an alternative energy source during hypoxia. In order to avoid the undesirable effects of medium, some researchers use PBS buffer with electrolytes instead (49). Apparently, this approach is far from physiologic

or pathologic conditions. Metabolic waste accumulation is also associated with ischemia, but probably received the least attention in I/R model assays. However, in the early phase of renal ischemia the changes in metabolite levels might be used as biomarkers for the diagnosis of AKI (50).

There are numerous approaches to measure hypoxic cellular response, such as the release of lactate dehydrogenase (LDH), hypoxia inducible factor-1α (HIF-1) protein expression, and bioreductive products containing nitroheterocyclic group like "EF5". The cells release LDH only when the membrane integrity has been disrupted (51). Since LDH is a fairly stable enzyme, it is easy to measure LDH activity from the medium using colorimetric assay. LDH catalyzes the conversion of lactate to pyruvate while it reduces NAD to NADH. NADH interacts with a specific probe, and measuring the absorbance detects the reaction velocity. HIF-1 complex is a unique oxygen response system being regulated by oxygen. The lack of oxygen activates HIF-1 complex, but the HIF-1 complex remains inactive by hydroxylation in the presence of physiological oxygen concentrations (52). Molecules containing nitroimidazole groups like "EF5" and "hypoxyprobe" are the most prevalent molecular probes for hypoxia. Cellular nitroreductase enzymes reduce the NO_2 group of nitroimidazole under normoxic conditions, which is a reversible process. However, in the absence of oxygen, the radical anion further reduces the NO_2 group to NH_2 and accumulates in the hypoxic tissue (53).

In addition, reperfusion injury is as important as the ischemic injury itself. The cellular damage continues and is even increased during reoxygenation. For example, the cells release more LDH after reoxygenation than during the hypoxic period (54). During the reperfusion phase *in vivo*, O_2 supply returns to normal level and CO_2 is washed out, while both nutrient supply and pH restore to pre-ischemic levels. In order to mimic reperfusion *in vitro*, we have to provide fresh media to the cells during reoxygenation to avoid nutrient depletion and waste accumulation.

1.4 Osmotic stress in the renal medulla

Even under physiological conditions, the renal medullary cells are exposed to significant changes in osmolarity, varying between 300 to 1200 mOsm in humans, but even broader range in rodents (55). Numerous in vitro data suggest that hyperosmolar

conditions induce the expression of several genes, including immediate early genes (56). Acute hyperosmolar conditions, for instance, can result in transforming growth factor-ß (TGF-ß) activation of cultured renal fibroblasts (57). TGF-ß plays a pivotal and pathological role in fibrotic diseases of several organs, including myocardial, pulmonary and kidney fibrosis (58-61). TGF-ß is present in the renal inner medulla in humans and rats, suggesting a physiological role of this cytokine. TGF-ß has been reported to inhibit sodium transport by the inner medullary collecting duct (IMCD) cells (62-65), whereas high water intake (and the consecutively reduced osmolarity) ameliorates tubulointerstitial injury by reducing TGF-ß mRNA expression (66). In contrary, high salt diet in rats increased the renal expression of TGF-ß (67).

TGF-ß can induce the transcription of many genes, including the transcription factors Egr-1 (early growth response factor-1) and the activator protein-1 (AP-1) complex, which has been associated with upregulation of extracellular matrix production (68-70). AP-1 is a heterodimeric molecule, composed of Jun and Fos nuclear oncoprotein families, being c-Jun and c-Fos the two major components of AP-1 (71). In vitro studies have previously shown that short term osmotic stress upregulates Egr-1 expression (72-74), however, less is known about the possible effect of hyperosmolarity on the expression of AP-1 components or collagens.

1.5 Screening

Screening is able to identify biologically active compounds in a large set. As compared to conventional assays, the screen measures biological processes, being a rigorous, well-developed and validated method, which ensures biologically relevant, reproducible and consistent results over years. Nowadays, both the academic field as well as the industry uses screening as a common experimental approach.

Two types of screens dominated the early stage of drug development: phenotypic screen and target-base screen. The phenotypic screen has been used to identify compounds causing changes in phenotype in a cellular or animal disease model, while target-base screen measures direct effect of the compounds on a target protein. Phenotypic screens have been usually used when the biology of diseases were not clearly understood. It could identify molecules that alter a disease phenotype and

influence pathway of yet undescribed one or more targets simultaneously. The challenge in this case is finding the target(s) of a recently identified candidate molecule (having disease-modifying effect). In the last few years, chemical proteomics has been used to identify molecule targets and it is a useful method to discover new therapeutic targets and identify new disease pathways. In contrast, target-based screening identifies candidate molecules with known target. The further optimization and toxicity studies of these tractable targets takes much less effort (75). Drug reposition is another viable screening method, an in vitro screening of known drugs or drug-like molecules to identify new therapeutic areas. The significant benefits of reposition are the lower cost and reduced development time. The repositioned drug has already passed several tests such as toxicity assays, which reduces the risk of failure for bringing it to the market (76).

High-throughput screening (HTS) is characterized by high efficiency, high speed and low cost. HTS means screening up to 10 000 compounds per day using 96-well to 1586-well microplates (77). An ultra-high-throughput screening can handle even 100 000 assays per day (78). There are several factors to consider during HTS screen development, such as the type of assay, the assay format, molecule library selection, delivery method of reagents and samples, assay detection, and data analysis. There are three basic assay types: 1) molecular target assay, 2) cell-free multicomponent assay and 3) cell- or organism-based assay. In every screen, there is a need to use positive and negative controls. The positive control produces the same result in the assay as the desired active molecule; the negative control is mostly the vehicle. Choosing the right controls is a critical step, because the controls determine and validate the biological response. As a basic requirement, the screening assay has to be reproducible for years. When screening only a small number of compounds (e.g. in the academic research), the screen setup uses 96-well microtiter plates. The assay formats used in the industry are either 384-well or 1536-well plates. Reducing assay volumes can minimize the assay costs; however, one has to consider the expenses of automatization investments.

During the primary screen, only the biologically active molecules with the expected effect are chosen (known as “hits”). As next step, selected hits are confirmed by generating dose-response curves using a fresh sample of the compound. Additionally, the dose-response curve also determines the half maximal inhibitory

concentration (IC_{50}) of the compound, to compare the effectiveness of candidate molecules. False positive hits are also filtered out during the hit confirmation process. HTS technology usually tests the compound's activity at a single concentration only, which leads to many false positive and false negative hits. False positive hits can be compounds that interfere with the assay signal, or in case of molecular target assay, the false positive compounds chemically react with the target, or inhibit the target. The extra cost and time spent on the analysis of these false positive hits can make the screen more expensive (79). Applying accurate measurements reduces the number of false negative hits, like using the most sensitive detection and running replicates. Using proper standardized hit identification process can improve the false positive/false negative ratio as well. Reducing the false negative hits maximizes the potential to identify a promiscuous binder (80). The aim of the hit-to-lead phase is to clarify hit series in order to produce selective and more potent compounds. Typically, this involves medical chemistry studies and intensive structure-activity relationship (SAR) investigations around the compound's structure. Animal experiments are used to validate the compound's activity in vivo, and for preclinical toxicity studies as well. Usually, only one or two drug candidate compounds are chosen out of 200 000 to 10^6 screened molecules (81) (Figure 2).

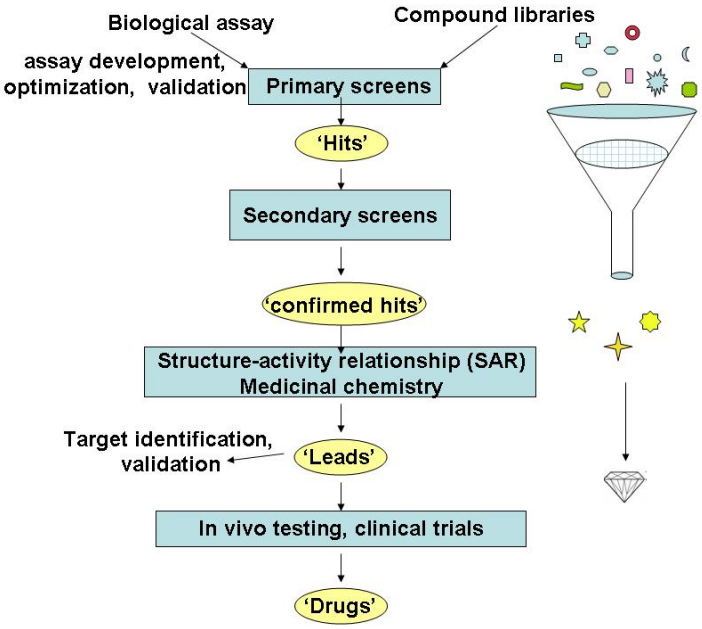

Figure 2. Drug discovery process. Screening identifies active molecules (hits), which have to accomplish several tests and optimization phases in order become a candidate drug. The candidate molecule can be introduced as a new drug to the market only after several successful preclinical and clinical trials. Thus, the total expenses of new drug's development might reach tens to hundreds millions of US dollars (82).

2. OBJECTIVES

Renal tubules are susceptible to injury of different etiologies, including ischemia, toxicity or sustained osmotic stress. Ischemia/reperfusion injury is a major cause of acute kidney injury. However, no effective modalities exist to prevent or treat ischemic tissue damage. Therefore, better understanding of ischemic cellular events, development of appropriate screening assays and cell based model systems are essential in order to identify new drug compounds that might fulfill the clinical demand in the near future.

The expression of several profibrotic genes have been so far implicated in the molecular response to acute osmotic stress of renal medullary cells. However, the molecular effects of sustained hyperosmolarity have not been investigated yet. As sustained hypertonicity is present in the renal medulla, we aimed to investigate how increased osmolarity might affect TGF-ß, Egr-1 and AP-1 expressions of cultured inner medullary collecting duct (IMCD) cells.

During our studies, our specific aims were the following:

1) set up cells-based hypoxia-reoxygenation model of tubular injury to mimic ischemia and reperfusion phase on LLC-PK cell line
2) better characterize the mechanism of both ischemic and reperfusion phase
3) apply the established *in vitro* model in order to search for compounds that ameliorate hypoxia-reoxygenation injury of renal proximal tubule cells
4) screen hits' confirmation
5) mechanism identification of novel hits
6) establish an *in vitro* model for sustained hyperosmolarity on IMCD cell line
7) investigate the effect of sustained hyperosmolarity on the expression of immediate early genes and collagens

3. METHODS

3.1. Reagents

A library of 1280 pharmacologically active compounds (LOPAC1280) was obtained from Sigma-Aldrich (St Louis, MO). The library includes drug-like molecules in the field of cell signaling and neuroscience. The compounds are dissolved at 10 mM in dimethyl-sulfoxide (DMSO) and dilutions were made either in DMSO or in phosphate-buffered saline (PBS, pH 7.4) to obtain 0.5% DMSO in the assay volume (Figure 3). Adenosine (ADE), inosine (INO), glucose, PJ34, 8-cyclopentyl-1,3-dipropylxanthine, 8-(3-chlorostyryl) caffeine, alloxazine, MRS 1523, erytro-9-(2-hydroxy-3-nonyl)adenine hydrochloride (EHNA), [4-amino-5-(3-bromophenyl)-7-(6-morpholino-pyridin-3-yl)pyrido(2,3-d)pyrimidine (ABT 702), oligomycin, carbonyl cyanide p-trifluoromethoxyphenylhydrazone (FCCP), antimycin A were purchased from Sigma-Aldrich (St Louis, MO), necrostatin-1 (NEC) from Calbiochem (EMD BioSciences, San Diego, CA), (carbobenzoxy-valyl-alanyl-aspartyl-[O-methyl]-fluoromethylketone) (Z-VAD-fmk) from Promega (Madison, WI). All compounds were dissolved in DMSO except for adenosine, inosine and glucose which were dissolved in culture medium.

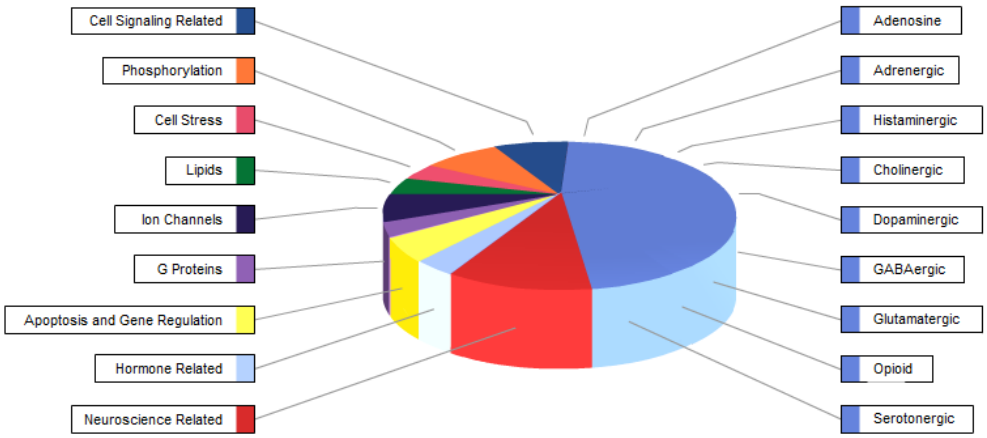

Figure 3. Content of LOPAC library by classes of action of the compound. Collection of assorted pharmacologically-active compounds for assay validation and high throughput screening.

(http://www.sigmaaldrich.com/life-science/cell-biology/bioactive-small-molecules/lopac1280-navigator.html)

3.2. Cell culture

LLC-PK1 porcine kidney proximal tubular cells, NRK rat renal proximal tubular epithelial cell line, HK-2 human renal proximal tubule epithelial cell and murine IMCD cells (mIMCD-3) were obtained from American Type Culture Collection (Manassas, VA). LLC-PK1 and NRK cells were maintained in Dulbecco's modified Eagle's medium (DMEM) (Hyclone, Logan, UT)) containing 1 g/l glucose supplemented with 10% fetal bovine serum (PAA Laboratories, Dartmouth, MA), 4 mM glutamine and 100 IU/ml penicillin and 100 µg/ml streptomycin (Invitrogen, Carlsbad, CA). HK-2 was maintained in DMEM containing 4.5 g/l glucose supplemented with 10% fetal bovine serum 4 mM glutamine and 100 IU/ml penicillin and 100 µg/ml streptomycin. IMCD cells were maintained in DMEM/F12 medium containing supplemented with 10% fetal bovine serum 4 mM glutamine and 100 IU/ml penicillin and 100 µg/ml streptomycin. From LLC-PK1, NRK and HK-2 cells, 3 000 cells/well were plated were plated into 96-well tissue culture plates and cultured for 5 days at 37 ºC in 5% CO_2 atmosphere. IMCD cells were plated into 6 cm dishes (500 000 cells/well) or 96 well plates (25 000 cells/well) and cultured to reach confluency at 37 ºC and 5% CO_2 atmosphere.

3.3. In vitro model of acute tubular necrosis

Culture medium was replaced with DMEM containing no glucose prior to the induction of hypoxia. In the pretreatment assay the drugs were added at 50 µM concentration in 5% of the culture volume (final concentration of DMSO was 0.5%). Culture plates were placed in gas-tight incubation chambers (Billups-Rothenberg Inc., Del Mar, CA) and the chamber atmosphere was replaced by flushing the chamber with 95% N2/5% CO_2 mixture at 25 L/min flow rate for 5 min. The hypoxia was maintained by clamping and incubating the chambers for 20 hours (or for the indicated period) at 37 °C. All assay plates subjected to hypoxia included vehicle-treated control wells with glucose-free medium (OGD) or medium containing 5 mM glucose (CTL). After hypoxia, glucose and serum concentration was restored by supplementing the culture

medium with glucose and FBS and the cells were incubated for 24 hours at 37 °C at 5% CO_2 atmosphere (83, 84). In the post-treatment assay the drugs were added immediately after the hypoxia at 50 μM final concentration in 5% of the culture volume (Figure 4). For western-blot analysis and fluorescent caspase assay, the glucose-free culture medium was replaced with fresh DMEM containing 1 g/l glucose and 10% FBS after the hypoxia.

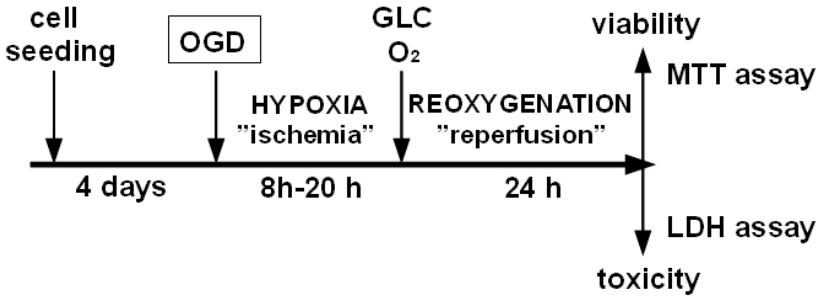

Figure 4. Experimental design and timeline. LLC-PK proximal tubule cells were grown to form confluent monolayer and then subjected to either glucose (GD) or oxygen (OD) or combined oxygen and glucose deprivation (OGD) for the designated time period to mimic ischemia.

3.4. In vitro model of sustained hyperosmolarity

IMCD cells were plated on 6 cm dishes (500 000 cell/dish) and cultured in DMEM/F12 medium containing 10% FBS and antibiotics. After confluency, the medium was switched to serum-free DMEM/F12 medium supplemented with 3,3′,5-Triiodo-L-thyronine (T3, Sigma-Aldrich), insulin-transferrin-selenium (ITS-G, Gibco), Bovine Serum Albumin (Sigma-Aldrich) and hydrocortisone (Sigma-Aldrich). In order to mimic the hyperosmolar conditions of the renal medulla, the medium osmolarity was gradually increased by adding NaCl and urea, from 330 mOsm reaching 900 mOsm on day 7. At specific osmolarities (330, 600, 900 mOsm), cells were harvested for MTT assay (on 96-well plates, n=8 replicates/group), RNA and protein isolation (on 6cm dishes, n=4 replicates/group).

3.5. MTT viability assay

In order to estimate the number of viable cells 3-(4,5-dimethyl-2-thiazolyl)-2,5-diphenyl-2H-tetrazolium bromide (MTT) was used. First, the cells were dissociated with 0.05 mM EDTA (at a final concentration of 2.5 µM) at 37 °C for 15 min at 5% CO_2 atmosphere to allow complete dye uptake, then 1/10 volume FBS containing 3-(4,5-dimethyl-2-thiazolyl)-2,5-diphenyl-2H-tetrazolium bromide (MTT, Calbiochem, EMD BioSciences, San Diego, CA) was added in 1/10 volume to reach final concentration of 0.5 mg•mL-1, and the cells were incubated for 3 hours at 37 °C at 5% CO_2 atmosphere. Cells were washed with PBS, dried overnight at room temperature and the formazan dye was dissolved in isopropanol. The amount of converted formazan dye was measured at 570 nm with background measurement at 690 nm on a Powerwave reader (Biotek).

3.6. Alamar Blue cell viability assay

Following the 24 hour-long recovery period, the cells were pretreated with EDTA at a final concentration of 2.5 µM for 15 min at 37 °C to allow complete dye uptake. Then FBS was added to the cells to neutralize EDTA and Alamar Blue (resazurin, 7-hydroxy-3H-phenoxazin-3-one-10-oxide) at a final concentration of 10 mg•mL-1. The cells were incubated for 3 h at 37 °C at 5% CO_2 atmosphere and fluorescence was measured on Synergy2 reader (Ex/Em: 530/590 nm) (Biotek, Winooski, VT, USA). The viability was calculated using dilution series of LLC-PK cells for calibration in Gen5 data reduction software.

3.7. Lactate dehydrogenase (LDH) assay

The cell culture supernatant (30 µl) was saved before the MTT assay and stored at 4˚C. For the assay the supernatant was mixed with 100 µl freshly prepared LDH assay reagent to reach final concentrations of 85 mM lactic acid, 1040 mM nicotinamide adenine dinucleotide (NAD), 224 mM N-methylphenazonium methyl sulfate (PMS), 528 mM 2-(4-Iodophenyl)-3-(4-nitrophenyl)-5-phenyl-2H-tetrazolium chloride (INT) and 200 mM Tris (pH 8.2). The changes in absorbance were read kinetically at 492 nm for 15 min (kinetic LDH assay) on a monochromator based reader (Powerwave HT,

Biotek). LDH release values are shown as Vmax (mOD/min) or percent values compared to the OGD group.

3.8. Immunocytochemistry of TGF-ß

IMCD cells (5000 cells/well) were seeded on BD multichamber slides and underwent the gradual increase in osmolarity as described above. At 330, 600 and 900 mOsm, cells were washed with ice-cold PBS and fixed with 4% paraformaldehyde for 30 minutes at room temperature. After washing with PBS, cells were blocked using 1x Powerblock (Biogenex, San Ramon, CA, USA) for 10 minutes and incubated with rabbit polyclonal TGF-ß1 antibody (1:50 in PBS, Santa Cruz) overnight at 4 ˚C. The slide was carefully washed twice with PBS and incubated with secondary antibody (Rabbit Link, Biogenex) for 30 minutes, washed and developed with Fast Red (Dako). Nuclei were counterstained with hematoxylin solution, then slides were mounted using Aquatex (Merck) and analyzed under light microscope.

3.9. Detection of TGF-ß, active Caspase-3 and PARP cleavage by western blotting

Cells were lysed in 400 µl denaturing loading buffer (20 mM Tris, 2% SDS, 10% glycerol, 6 M urea, 100 µg/ml bromophenol blue, 200 mM ß-mercaptoethanol), sonicated and boiled. Lysates (10 µl) were resolved on 4-12% NuPage Bis-Tris acrylamide gels (Invitrogen, Carlsbad, CA) and transferred to nitrocellulose. Membranes were blocked in 10% non-fat dried milk and probed overnight with anti-TGFß1 antibody (1:200, SantaCruz Biotechnology, Santa Cruz, CA), anti-caspase-3 antibody (1:100, Chemicon, Temecula, CA) or anti-PARP antibody (1:2000, Cell Signaling, Boston, MA). Anti-rabbit-horseradish peroxidase conjugate (HRP, 1:2000, Cell Signaling) and Pierce enhanced chemiluminescent substrate (Pierce ECL, Thermo Fisher Scientific Inc., USA) were used to detect the chemiluminescent signal in a CCD-camera based detection system (GBox, Syngene USA, Frederick, MD). To normalize signals, membranes were re-probed with an antibody against α-tubulin. The membranes were stripped in 62.5 mM Tris, 2% SDS, 100 mM ß-mercaptoethanol at 60 ˚C for 30 min, blocked overnight in 5% non-fat dried milk and re-probed with anti-tubulin (1:4000, Sigma St. Louis, MO) monoclonal antibody. After the application of anti-

mouse-HRP conjugate (1:4000, Cell Signaling) and ECL, chemiluminescence was detected with the same imaging system. The chemiluminescent signal of TGF-ß at 25 kDa, active caspase-3 at 17 kDa, full length PARP-1 at 120 kDa and tubulin at ~50 kDa were quantitated with Genetools analysis software.

3.10. Gene expression analysis of IMCD cells

IMCD cells for gene expression analysis were harvested using 1 ml of Trizol reagent per well (Life Technologies, USA) for phenol/chloroform extraction of total RNA according to the manufacturer's protocol. 2 μg RNA was reverse transcribed (High Capacity cDNA Reverse Transcription kit, Applied Biosystems, Forster City, CA, USA) using random primers. PCR reactions were performed on a BioRad CFX thermal cycler (BioRad, Hercules, CA, USA) using the Power SYBR Green PCR Master Mix (Applied Biosystems). Specificity and efficiency of the PCR reaction was confirmed with melting curve and standard curve analysis, respectively. Duplicate samples were normalized to glyceraldehyde-3-phosphate dehydrogenase (Gapdh) expression. Mean values are expressed with the formula 2-ΔΔCt. Primer sequences were as follows:

cFos forward 5-TTTCAACGCCGACTACGAGG-3;
cFos reverse 5-GCGCAAAAGTCCTGTGTGTT-3;
cJun forward 5-GCACATCACCACTACACCGA-3;
cJun reverse 5-GGGAAGCGTGTTCTGGCTAT-3;
mCol3a1 forward 5-TGGAAAAGATGGAACAAGTGG-3;
mCol3a1 reverse 5-CCAGACTTTTCACCTCCAAC-3;
mCol4a1 forward 5-CCTGCTAATATAGGGTTCGAG-3;
mCol4a1 reverse 5-CCAGGCTTAAAGGGAAATCC-3;
mEgr1 forward 5-TTCAATCCTCAAGGGGAGCC-3;
mEgr1 reverse 5-TAACTCGTCTCCACCATCGC-3;
mTgfb1 forward 5-CACCATCCATGACATGAACC-3;
mTgfb1 reverse 5-TCATGTTGGACAACTGCTCC-3.

3.11. Measurement of caspase-3 activity using a fluorescent substrate

LLC-PK1 cultures were exposed to 20 hours of combined oxygen-glucose deprivation in 96-well plates. Following 0-1-3-8-24 h reoxygenation, cells were lysed and caspase-3 activity was measured by CaspACETM Fluoremetric Assay System (Promega, Madison, WI) according to the manufacturer's recommendations. Cell lysates were mixed with caspase-3 specific fluorescence substrate, fluoro-chrome-7-amino-4-methyl-coumarin (Ac-DEVD-AMC). Cleaved generated free AMC that was detected using fluorescence reader (Ex/Em: 360/460nm). The fluorescence signal of free AMC, which is proportional to caspase-3 activity present in the sample, is shown as relative fluorescence units (RFU).

3.12. Trypan blue exclusion test

LLC-PK1 cells were exposed to OGD or glucose deprivation only for 20 hours, then trypan blue dye was added to the cells at the final concentration of 0.01% for 10 min. Excess dye was aspirated and the cells were visualized using a phase contrast microscope (Nikon TS-100F, Nikon Instruments, Inc.).

3.13. Permeability measurement

The apical membrane of LLC-PK cells is nonpermeable to MTT, Calbiochem, EMD BioSciences, San Diego, CA), thus the confluent monolayer of the cells excludes the dye, while the disruption of the monolayer allows dye uptake through the basolateral surface. LLC-PK1 cells underwent 20 hour-long OGD, then MTT was added at a final concentration of 0.5 mg•mL-1, and the cells were incubated for 3 hours at 37 °C at 5% CO_2 atmosphere. The formazan dye taken up by the cells was reduced with ascorbic acid and was dissolved in isopropanol. The absorbance was measured at 570 nm with background measurement at 690 nm. The increase in the amount of dye uptake is expressed as fold increase compared to control cells deprived of glucose only.

3.14. Measurement of cellular ATP content

LLC-PK cultures were exposed to 20 hours of combined oxygen-glucose deprivation and 0-8-24 h reoxygenation in 96-well plates. ATP concentration was determined by the commercially available CellTiter-Glo® Luminescent Cell Viability Assay (Promega, Madion, WI). The cells were lysed in 100 µL of CellTiter-Glo reagent according to the manufacturer's recommendations and the luminescent signal was recorded for 1s on a high sensitivity luminometer (Synergy 2, Biotek,Winooski, VT, USA). The assay is based on ATP requiring luciferen-oxyluciferin conversion mediated by a thermostable luciferase that generates a stable "glow-type" luminescent signal.

3.15. Bioenergetic measurements using the Seahorse analyzer

An XF24 Analyzer (Seahorse Biosciences, Billerica, MA) was used to measure metabolic changes in LLC-PK cells. The XF24 creates a transient 7 µl chamber in specialized microplates that allows real-time measurement of oxygen and proton concentration changes via specific fluorescent dyes and calculates OCR (oxygen consumption rate) and ECAR (extracellular acidification rate), measures of mitochondrial respiration and glycolytic activity. The OCR and ECAR values represent the metabolism of cells, but may also reflect the number of viable cells. LLC-PK cells underwent OGD as described above and were either used immediately for metabolic analysis or a 24 hour-long recovery period was allowed prior to metabolic measurements. For all bioenergetics measurements, the culture medium was changed to unbuffered DMEM (pH 7.4) containing 5 mM glucose, 2 mM L-glutamine and 1 mM sodium pyruvate. After determining the basal OCR and ECAR values, oligomycin, FCCP and antimycin A were injected through the ports of the Seahorse Flux Pak cartridge to reach final concentrations of 1 µg/ml, 0.3 µM and 2 µg/ml, respectively, to determine the amount of oxygen consumption linked to ATP production, the level of non-ATP-linked oxygen consumption (proton leak) as well as the maximal respiration capacity and the non-mitochondrial oxygen consumption. The values of oxygen consumption rate (OCR) and extracellular acidification rate (ECAR) reflect the metabolic activities of the cells and the number of cells.

3.16. Statistical analysis

Data are shown as mean ± SEM values or mean ± SD. One-way analysis of variance (ANOVA) was used to detect differences between groups. Post hoc comparisons were made using Tukey's test. A value of $p < 0.05$ was considered statistically significant. All statistical calculations were performed using Graphpad Prism 6 analysis software (GraphPad Software, Inc., La Jolla, CA)

.

4. RESULTS

4.1 Establish an in vitro model of renal ischemia-reperfusion injury

In order to establish an *in vitro* model of ATN, renal proximal tubule cells were exposed to oxygen-glucose depletion, as mainly proximal tubules are damaged during ischemic ATN. The most relevant feature of ischemia-reperfusion is oxygen deficiency; therefore we exposed the cells to partial or complete oxygen depletion in the presence of different glucose concentrations, in order to investigate the effects of different oxygen and glucose depletion conditions. Various hypoxia periods were applied (12h, 16h, 20h, 24h, 36h) during complete and partial hypoxia. After hypoxia, the medium was replaced with fresh, glucose containing DMEM and the cells were incubated for 24 hours at 37 °C at 5% CO_2 atmosphere to mimic *in vitro* the "reperfusion" or reoxygenation injury. Finally, we determined the cellular viability by MTT assay.

The partial hypoxia caused 50% reduction in tubular cell viability, but the total hypoxia reduced the viability to only 10%. In the presence of 5 mM glucose, the longer (36h) hypoxia caused a nearly 20% viability regardless of oxygen concentration. Therefore, we applied hyperglycemic control samples for each hypoxia conditions, which cells retained their viability regardless of the hypoxia condition (Figure 5).

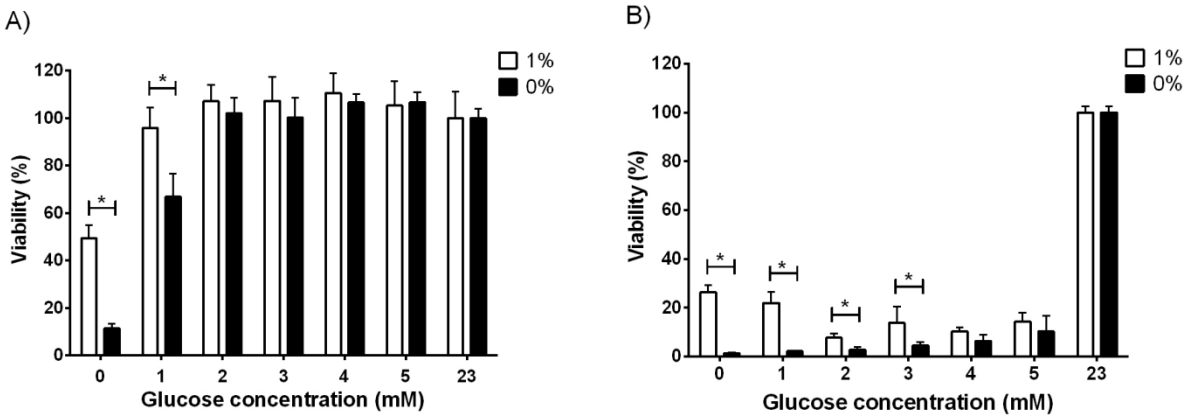

Figure 5. Cellular viability during complete oxygen-glucose deprivation. The HK-2 cells subjected to 16 hours (A) and 36 hours (B) of partial hypoxia (at 1% O_2) and complete hypoxia (total O_2 deprivation) along different glucose concentrations and followed by a 24 hour-long reoxygenation. Cellular viability was evaluated by MTT assay. The shown viability values are expressed as relative to cells that were treated

with 23 mM glucose (last bars on both graphs). (Data are shown as mean ± SD values. *$p<0.05$)

Our next step was to compare different proximal tubular cell lines, such as human renal proximal tubular epithelial cell line (HK-2), rat renal proximal tubular epithelial cell line (NRK) and porcine kidney proximal tubular cells (LLC-PK). As the first experiments on HK-2 cells resulted in minimal viability after prolonged (36h) hypoxia, we exposed the different proximal tubule cells to 16 and 20 hours oxygen-glucose deprivation (OGD).

Although all three cell lines showed reduction in viability after OGD, the different cell lines depicted variable tolerance to the extent of glucose depletion and hypoxia. HK-2 was the most sensitive cell line, 16 hours of OGD reduced the viability to 10% in the presence of 5 mM glucose. This might be explained by the fact that HK-2 cells are normally maintained in high-glucose (4.5 g/l or 25 mmol/l) medium. In NRK cells, 16 hours of oxygen depletion reduced the viability by 50% in the absence of glucose (0 mM), but a 20h of OGD further reduced cell viability to 20% in 1 mM but to 0% in 0 mM glucose media, respectively. LLC-PK cells behaved similar to NRK, as 16h of OGD reduced the viability to 80% in 0 mM glucose and 20h of OGD reduced further to 20% but only in 0 mM glucose (Figure 6).

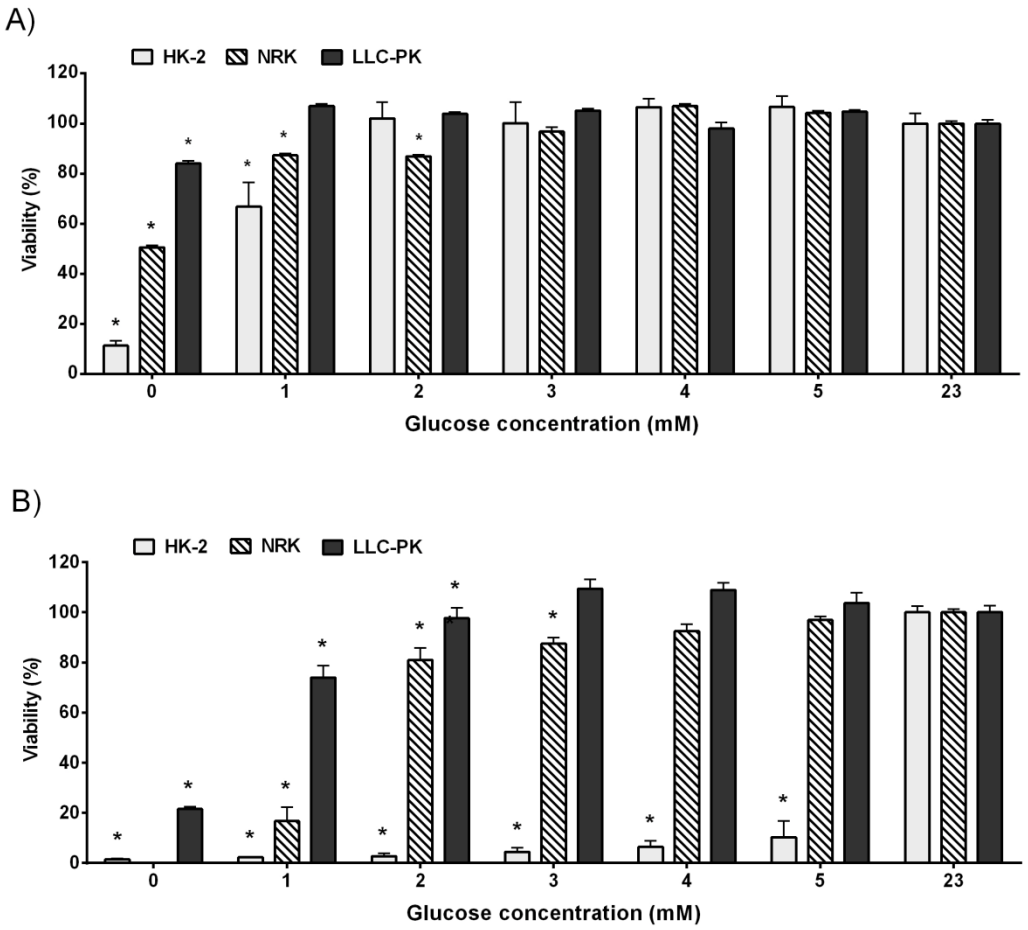

Figure 6. The reduction of cellular viability in different cell lines exposed to oxygen depletion in the presence of different glucose concentrations. Three different cell-lines showed reduction in viability depending on glucose concentration during oxygen depletion. The cells were exposed to (A) 16 hours and (B) 20 hours of hypoxia at indicated glucose concentrations and 24 hours reoxygenation. The viability was evaluated after the period of reoxygenation by MTT assay and the viability values are expressed as relative to control cells that were treated with 23mM glucose (last bars on the graph). (Data are shown as mean ± SD values. *$p<0.05$ compared to 23 mM glucose.)

Despite all cell lines show reduced viability under hypoxic condition, only the LLC-PK cells were suitable to model the postischemic injury. We measured LDH release to evaluate the cell death during the OGD and reoxygenation period. LDH is an intracellular enzyme released during cell death, therefore used as indicator of necrosis. LLC-PK cells underwent 20 hours of OGD and 24 hours of reoxygenation period. The

released LDH enzyme was measured immediately after hypoxia and after the following reoxygenation period in the cell culture supernatants. The oxygen-glucose depletion induced only 1.5 fold increase in LDH activity during the hypoxia, but the reoxygenation period further increased LDH activity by 3-fold in the supernatants as compared to the CTL cells. These results indicate that the reduction of viability occurs during the reoxygenation period (Figure 7).

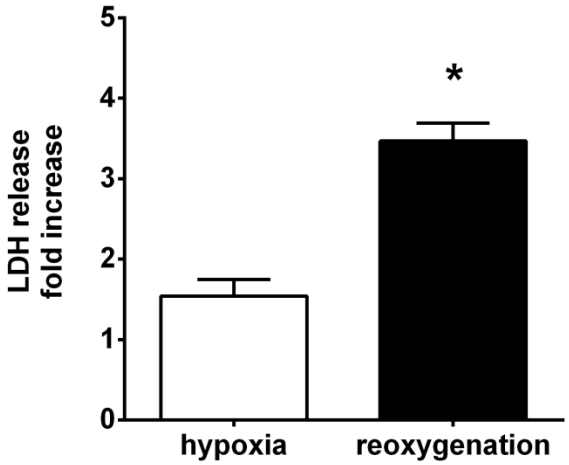

Figure 7. Activity of released LDH enzyme during hypoxia and reoxygenation. LLC-PK cells were exposed to 20 hours OGD and 24 hours reoxygenation period. LDH activity was measured in cell culture supernatants of samples immediately after the hypoxia and after the reoxygenation period. Fold increase is shown relative to CTL (the cells exposed to OD only). (Data are shown as mean ± SD values. *$p<0.0001$)

Aditionally, we studied the effect of FBS during oxygen depletion. LLC-PK cells were exposed to 24 hour-long complete oxygen depletion in the prescence of different FBS (Figure 8A) and glucose concentrations (Figure 8B) Cell viability at different FBS concentrations increased in a dose dependent manner during oxygen and glucose depletion. Not surprisingly, the complete absence of FBS and glucose resulted in minimal viability. However, there was hardly detectable difference in cell viability from 1 mM glucose or above, as at 1 mM glucose concentration the cell viability increased up to 80% even in the absence of FBS.

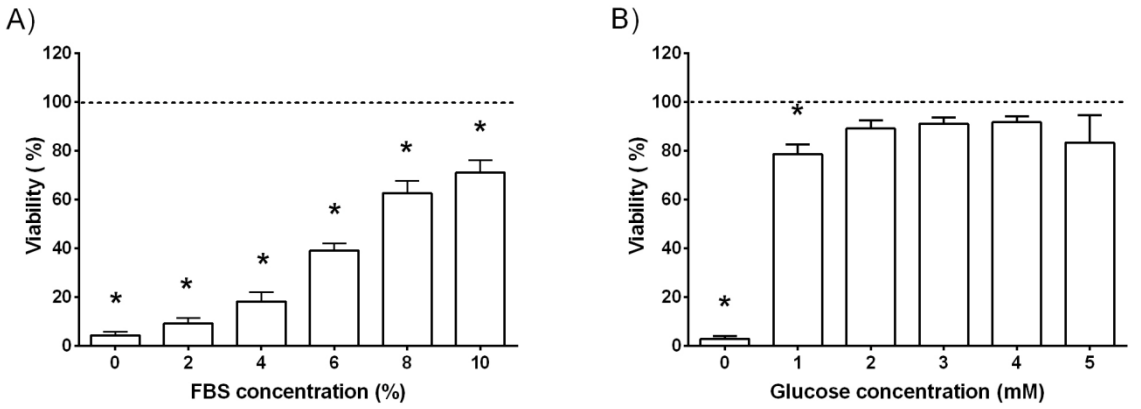

Figure 8. LLC-PK cell viability changes in the presence of different FBS and glucose concentrations. The cells exposed to 20 hours oxygen and glucose depletion in the presence of different FBS concentration (A), and oxygen depletion in the absence of FBS at different glucose concentrations (B). After OGD, both FBS and glucose concentrations were normalized and the viability was measured by MTT assay after a 24 hour-long recovery period. Viability values are expressed as relative to CTL (5mM glucose and 10% FBS), the CTL group is labeled with the dashed line. (Data are shown as mean ± SD values. *$p<0.05$ compared to CTL).

Considering that acidosis develops during ischemia, the cells derive more energy from glycolysis which generates protons, leading to the reduction of renal pH (85) the pH reduction was tested. The cells were exposed to 20 hours OGD at different (5% or 18%) CO_2 atmosphere followed by 24 hour reoxygenation at normal 5% CO_2 atmosphere. Interestingly, at higher (18%) CO_2 concentration, that theoretically causes acidosis, we observed increased cell viability as compared to normal (5%) CO_2 atmosphere (Figure 9).

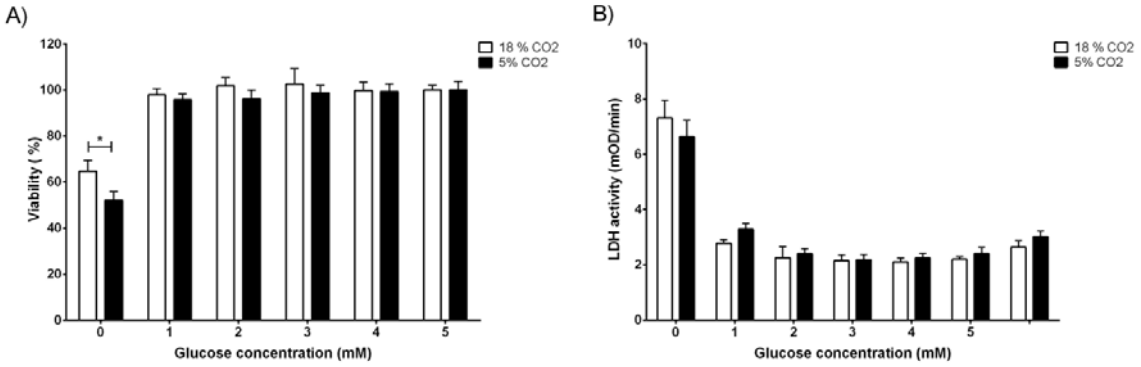

Figure 9. Cells viability at different CO_2 atmosphere during OGD. LLC-PK cells underwent 16 hour-long OGD at 5% or 18% CO_2 atmosphere. Cell viability was measured by MTT assay (A) after the glucose and oxygen were resupplied for 24 hours. LDH release was evaluated by measuring the LDH activity in the supernatant (B). Viability values are expressed as relative to control cells treated with 5mM glucose at 18% CO_2 or 5% CO_2, atmosphere. (Data are shown as mean ± SD values. *$p<0.0001$.)

We established a cell culture model of ischemic acute tubular necrosis by deprivation of oxygen and glucose followed by a recovery period, to mimic the reperfusion injury. We cultured LLC-PK porcine proximal tubular cells for 4 days prior to the hypoxic challenge in order to form a confluent polarized monolayer. Then the cells were exposed to combined deprivation of both oxygen and glucose (OGD) or only oxygen deprivation (OD) in a medium containing 5 mM glucose (used as control), followed by a 24 hour-long recovery period. Glucose and serum concentrations were restored during the recovery period. The cell viability changed depending on the length of oxygen-glucose deprivation: an 8 hour-long OGD had no effect, but an OGD of 12, 16, 18 or 20 hours reduced the viability by 15%, 30%, 65% or 80%, respectively (Figure 10).

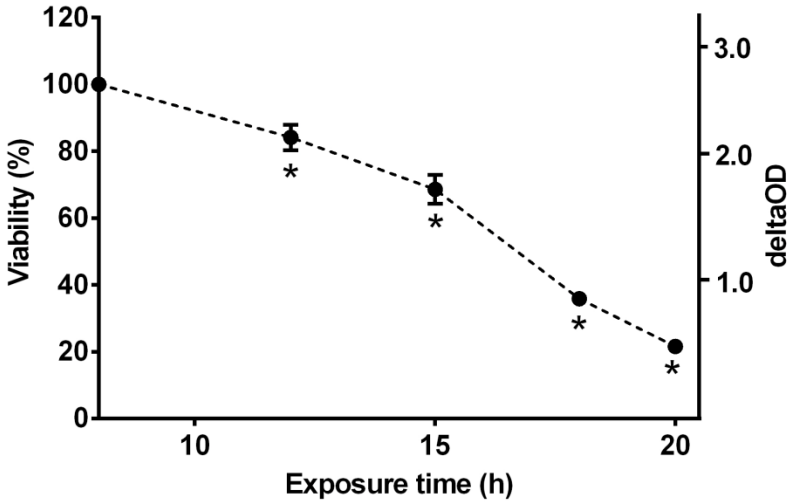

Figure 10. Reduction of viability depends on the length of oxygen-glucose depletion. The LLC-PK cell were exposed to OGD for the indicated length in order to mimic ischemic injury. Reperfusion injury was imitated by resupplying glucose and oxygen for 24 hours prior to the evaluations of cellular viability by MTT assay and cell death by LDH assay. The shown viability values are expressed as relative to control cells that were maintained under normoglycemia and normoxia for the same length. (Data are mean ± SD values, *$p<0.05$ compared to CTL)

4.2 Energy depletion and loss of cell barrier function during ischemia-reperfusion.

We investigated the ischemia induced dysfunction of cell barrier, caused by energy depletion, using trypan blue staining. OGD induced the loss of trypan blue excluding ability of the cells. While oxygen deprivation alone had no effect on trypan blue exclusion (Figure 11A), near 100% of the cells subjected to OGD were stained with trypan blue (Figure 11B). The inability to exclude or actively remove trypan blue from the cells reflect the loss of barrier function of the cell membrane, or the lack of energy to properly exclude and/or remove the dye.

The apical membrane is impermeable to MTT, thus the confluent LLC-PK cells do not take up and retain MTT without the disruption of the monolayer's barrier function. Glucose deprivation induced a low, but measurable MTT uptake by the cells, and OGD induced a 3-fold increase in the amount of MTT taken up by the cells (Figure 11C).

OGD induced a severe reduction in cellular ATP content: a 20 hour-long exposure reduced the ATP content below 5% of the control. The 24 hour-long recovery period increased ATP content at least 4-fold, reaching approximately 20% of the controls (Figure 11D). As it was mentioned above, OGD did not induce an immediate increase in the LDH release form the cells: there was no detectable difference between the LDH release of the cells subjected to OGD and control cells following the hypoxia (Figure 11E). However, during the recovery period the LDH release increased significantly in the OGD group.

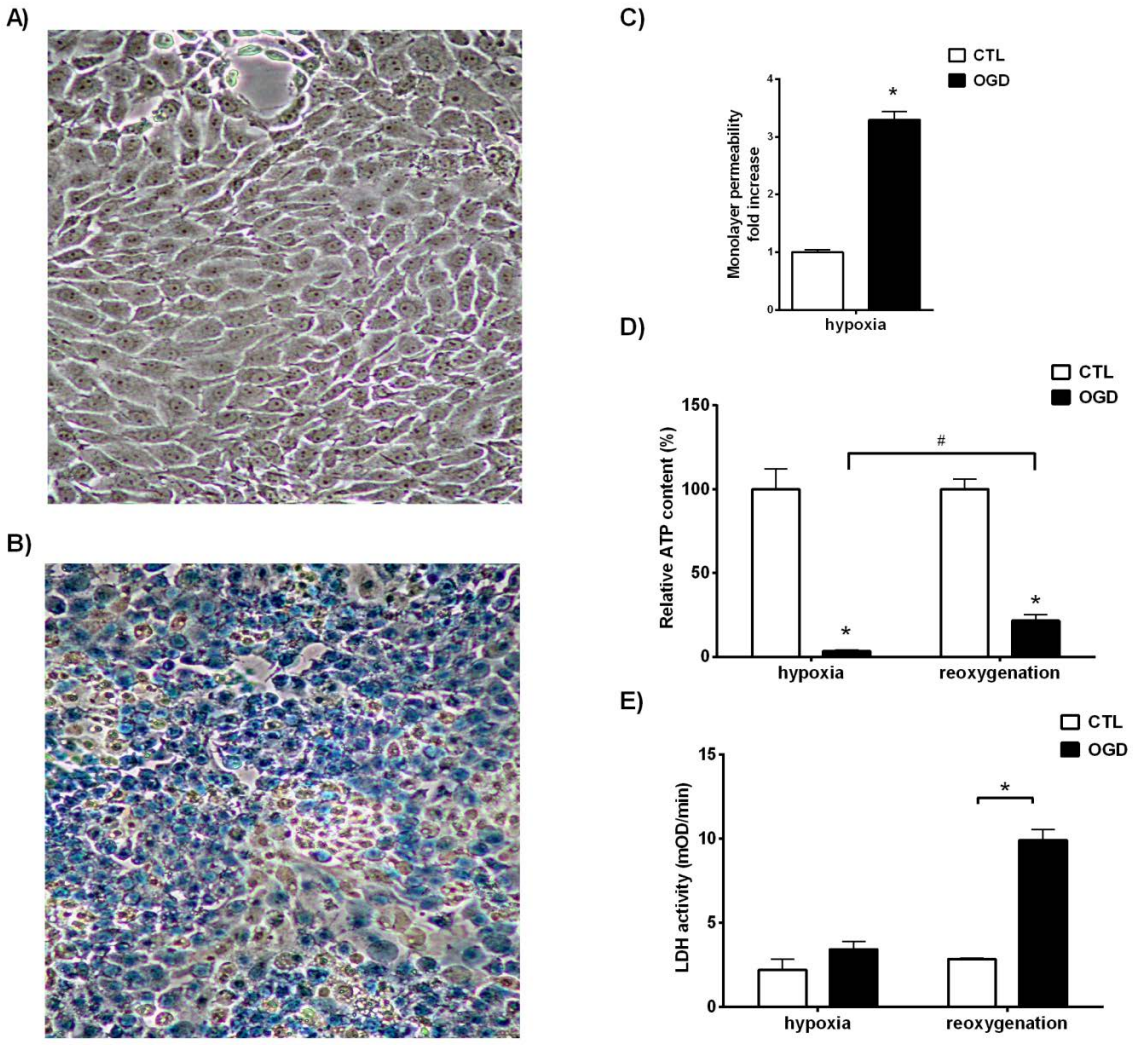

Figure 11. Cellular dysfunction, ATP depletion and cell death after OGD. LLC-PK cells were subjected to hypoxia with excess glucose (CTL, A) or with simultaneous glucose deprivation (OGD, B) for 20 hours and were stained with trypan blue. Representative micrographs are shown. The permeability of the monolayer was

measured immediately after hypoxia and fold increase is shown relative to CTL (C). Cellular ATP content (D) was measured from cell lysates prepared immediately following the hypoxia ("hypoxia") and after a 1 day-long recovery ("reoxygenation"). Relative ATP contents are shown compared to controls. LDH activity was measured in cell culture supernatant in samples taken immediately after the hypoxia or after the 24 hour-long reoxygenation (E). The measured enzyme activity values are shown in mOD/min. (Data are shown as mean ± SD values, *$p<0.0001$ compared to CTL, #$p<0.0001$ compared to the respective post-hypoxia value)

4.3 Multiple pathways are implicated in the OGD induced cell death in LLC-PK cells

In order to better characterize the mechanism of the late phase cell death after OGD, we tested the effect of compounds that selectively inhibit various forms of cell death. The cells were treated after the ODG with caspase inhibitor Z-VAD-fmk, the necroptosis inhibitor necrostatin-1 or poly(ADP-ribose)polymerase (PARP) inhibitor PJ34. Neither the necrosis inhibitor PJ34 nor the inhibition of necroptosis provided protection against the OGD induced cell death (Figure 12). On the other hand, inhibition of apoptosis using Z-VAD-fmk resulted in a significant increase in cellular viability. Caspase inhibition induced a two-fold increase in the viability after severe OGD, still the majority of the cells receiving Z-VAD-fmk treatment died eventually. Caspase inhibitor treatment preceding the OGD was similarly effective, but it had no benefit over the post-OGD treatment.

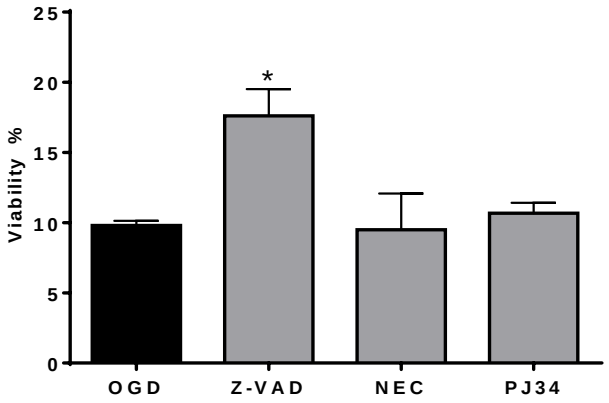

Figure 12. Effect of different compounds that inhibit various forms of cell death. LLC-PK cells were subjected to OGD for 20 hours, then resupplied with oxygen and glucose and treated with Z-VAD-fmk (Z-VAD), necrostatin-1 (NEC) or PJ34 at 10 µM. The viability was measured after the 24 hour-long recovery period by MTT assay and are expressed as relative to control cells (the cells exposed to OD only). (Mean ± SD values are shown, *$p<0.05$ compared to OGD)

We also studied the time course of caspase activation by Western blotting and using an activity assay. Active caspase-3 was hardly detectable in the samples immediately after the OGD, but appeared within 1 hour of the reoxygenation period and was detectable subsequently for hours (Figure 13A). Similarly, the caspase activity assay showed increased caspase-3 activity 1 hour following the end of the OGD and the activity further increased in the following hours peaking by 8 hours of the reoxygenation period (Figure 13B). However, active caspase-3 was not detectable by Western blotting at the end of the 24 hour-long recovery period, and also the caspase activity returned to baseline level by that time.

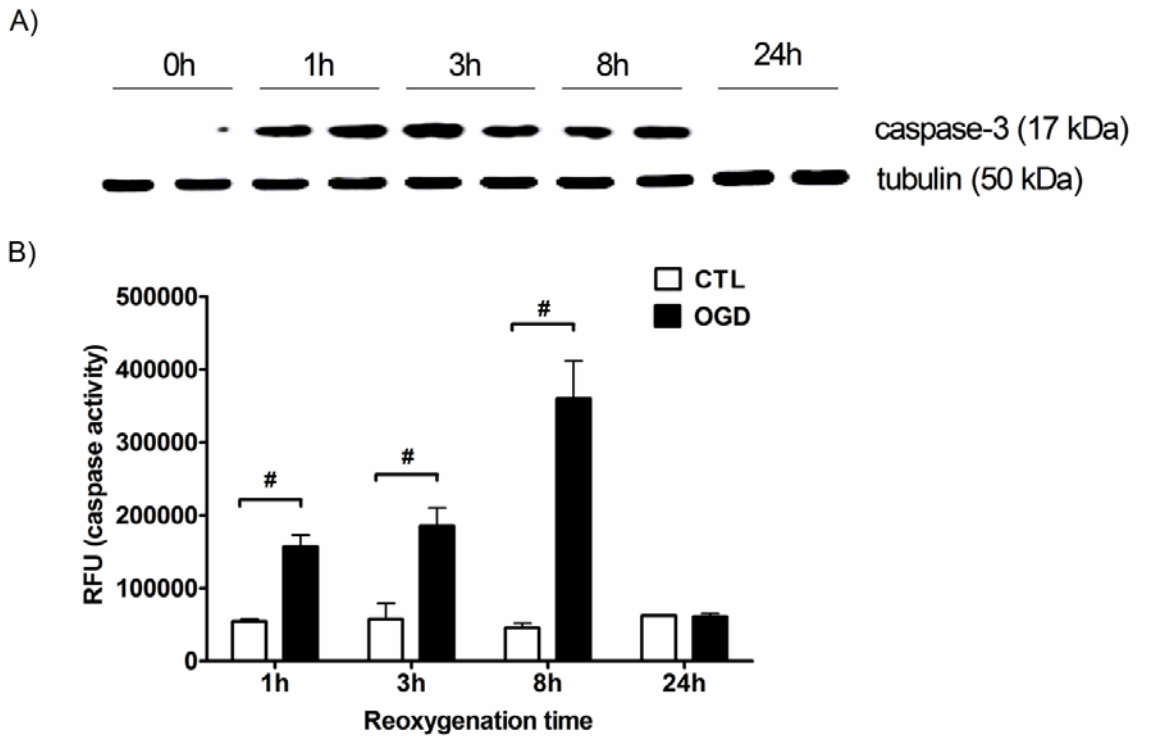

Figure 13. Caspase-3 activation during reoxygenation. Cells were subjected to 20 hour-long OGD and maintained under normoxia with glucose supplementation for the indicated time for the detection of active caspase-3 protein (A) and caspase activity (B). Representative Western blot images with tubulin signal as loading control are shown (A). Caspase-3 activity (B) was measured with fluorescent substrate and relative fluorescence (RFU) values of the cleavage product are shown. (Mean ± SD values are shown, #$p<0.05$ compared to control cells which exposed to OD only)

Caspases cleave various proteins during the apoptotic process, including PARP, a nuclear enzyme associated with necrotic cell death. Caspase cleavage of PARP-1 removes the DNA-binding domain of the protein from its catalytic domain, creating 30 kDa and 89 kDa fragments. We detected a decrease in full length (120 kDa) PARP-1 during the reoxygenation phase: 1 hour following the beginning of the reoxygenation the amount of full length PARP-1 significantly decreased, followed by further reduction in PARP-1 level. Full length PARP-1 was hardly detectable by 8 hours and it completely disappeared at the end of the 24 hour-long recovery period. The decrease of full-length PARP-1 was associated with an increase of cleavage fragments. The caspase-specific 89 kDa fragment appeared in some of the samples taken immediately

after the OGD and reached peak levels by 3 hours of reoxygenation, then started to decline, but remained detectable by the end of the 24 hour-long recovery period. Other proteases that cleave PARP-1 include calpain, cathepsin B and granzyme B which create 70 kDa, 64 kDa and 50 kDa fragments, respectively. The calpain specific 70 kDa fragment was detectable 1 hour following the OGD (but not immediately at the end of the OGD), and was present in all subsequent samples at high levels throughout the reoxygenation period. The cathepsin B specific 64 kDa fragment was detectable at low levels in samples taken 1 hour after the OGD and remained detectable up to 8 hours of the recovery period. The 50 kDa fragment associated with granzyme B mediated cleavage was present in the samples from the end of the OGD and remained detectable throughout the 24-hour follow-up. All proteolytic fragments of PARP reached the highest level in the samples taken 3 hours after the beginning of the reoxygenation. The calpain specific fragment was present in the highest amount in all the samples taken after 1 hour of reoxygenation or later (Figure 14).

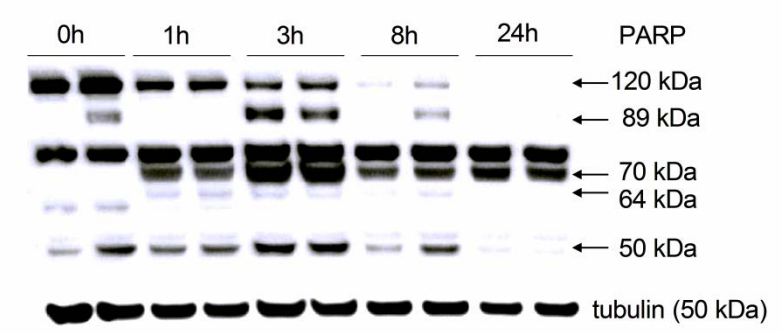

Figure 14. Detection of PARP-1 protein activation and cleavage by different proteases. Cells were subjected to 20 hour-long OGD and indicated reoxygenation period with glucose supplementation and PARP protein was detected at the indicated time. Representative Western blot with tubulin signal as loading control are shown.

4.4. Diverse compounds protects against hypoxia-reoxygenation injury in LLC-PK cells

We searched for compounds that ameliorate hypoxia-reoxygenation injury of renal proximal tubule cells in two settings: cells were subjected to 20 hours of OGD

followed by a 24 hour-long reoxygenation period with the test compounds either added prior to the OGD induction (pre-OGD screen) or immediately after the onset of the reoxygenation (post-OGD screen) (Figure 15).

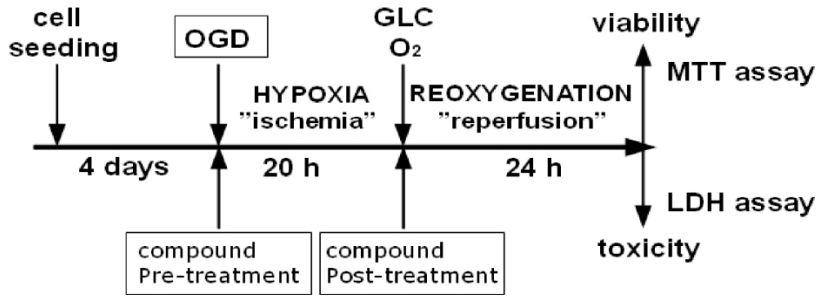

Figure 15. Screen design. LLC-PK proximal tubule cells were grown to form confluent monolayer and then subjected to OGD for 20 hours to mimic ischemia. Reperfusion injury was imitated by glucose and oxygen re-supplementation for 24 hours, then the cell survival was evaluated by the MTT and LDH assays. Test compounds were screened for cytoprotection by treating the cells either prior to the OGD ("Pre-treatment") or following the OGD ("Post-treatment).

The majority of the compounds had negligible effect on the OGD induced injury. Some compounds reduced the viability either by enhancing the injury or by exerting a cytotoxic effect on LLC-PK cells. Compound treatment following the OGD had less pronounced effect than the pre-treatment. The largest viability increase was no more than 15% in the post-OGD screen, while in the pretreatment screen it attained 45%. The number of compounds that markedly reduced or increased the viability was similar in both assays. Most of the compounds that showed some activity had dissimilar effects depending on the timing of the treatments. The majority of the compounds that markedly reduced the viability in one of the two screens, had little effect in the other screen. Similarly, the compounds showing the highest level of protection in one set-up did not affect the viability in the other screen (with one notable exception) (Figure 16).

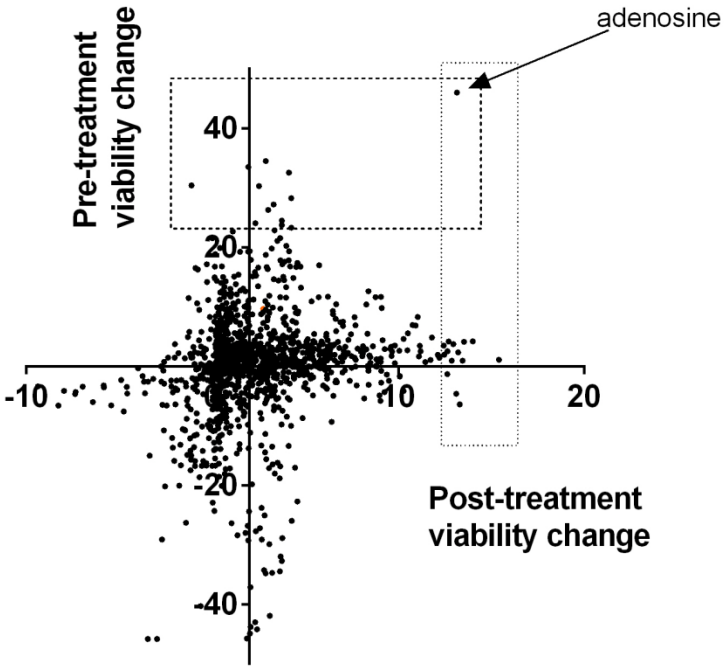

Figure 16. The compound-induced viability changes in the screen. Cells were subjected to 20 hour-long OGD and 24 hours reoxygenation with glucose supplementation, the cell survival was evaluated by the MTT assays. Test compounds were screened by treating the cells either prior to the OGD ("Pre-treatment") or following the OGD ("Post-treatment). The viability changes induced by the compound treatment are shown as percent values compared to the vehicle treated cells (zero value) on the dot plot. The effect of the post-treatment is shown on the x-axis and the changes in the pre-treatment screen are represented on the y-axis. The screens were performed in replicates and the average values are shown.

The compounds exerting the highest protective activity in the screens are summarized in Table 1. **Adenosine** was the only compound that showed high activity in both assays. In fact, it was the only compound that increased the viability by more than 40% in the pretreatment screen, and was among the top 10 compounds in the post-OGD screen with 13% increase in the viability. Among the protective compounds in the pre-OGD screen were disulfiram and inhibitor of alcohol metabolism, tyrosine kinase inhibitors of the epithelial growth factor receptor (EGFR) class. In the post-OGD screen the compounds showing the highest activity included dopaminergic and cholinergic

compounds, the nitric oxide synthase (NOS) inhibitor aminoguanidine, a phosphodiesterase (PDE) inhibitor, or the amino acid L-aspartate. Interestingly, these compounds did not improve the viability by similar extent if applied earlier, prior to the OGD and were present in the assay medium throughout the hypoxia.

The high activity of adenosine in our screens and the fact that adenosine is known to be released from the cells during ischemia or inflammation and may reach similar local concentration urged us to search for potentiators of adenosine. We performed two additional screens in which the same compound library was screened with 30 μM adenosine pretreatment either with pre-OGD or post-OGD addition of the test compounds. In these screens, the highest-ranking compounds included only two of the drugs that emerged as protective in the previous screens: adenosine in the pre-OGD and L-aspartic acid in the post-OGD regimen. Adenosine was among the most potent compounds in the pre-OGD combination screen, showing that higher concentration of adenosine has further benefit and it affects the cell survival more than most other treatments. Also, many compounds that increased cell survival without adenosine had the opposite effect in the combination screen: these antagonized the protective effect of adenosine, especially when they were applied prior to the hypoxia. Interestingly, half of the most protective compounds were identical in the two combination screens, and many of the compounds that showed some protective effect in one of the assays had similar effect in the other assay. Altogether, these data show that a few of the compounds can exert additional protective effect via multiple disparate mechanisms; the purine nucleoside adenosine is a highly effective protective agent that can be used safely at various time points during the injury.

Table 1. The hit molecules showing the highest protective effect in screens. Hypoxia-reoxygenation injury was induced in LLC-PK cells and the LOPAC library was screened for protective effect in various set-ups. From each screen, the 5 highest-ranking cytoprotective compounds are shown with the respective activity in the other assays and the known biological function. (I.) In the pre-treatment screen (PRE) the compounds (50 µM) were applied prior to the OGD, (II.) in the post-treatment screen (POST) the cells received the compounds after the OGD. Adenosine pretreatment (30 µM) was combined (III.) with compounds pre-treatment (ADE PRE) and (IV.) with the application of the test compounds following the OGD (ADE POST). The shown cytoprotective effect represents the viability increase compared to the OGD in PRE and POST screens or compared to the adenosine-treated cells subjected to OGD (ADE) in ADE PRE and ADE POST screens. (The viability values of CTL, OGD and ADE groups were 100%, 40% and 70%, respectively.)

Compound	*Known biological activity*	*Cytoprotection (%)*			
		PRE	*POST*	*ADE PRE*	*ADE POST*
I. Pre-treatment screen					
Adenosine	*endogenous neurotransmitter*	**46.0**	13.2	16.6	-0.8
Disulfiram	*aldehyde dehydrogenase inhibitor*	**34.5**	2.9	-9.2	0.8
2-Phenylaminoadenosine	*selective adenosine A2 receptor agonist*	**33.5**	1.9	-4.2	2.6
Tyrphostin AG 537	*tyrosine kinase inhibitor*	**32.6**	4.1	-14.4	7.1
Riluzole	*glutamate release inhibitor*	**30.4**	-1.1	-2.1	10.6
II. Post-treatment screen					
N-Acetyldopamine monohydrate	*dopamine analog possessing antitumor activity*	1.1	**15.4**	3.1	-3.5
Enoximone	*phosphodiesterase inhibitor*	4.2	**14.0**	-6.0	4.5
R(-)-N-Allylnorapomorphine HBr	*dopamine receptor anatagonist*	4.1	**13.5**	7.8	10.4
L-Aspartic acid	*amino acid, participant in gluconeogenesis*	1.0	**13.5**	8.3	24.8
Amperozide HCl	*serotonin receptor antagonist*	-6.4	**13.3**	-73.0	6.5
III. Adenosine combined pre-treatment screen					
γ-D-Glutamylaminomethylsulfonic acid	*kainate/quisqualate glutamate receptor antagonist*	1.4	2.0	**27.0**	3.2
Hydrocortisone 21-hemisuccinate	*glucocorticoid steroid*	1.6	3.0	**25.1**	11.7
Tyrphostin AG 126	*TNF-α and NO synthesis inhibitor*	16.5	-0.9	**18.1**	3.6
4-Amino-1,8-naphthalimide	*poly(ADP-ribose) polymerase (PARP) inhibitor*	8.9	4.6	**16.9**	21.9
Adenosine	*endogenous neurotransmitter*	46.0	13.2	**16.6**	-0.8
IV. Adenosine combined post-treatment screen					
Arecaidine propargyl ester HBr	*M2 muscarinic acetylcholine receptor agonist*	-1.4	3.5	-16.1	**35.6**
L-Aspartic acid	*amino acid, participant in gluconeogenesis*	1.0	13.5	8.3	**24.8**
Centrophenoxine HCl	*cholinergic nootropic agent*	1.0	6.1	8.5	**24.0**
Caffeic acid phenethyl ester	*NF-kB inhibitor*	1.7	3.6	12.4	**22.5**
4-Amino-1,8-naphthalimide	*poly(ADP-ribose) polymerase (PARP) inhibitor*	8.9	4.6	16.9	**21.9**

4.5. Adenosine and inosine increase the survival after OGD with similar efficacy

Adenosine possesses marked cardiovascular effects that may limit its systemic use, thus we also tested its metabolite, inosine that has less cardiovascular activity but retains most of adenosine's anti-inflammatory activity (86). Both adenosine and inosine increased cell survival in a dose dependent manner. The protective effect of these purine nucleosides was similar to that of glucose (Figure 17A and B). Adenosine exerted a significant cytoprotection at 30 µM as measured with the MTT assay, while inosine and glucose were less effective, though both adenosine and glucose decreased the LDH release already at 10 µM (Figure 17C). 100 µM of any of the three compounds (adenosine, inosine or glucose) induced a significant viability increase and significant reduction of LDH release. All three compounds mostly reverted the hypoxic injury at 300 µM with slight improvement at 1000 µM. The MTT assay indicated complete reversal of the injury at 300 µM for all three compounds, while the alamar blue assay showed only 90% restoration for adenosine and inosine and approximately 75% functional recovery after glucose treatment. The LDH release was also lower in the purine-treated wells than in the wells receiving glucose treatment in the 100-1000 µM range.

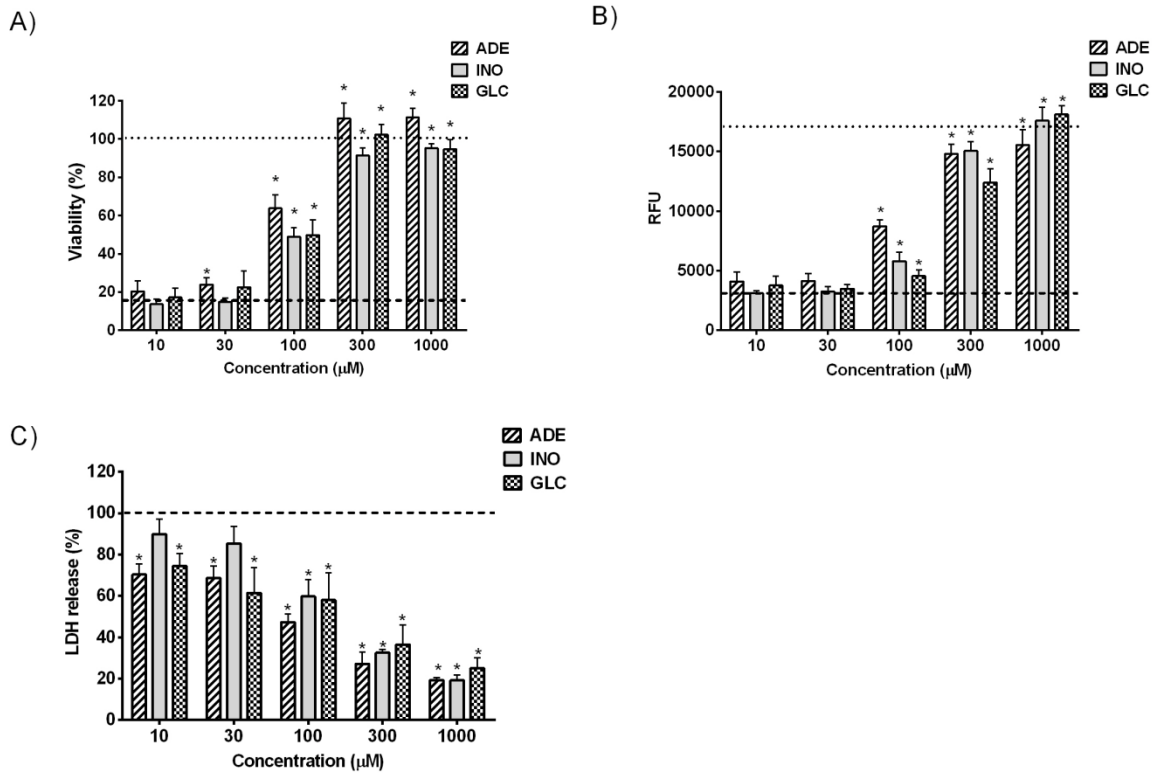

Figure 17. The protective actions of adenosine and inosine against the OGD induced proximal tubule injury. LLC-PK cells were subjected to 20 hour-long OGD in presence of the indicated concentration of adenosine (ADE), inosine (INO) or glucose (GLC) and then re-supplemented with glucose and oxygen for 24 hours. The viability was measured by MTT (A) and alamar blue (B) assays. The viability values measured by MTT assay are expressed as relative to control cells, which were exposed to OD only. LDH release was evaluated by measuring the LDH activity in the supernatant (C). The viability value of the OGD group is labeled with the dashed line, and the CTL viability is shown as dotted line. The decrease in LDH release is shown as percent value of the LDH activity of the vehicle treated cells (OGD). (Data are shown as mean ± SD values, *$p<0.05$ compared to OGD group)

We studied cytoprotection of adenosine and inosine in wide range dose response during OGD to determine toxicity and the "safe" level. The cells were treated from 3 μM to 5 mM concentration of adenosine and inosine in a dose-dependent manner. The cytoprotection reached the maximum level around at 300 μM and holded to 5 mM. We

could not reach the toxic level with the applied 5 mM maxmimum concentration (Figure 18).

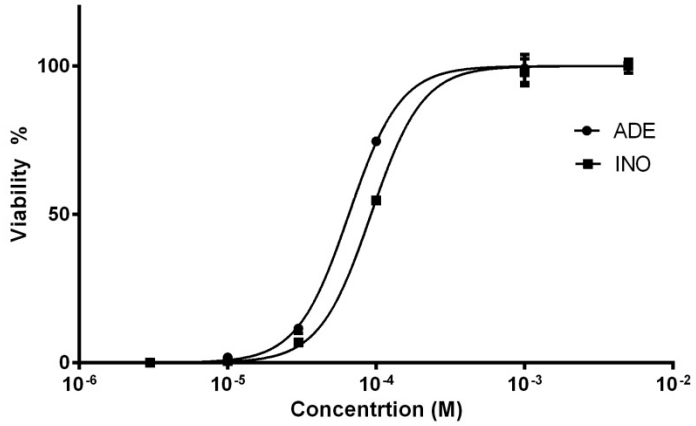

Figure 18. Potency of adenosine and inosine. LLC-PK cells were subjected to 20 hour-long OGD in presence of wide dose interval adenosine and inosine. The viability was measured 24 hour-long recovery period by MTT assay and expressed as relative to CTL (cells exposed to OD only). The half-maximal effective concentration (EC_{50}) of adenosine was 68 µM (A) of inosine was 89 µM (B). (Data are shown as mean ± SD values).

We tested the cytoproective effect of other purin and pyrimidin bases during the OGD to determine the mode of action. The cells were treated with 300 µM of adenosine, cytidine, guanosine, thymidine, uridine, adenine, cytosine, guanine, thymine and uracil and exposed to 20 hour-long OGD. Cell viability was measured after 24 hours recovery period. Although cytidine, guanosine and uridine were cytoprotective to some extent against hypoxic injury, only adenosine pretreatment could preserve cell viability (Figure 19).

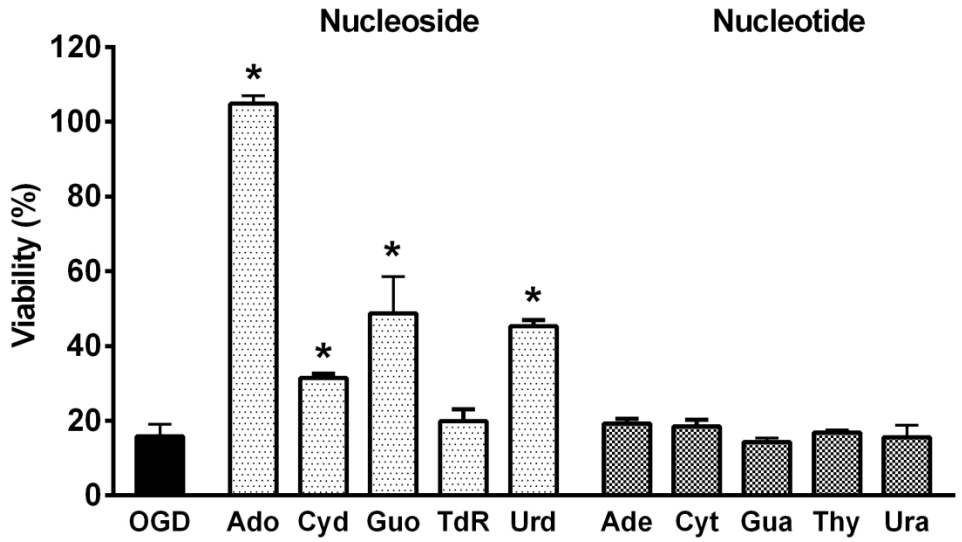

Figure 19. Effect of purine and pyrimidine bases against the OGD induced proximal tubule injury. LLC-PK cells were subjected to 20 hour-long OGD in presence of 300 µM adenosine (Ado), cytidine (Cyd), guanosine (Guo), thymidine (TdR), uridine (Urd), adenine (Ade), cytosine (Cyt), guanine (Gua), thymine (Thy) and uracil (Ura). The viability was measured by MTT assay after 24 hour-long recovery period and expressed as percent values of controls (cells exposed to OD only) (Data are shown as mean ± SD values, *$p<0.05$ compared to OGD)

We also tested whether purine nucleoside treatment can prevent the OGD induced caspase activation and PARP cleavage. OGD induced caspase activation during the reoxygenation phase which was significantly reduced by inosine pretreatment (Figure 20A). PARP is cleaved by various proteases during the recovery phase including caspases. OGD induced a severe reduction of full length PARP, 8 hours after the beginning of reoxygenation only 10% of intact PARP remained detectable, while adenosine pretreatment protected PARP and restored it to 60% of the control level (Figure 20B).

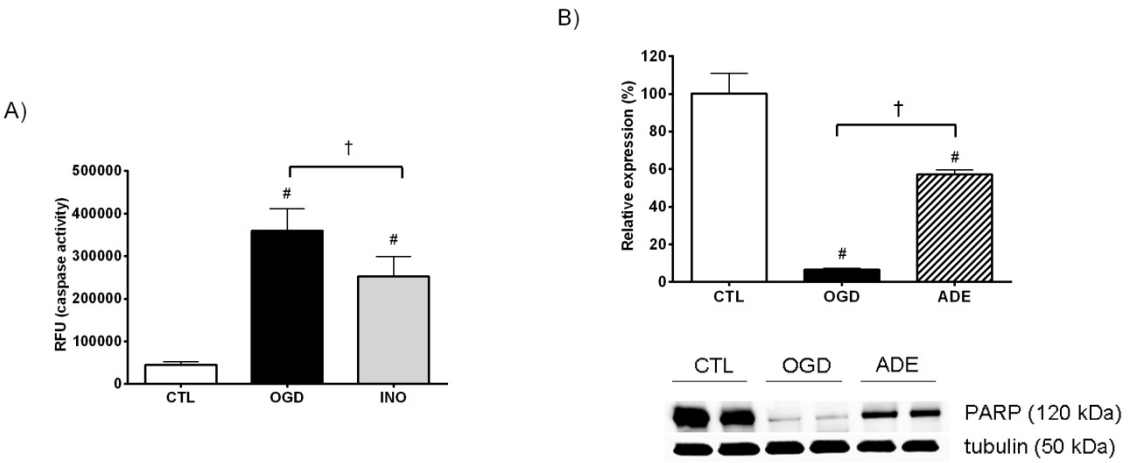

Figure 20. Treatment of adenosine and inosine reduce the caspase activation and PARP cleavage during the reoxygenation phase. Cells were subjected to 20 hour-long OGD with the absence (OGD) or presence of 100 µM inosine (INO) and caspase-3 activity was measured after 8 hours of reoxygenation. Caspase-3 activity was measured with fluorescent substrate and relative fluorescence (RFU) values of the cleavage product are shown (A). Cells were subjected to 20 hour-long OGD with the absence (OGD) or presence of 300 µM adenosine (ADE) and the amount of full-length PARP1 was evaluated by Western blotting (B). Representative blot of PARP and normalization signal tubulin and results of the densitometric analysis are shown. The bar graph represents the PARP (120 kDa) signal normalized to tubulin as relative PARP expression compared to the CTL (cells exposed to OD only). (Data are shown as mean ± SD values, #$p<0.05$ compared to CTL, †$p<0.05$ compared to OGD group)

4.6. The cytoprotective effect of purine nucleosides requires intracellular metabolism

Adenosine was shown to protect against ischemia-reperfusion injury and inflammation and the various adenosine receptors were implicated in the protective action suggesting that these receptors are essential in the protective function of adenosine in hypoxia-reoxygenation based injuries. We tested whether blockade of the adenosine receptors prevents the protective action of adenosine or inosine against the OGD induced cell death in LLC-PK cells. Treating the cells with A1 receptor antagonist CDPX or A2A receptor antagonist 8-(3-chlorostyryl)-caffeine or A2B receptor

antagonist alloxazine or with A3 receptor antagonist MRS 1523 did not reduce the viability increase attained by adenosine or inosine (Figure 21A and B). Neither affected the adenosine receptor antagonists the adenosine or inosine induced decrease of the LDH release in LLC-PK cells exposed to OGD (Figure 21C and D). These data indicate that receptor-independent actions are involved in the protective actions of adenosine and inosine in LLC-PK cells.

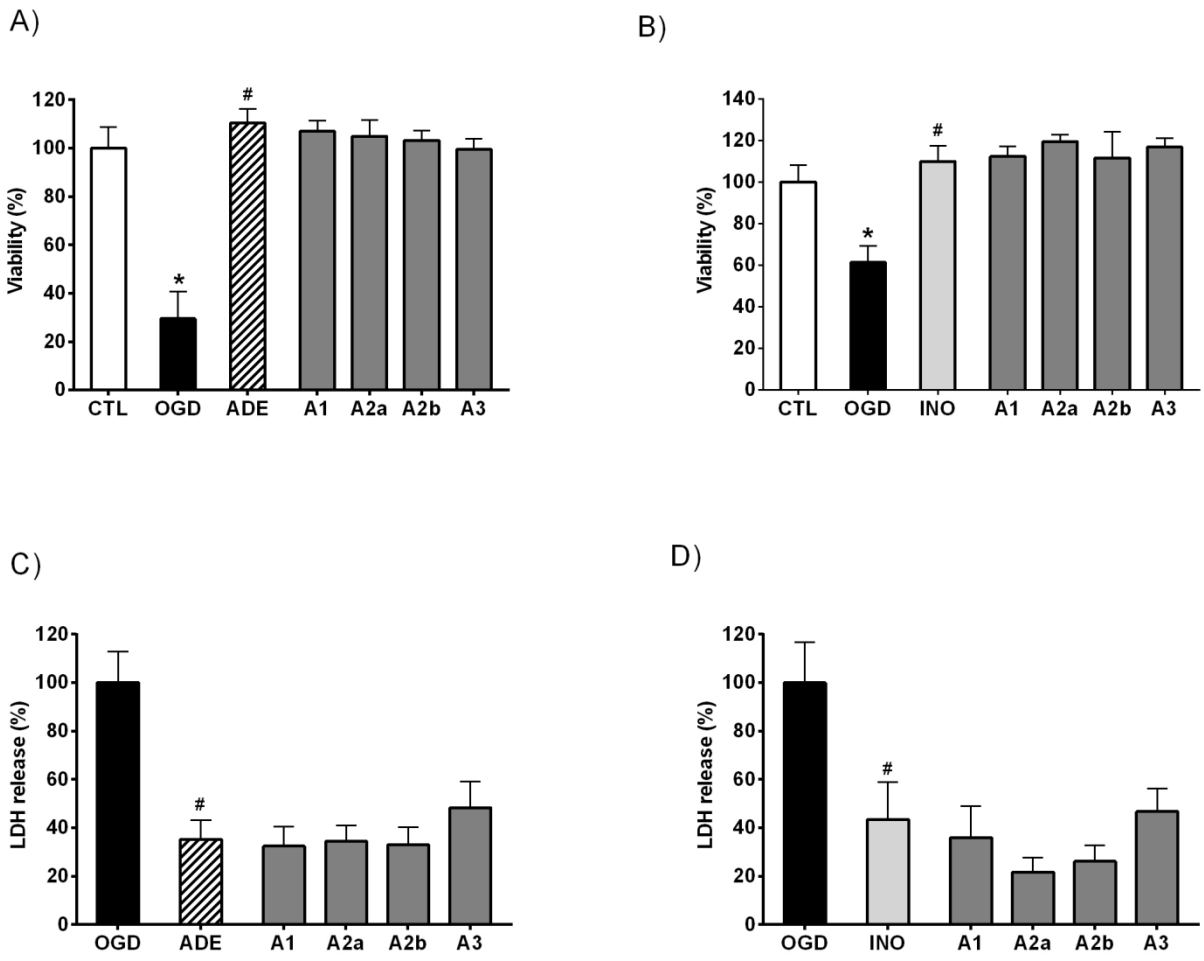

Figure 21. The effects of adenosine receptor antagonist on adenosine- and inosine-mediated protection in LLC-PK cells subjected to OGD. The cells were exposed to 20 hour-long OGD followed by a 24 hour-long recovery period in the presence of 1000 uM of adenosine (ADE) (A,C) or inosine (INO) (B,D) and the respective receptor antagonists (3 μM): A1 receptor antagonist CDPX (A1), A2A receptor antagonist 8-(3-Chlorostyryl)caffeine (A2A), A2B receptor antagonist alloxazine (A2B), A3 receptor antagonist MRS 1523 (A3). The cellular viability was evaluated by the MTT assay (A,

B) and expressed as percent values of controls (cells exposed to OD only). LDH activity (C,D) was measured in the supernatant and shown as percent value of the vehicle treated controls (OGD). Mean ± SD values are show. (*p<0.05 compared to CTL, #p<0.05 compared to OGD.)

We blocked adenosine deaminase (ADA), the enzyme that converts adenosine to inosine within the cells, with pharmacological inhibitor EHNA. As expected, EHNA did not reduce the protective effect of inosine or glucose totally. However, EHNA significantly decreased the viability of the adenosine treated cells subjected to OGD and also significantly increased the LDH release from the cells. Surprisingly, ADA inhibition did not abolish the adenosine-mediated protection completely. Adenosine is phosphorylated by adenosine kinase (AK) within the cells to produce AMP, adenosine kinase inhibitor, ABT 702 also reduced the adenosine and inosine induced viability increase after OGD in LLC-PK cells. The AK and ADA inhibition resulted in comparable viability decrease in the adenosine treated cells, and similar increase in the LDH release. In addition, AK inhibition similarly affected the viability and LDH release in both the adenosine and the inosine treated cells, whereas it had no significant effect on the glucose treated cells. The simultaneous inhibition of ADA and AK completely abolished the protective effect of adenosine and inosine. The combination of EHNA and ABT 702 significantly reduced the glucose mediated viability increase and increased the LDH release (Figure 22).

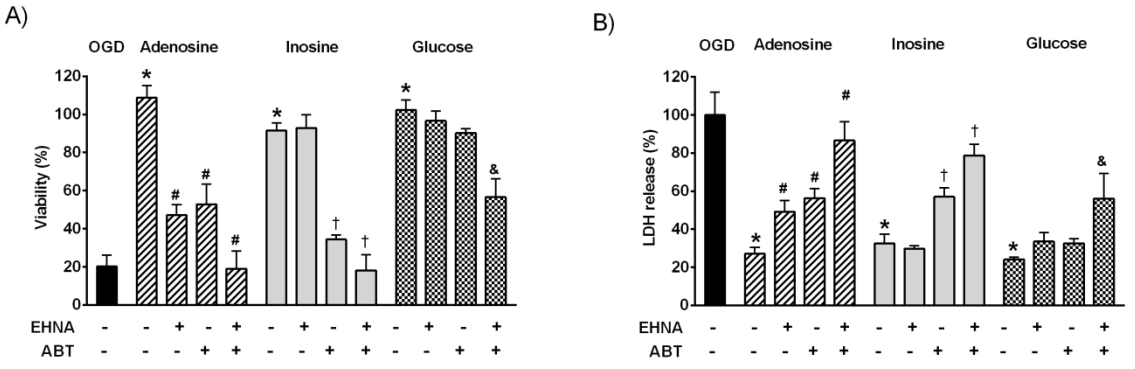

Figure 22. The role of adenosine deaminase (ADA) and adenosine kinase (AK) in the cytoprotective effects of adenosine, inosine and glucose in hypoxia-reoxygenation injury. LLC-PK cells pretreated with ADA inhibitor EHNA (10 μM) and/or AK inhibitor ABT 702 (ABT, 30 μM) were subjected to 20 hour-long oxygen-

glucose deprivation in the absence (OGD) or presence of 300 μM adenosine, inosine or glucose. Following the oxygen-glucose deprivation, the cells were re-supplied with oxygen and glucose for 24 hours and the viability was evaluated by MTT assay and expressed as percent values of controls (cells exposed to OD only) (A). LDH activity was measured in the supernatant (B), data are percent values of the activity measured in the supernatant of the OGD group. (Mean ± SD values are show. *$p<0.05$ compared to OGD, #$p<0.05$ compared to adenosine, †$p<0.05$ compared to inosine, &$p<0.05$ compared to glucose).

4.7. Adenosine and inosine accelerate the post-hypoxic recovery

ATP depletion plays a crucial role in the pathogenesis of hypoxia-reoxygenation injury and the requirement of AK activity in the protection mediated by adenosine and inosine suggested that these purine nucleosides act via promoting ATP synthesis and preserving the ATP content during hypoxia. We measured the ATP content of the cells receiving 300 μM adenosine, inosine or glucose treatment prior to the OGD. The OGD induced a 60% decrease in the viability and the compound treatments fully restored the viability of the cells according to the viability assay. Both adenosine and inosine significantly increased the cellular ATP content as measured immediately after the OGD. The ATP content dropped to 5% in LLC-PK cells subjected to OGD and both purine nucleosides elevated the ATP content to 20%, while the presence of glucose in equal amounts increased the ATP content to 10% only. During the recovery period, ATP concentration increased gradually in all groups. The ATP content of the cells subjected to OGD reached 10% and 20% after 8 and 24 hours of reoxygenation, respectively. In the cells exposed to hypoxia in the presence of glucose the ATP content was 30% and 60% after 8 and 24 hours of reoxygenation, while in the cells supplemented with purines the ATP content exceeded 60% by 8 hours and was completely restored by 24 hours. The cellular ATP content decreased severely during the OGD, and both glucose and purine pretreatment helped preserving the ATP content to some extent, still this effect seems to be moderate. In the presence of adenosine or inosine, LLC-PK cells tolerated such severe ATP depletion with full recovery that might induce cell death in other cells. The purines also enhanced the restoration of the ATP content, since they resulted in a steeper increase in the ATP content and they fully

replenished the cellular ATP concentration by 24 hours, while glucose supplementation also fully prevented cell death, still resulted in a significantly lower cellular ATP concentration at the end of the 24 hour-long follow-up (Figure 23).

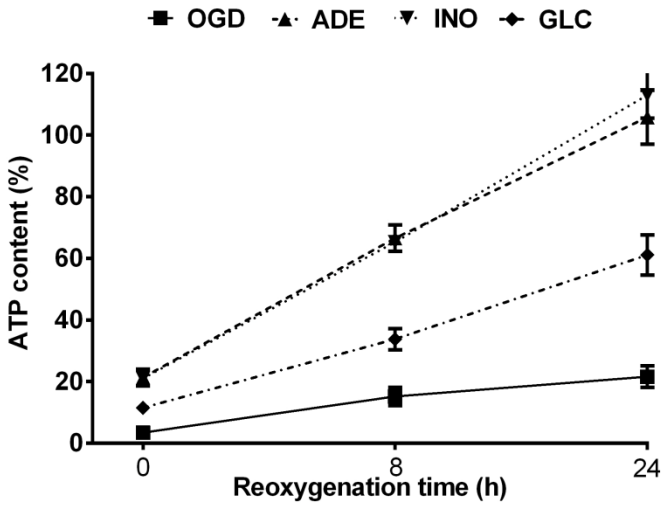

Figure 23. The posthypoxic ATP content of the cells after purine nucleoside supplementation. LLC-PK cells were subjected to 20 hour-long OGD in the absence (OGD) or presence of 300 µM adenosine (ADE), inosine (INO) or glucose (GLC), then re-supplemented with glucose and oxygen and incubated up to 24 hours. The ATP content was determined at the indicated reoxygenation time and expressed as percent values of control cells (cells exposed to OD only). (Data are shown as mean ± SD values.)

We blocked ADA and AK function during the reoxygenation period to test whether these enzymes also take part in the recovery after hypoxia. Both the post-hypoxic ADA and AK inhibition decreased the viability, proving the requirement of ADA and AKA function during the reoxygenation period. ADA or AK inhibition after the OGD significantly reduced the viability of the adenosine-pretreated cells. Interestingly, EHNA significantly reduced the viability of inosine and glucose treated groups, possibly by blocking the utilization of endogenous adenosine via the pentose phosphate pathway. AK inhibition resulted in a more pronounced viability reduction in all treatment groups. The effect of ADA and AK inhibition was summative, showing the synergistic actions of ADA and AK during the recovery period (Figure 24). These data strongly suggest that metabolism of endogenous or exogenous adenosine and inosine

are also used for ATP production during the post-hypoxic reoxygenation period. These molecules are able accelerate the recovery even in the presence of sufficient glucose supply and the use of these purine nucleosides plays a fundamental role in post-hypoxic cell survival.

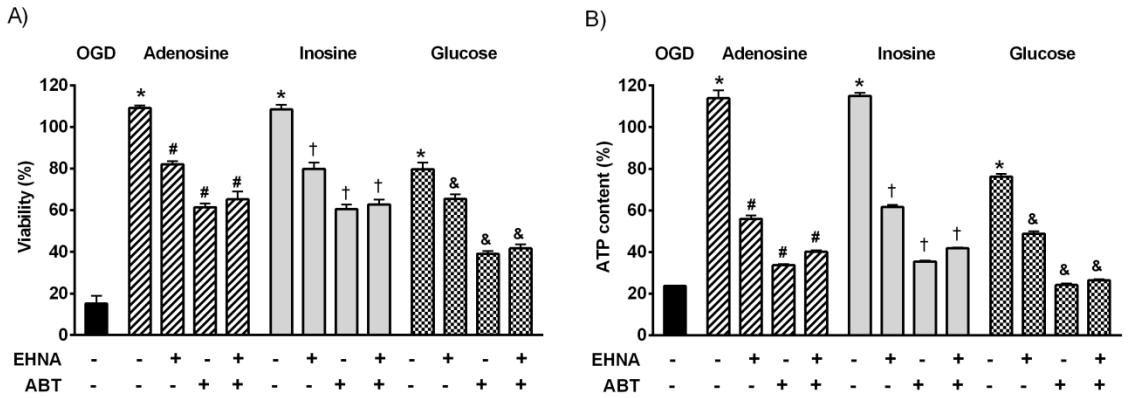

Figure 24. The effect of ADA and AK inhibition on the recovery phase. LLC-PK cells were subjected to 20 hour-long oxygen-glucose deprivation in the absence (OGD) or presence of 300 µM adenosine (ADE), inosine (INO) or glucose (GLC), then re-supplemented with glucose and oxygen and incubated up to 24 hours. After the hypoxia the cells were also treated with ADA inhibitor EHNA (10 µM) and/or AK inhibitor ABT 702 (ABT, 30 µM) and cellular viability was evaluated by MTT assay after 24 hours. Viability values and ATP content are shown as percent values of controls (cells exposed to OD only). (Data are shown as mean ± SD values. *$p<0.05$ compared to OGD, #$p<0.05$ compared to adenosine, †$p<0.05$ compared to inosine, &$p<0.05$ compared to glucose.)

4.8. Adenosine and inosine ameliorate the OGD induced metabolic suppression in LLC-PK cells

Adenosine preserves the cellular ATP content during OGD and blockade of ADA, the enzyme responsible for the conversion of adenosine to inosine, the first step required for metabolism of adenosine via the pentose-phosphate pathway, reduces the protective effect of adenosine. These data suggest that adenosine as a ribose source is used in place of glucose to maintain ATP generation during OGD. Thus we tested whether adenosine pretreatment directly affect the cellular metabolism using the Seahorse metabolic analyzer.

LLC-PK cells were subjected to OGD with 300 μM adenosine pretreatment and the cellular metabolism was measured immediately following the hypoxia and after a 24-hour-long recovery period. OGD induced very severe reduction in both aerobic and anaerobic metabolism, the oxygen consumption rate (OCR) of the cells was lower than the detection limit of the instrument while extracellular acidification rate (acid production), the measure of the anaerobic metabolism, was below 10% of the controls. (The Seahorse analyzer uses fluorescent detection method to measure changes of partial pressure of oxygen in the assay medium and is unable to reliably detect a drop less than 50 mmHg or OCR values under 30-40 pMoles/min.) Adenosine pretreatment completely preserved the anaerobic metabolism in the cells and resulted in approximately 40% decrease in the oxygen consumption. Anaerobic metabolism is often described with the proton production rate (PPR) that is calculated from the pH changes of the assay medium and it is also expressed in a logarithmic scale as ECAR in pH/min. The assay medium acidification is proportional to the CO_2 production as glucose represents the major energy source during the measurement. During glucose metabolism CO_2 is produced in an anaerobic fashion while the protons retrieved from glucose are not released from the cell but proceed to the oxidative phosphorylation. The Seahorse analyzer measures the water production from the retrieved protons as OCR. The acidification rate of the controls and the adenosine-pretreated cells was comparable; showing that adenosine supplementation completely preserved the cellular machinery required for anaerobic glucose metabolism, while it was severely damaged in oxygen-glucose deprived cells. Proton leak is implicated in the mitochondrial damage and it can be measured with the Seahorse analyzer as the difference between the OCR values after oligomycin and antimycin addition. There was no detectable proton leak in the adenosine-pretreated cells after hypoxia, but there was a reduction in the mitochondrial potential (shown by the lower OCR after FCCP addition). These data suggest that rather the decreased mitochondrial potential (possibly as a result of lower proton production during the OGD) than mitochondrial dysfunction cause the lower basal mitochondrial oxygen consumption and aerobic metabolism after adenosine treatment. We also tested the metabolic function in the cells subjected to hypoxia 24 hours later when the ATP content of the cells was fully restored in the adenosine-pretreated cells. There was very little improvement in both the aerobic and anaerobic metabolism in the cells subjected

to OGD without treatment. The aerobic metabolism markedly improved in the adenosine pretreated cells, reaching 90% of the OCR values of the controls, and the anaerobic metabolism of the cells was indistinguishable from the controls. The mitochondrial potential also increased in the adenosine treated cells, but it was still lower than in the controls. We can postulate that the protons produced during anaerobic glucose breakdown but not used in the oxidative phosphorylation can account for the increase in the mitochondrial potential during the recovery phase (Figure 25).

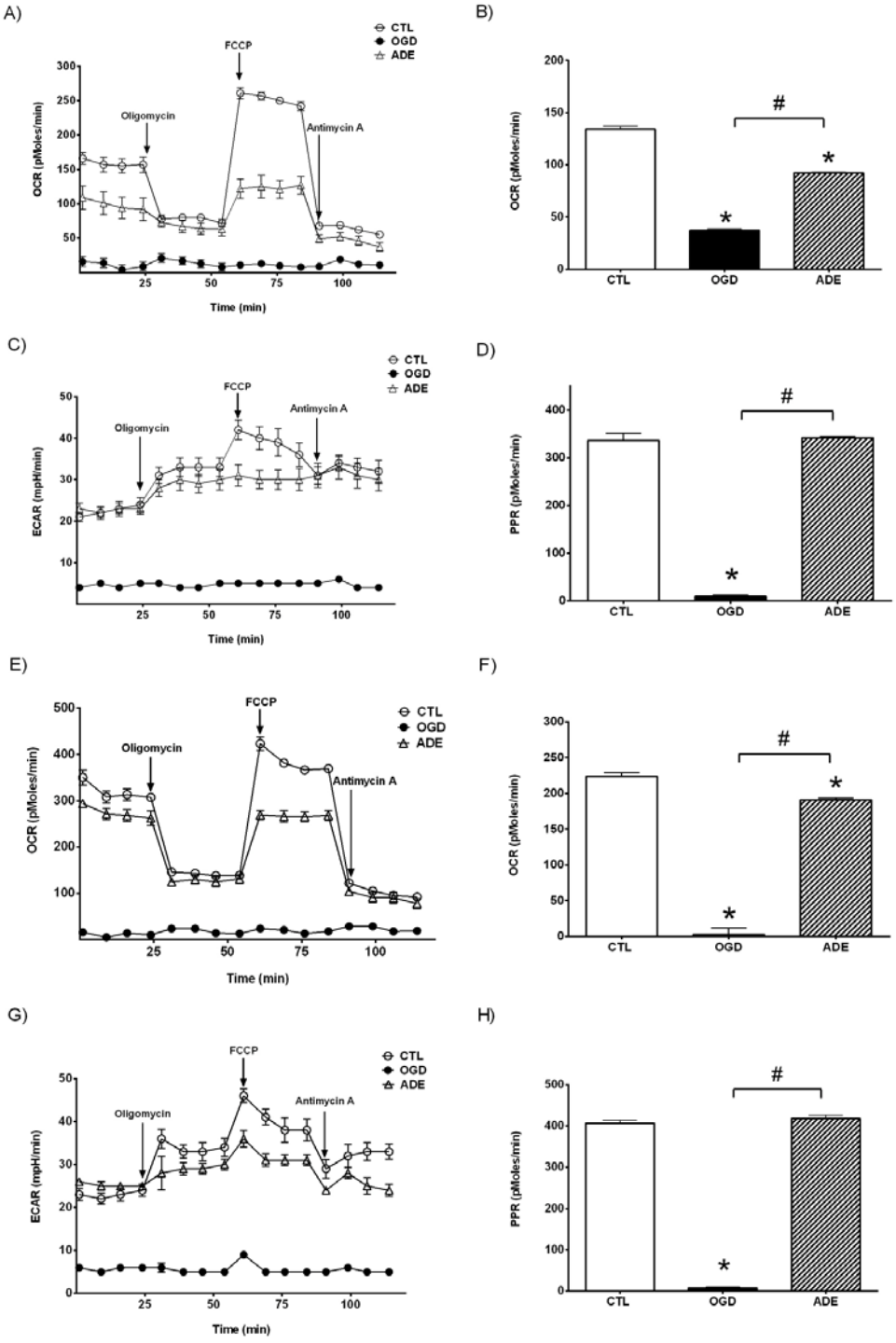

Figure 25. Seahorse metabolic analysis of LLC-PK cells subjected to hypoxia-reoxygenation injury. LLC-PK were subjected to oxygen-glucose deprivation in the absence (OGD) or presence of 300 µM adenosine (ADE) for 20 hours and analyzed immediately (A-D) or re-supplemented with glucose and oxygen and incubated for 24

hours prior to the measurement (E-F). Oxygen consumption rate (OCR) and the extracellular acidification rate (ECAR) were determined prior to and after the addition of oligomycin, FCCP and antimycin A (A,C,E,F), as indicated on the figure. The basal respiration (B,F) as the difference between the OCR prior to oligomycin and after antimycin A and the respective proton production rates (PPR) are also shown (D,H). Data are shown as mean ± SEM values. *$p<0.05$ compared to CTL, #$p<0.05$ compared to OGD.

4.9. Hyperosmolarity decreases cell viabilty and induces TGF-ß overexpression in IMCD cells

The progressive increase of osmolarity resulted in decreased viability of IMCD cells as shown by MTT assay. Compared to controls (at 330 mOsm), reaching 600 mOsm in the medium led to 40% fall in viabilty, and a further 10% decrease was observed when we increased the osmolarity to 900 mOsm (Figure 26A). In parallel with the decreased viability, we observed marked increase in TGF-ß mRNA and protein expressions due to hyperosmolarity. TGF-ß mRNA expression increased from 330 mOsm to 600 mOsm and from 600 to 900 mOsm by 1.5 fold and further 1.6 fold, respectively (Figure 26B). This was accompanied by a similar increase in TGF-ß protein expression by 3-fold and 2.4-fold, respectively. This observation was confirmed by immunocytochemistry as well (Figure 26C).

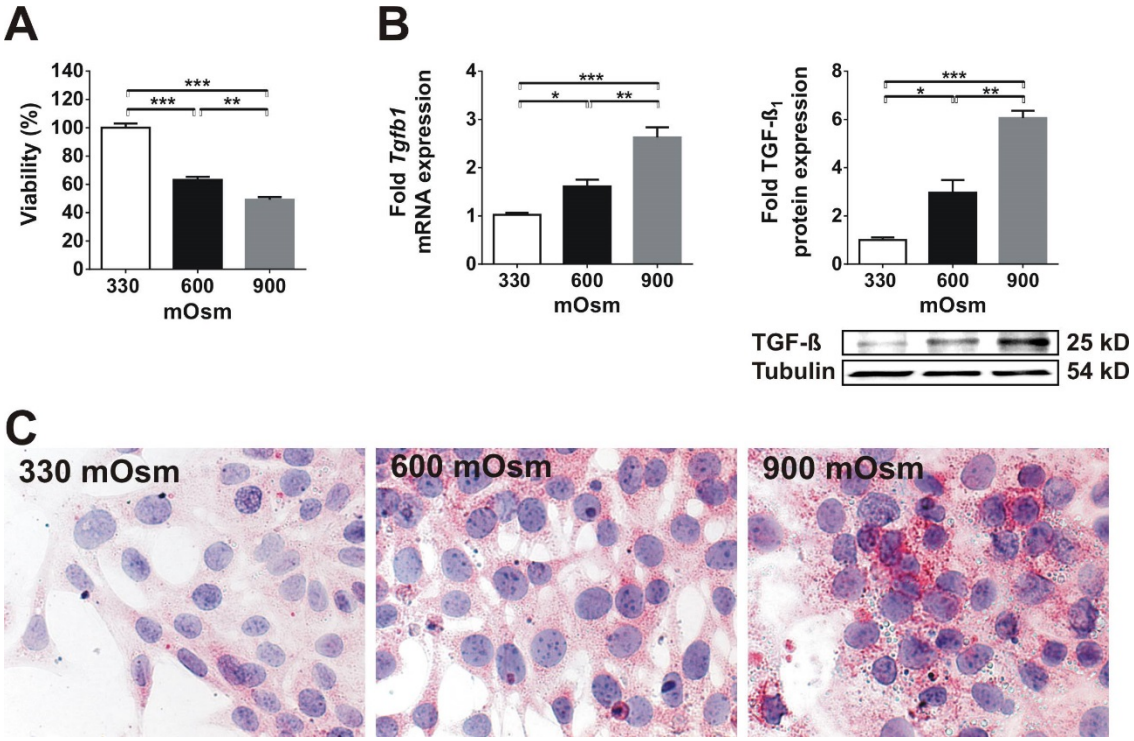

Figure 26. Effect of chronic increase in medium osmolarity on viability and TGF-ß expression of IMCD cells. (A) Chronic hyperosmolarity significantly reduced the viability of IMCD cells (n=8/group). (B) The expression of TGF-ß, however, increased dramatically both at mRNA and protein level (n=4/group). (C) Accordingly, immunocytochemistry depicted significant TGF-ß staining at 600 mOsm and even stronger staining at 900 mOsm (n=3/group). Data are presented as mean ± SEM. * $p<0.05$, ** $p<0.01$, *** $p<0.001$ (one-way ANOVA with Tukey's post-hoc test).

4.10. Increased osmolarity induces the expression of profibrotic genes in IMCD cells

As TGF-ß is one of the key growth factors that participate in the pathomechanism of fibrosis, we investigated whether its increased expression due to hyperosmolarity could contribute to fibrotic gene expression in vitro. Surprisingly, the progressive increase in osmotic concentration led to a gradual 2-fold increase in early growth response factor-1 (Egr-1) expression, accompanied by mild and late overexpression of collagen-3 but marked and early overexpression of collagen-4 (Figure 27A). The mRNA expression of Egr-1 correlated well to TGF-ß ($p<0.0001$, Figure 27B) but Egr-1 also correlated significantly to both type III and type IV collagen expressions, which indicates that hyperosmolarity might induce extracellular matrix overproduction via activation of Egr-1. The members of AP-1 transcription factor, c-Fos and c-Jun were significantly upregulated at sustained hyperosmolarity reaching 900 mOsm, but remained unchanged at 600 mOsm (Figure 27C).

4.11. TGF-ß induces Egr-1 and collagen-IV production in IMCD cells

In order to elucidate whether the overexpression of profibrotic genes in IMCD cells under hyperosmolar environment are mainly a result of increased TGF-ß, we investigated the effect of direct TGF-ß administration on IMCD cells in normal osmolarity. TGF-ß treatment (10 ng/ml) of IMCD cells resulted in 2-fold increased Egr-1 mRNA expression (Figure 28A) accompanied by only mild, 30% increase in type IV collagen expression (Figure 28C). Surprisingly, type III collagen expression of TGF-ß treated cells was similar to non-treated controls (Figure 28B). This experiment shows that even a mild hyperosmolarity of 600 mOsm exerts stronger effect on IMCD gene expression as compared to the potent profibrotic TGF-ß.

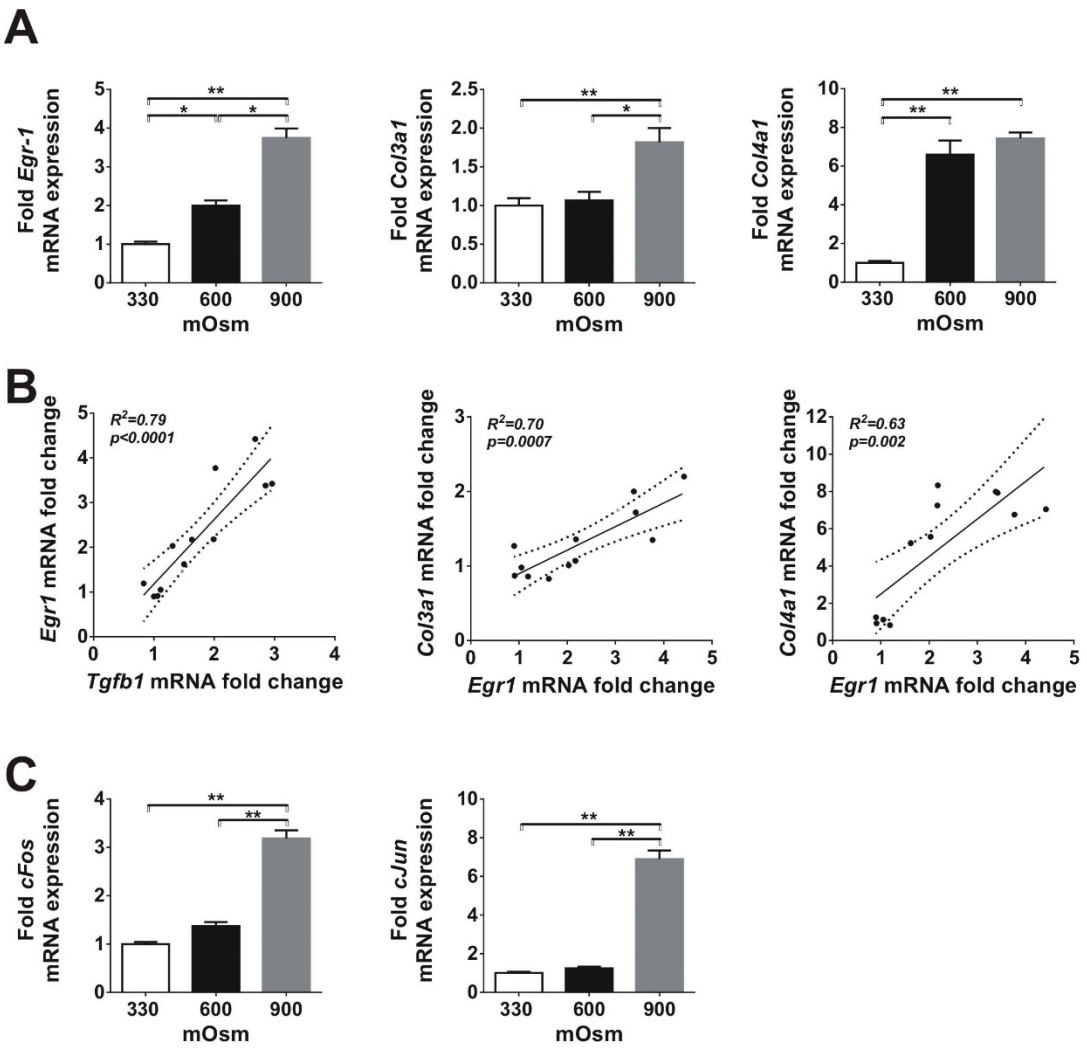

Figure 27. Effect of chronic hyperosmolarity on the expression of profibrotic genes and transcription factors in IMCD cells. (A) The progressive increase of medium osmolarity induced overexpression of the Egr-1 mRNA. Mild type III collagen upregulation was induced only by 900 mOsm, dramatic (6-fold) type IV collagen overexpression was observed at medium osmolarity of 600 mOsm. (B) Egr-1 and TGF-ß mRNA expressions showed the strongest correlation. Both type III and type IV collagen expressions correlated well to the expression of the profibrotic Egr-1. (C) Components of the transcription factor AP-1, cFos and cJun, were strongly overexpressed only at high osmolar concentration of 900 mOsm. Data are presented as mean ± SEM, n=4/group. * $p<0.05$, ** $p<0.01$ (Kruskal-Wallis test with Dunn's post-hoc test).

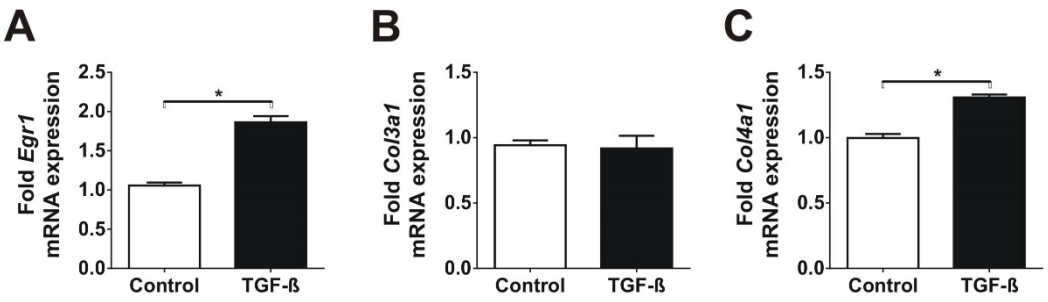

Figure 28. Effect of TGF-ß administration on IMCD cells under normal osmotic concentration. TGF-ß administration for 48h significantly upregulated Egr-1 mRNA expression by 2-fold (A) but had no effect on type III collagen expression (B). As compared to the effects of increased osmotic concentration, TGF-ß administration induced only a mild type IV collagen overexpression (C). Data are presented as mean ± SEM, n=3/group. * $p<0.05$ (Mann-Whitney test)

5. DISCUSSION

5.1. Oxygen-glucose deprivation induces cell death via various mechanisms in LLC-PK renal proximal tubule cells

Severe depletion of ATP occurs in the tubular cells as a result of hypoperfusion in acute renal injury and it is assumed to play a central role in the pathogenesis of renal injury (87). The depletion of ATP in the tubular cells may induce cell death via several way such as apoptosis, necroptosis and autophagy simultaneously (88). Historically, all these cell death processes were called necrosis in the kidney tubules and led to the nomenclature of acute tubular necrosis (ATN). However, the nomenclature of tubular necrosis might be misleading, although ATN labels a severe tubular injury that is not fully reversible and certainly involves energy depletion and tubular cell death (89-91).

In our experiments, we established a cell culture model of acute renal injury that shares several common features with the human disease. We deprived proximal tubular cells, the primary targets of ATN, of both oxygen and glucose (OGD) for an extended period to mimic the ischemic origin of acute tubular necrosis and modeled reperfusion by providing glucose and oxygen back to the cells (Figure 15). Our purpose was to induce a sublethal injury to the cells during the reperfusion phase following OGD, in order to resemble the in vivo ischemic tissue damage. Only the LLC-PK cells showed reduced viability and significant damage during the reperfusion, therefore we chose LLC-PK cells as a suitable model of the in vivo reperfusion injury. OGD induced a gradual decrease in viability in our cellular model of ATN. The loss of viable cells was proportional to the exposure length, whereas neither oxygen deprivation nor glucose deprivation alone induced a significant reduction in viability over the same period. This shows that the tubular cells possess energy reserve that can be utilized in case of hypoperfusion. Thus, the cells can switch to solely anaerobic metabolism and produce sufficient ATP to survive and maintain the major cellular functions without any oxygen supply for a relatively long period.

The severe decrease of renal blood flow stops the oxygen and glucose supply and simultaneously reduces the filtrate production and functional needs of the tubular cells, reducing the ATP consuming transfer processes and better preserving the cellular energy reserve. We found that a severe reduction of the cellular ATP content was

detectable after the OGD that was associated with the loss of the barrier function of the monolayer and the inability of the cells to maintain the energy consuming transports. The cellular LDH release did not increase significantly during OGD, showing that the cells, though dysfunctional, were still viable. In fact, both the cellular ATP content and the transport and barrier functions were mostly reverted when measured after a 24 hour-long recovery period that allowed resupply of oxygen and glucose to the cells, while there was a significant increase in the LDH release during this period (Figure 11). Glucose deprivation alone also slightly reduced the cellular ATP content that was recoverable and had no impact on the measured cellular functions or viability (Figure 23). Interestingly, urinary LDH concentration increases relatively late in acute kidney injury (AKI) patients. Consistent with the clinical findings, OGD induced a cellular dysfunction in tubular cells, but increased LDH release and definitive cell death occurred only during the recovery period following the OGD.

Pharmacological inhibition of caspase activity exerted a partial protection against the OGD induced viability reduction either applied prior to or following the OGD, whereas neither the poly(ADP-ribose)polymerase (PARP) inhibitor PJ34, nor the necroptosis inhibitor necrostatin possessed any protective effect (Figure 12). Caspase activation is well documented in renal ischemia, and caspase inhibition possesses a protective effect *in vivo* (92-95). We detected a transient caspase activation after the OGD period that peaked between 3-8 hours following the OGD and was over by 24 hours. Active caspases stop various high energy requiring enzymatic processes by proteolytic cleavage of key enzymes, thus favor the energy preservation for the apoptotic process within the cells. This includes the cleavage of the DNA repair enzyme PARP that is widely associated with necrotic cell death. In our model the appearance of the 89 kDa PARP fragment, that is associated with caspase mediated cleavage (96), strongly followed the pattern of caspase activation detected by Western blotting using an active caspase-3 specific antibody and a fluorescent substrate based activity assay (Figure 13). Mitochondrial dysfunction, depolarization and leakage (damage) are observed in ATN (97-100) and can be the initiator of caspase activation. We also observed mitochondrial dysfunction in tubular cells after the OGD characterized by the loss of mitochondrial potential, severe reduction of oxygen consumption and ATP production (Figure 19, 14). Thus, caspase activation and apoptosis are implicated in cell

death in this model, albeit inhibition of caspase activity possesses a relatively minor benefit in our model system. On the other hand, several proteases were also recognized as key contributors to cellular damage in ischemic renal injury, as the inhibition of these proteases or proteasomes confer protection against the renal damage (101-103). The proteases that are implicated include calpain (104, 105), cathepsin (106, 107) and granzyme B (108-111), since inhibition of these proteases ameliorate renal ischemia-reperfusion injury. Interestingly, these proteases all cleave PARP but at various recognition sites and generate various fragments that lack the ADP-ribose polymerase function of full length PARP. While caspase cleavage generates 89 and 21 kDa fragments, granzyme B produces a 64 kDa, cathepsin-b creates a 50 kDa and calpain generates 70 and 40 kDa fragments, leaving a "fingerprint" behind (112-117). The presence of PARP fragments in our model strongly suggests activation of calpain, cathepsin and granzyme B during the reoxygenation period. While cathepsin specific fragments are present already at the beginning of the reoxygenation phase, calpain and granzyme B activity appear in samples taken 1 hour later. All of these proteolytic activities peak after 3 hours of reoxygenation, similar to the caspase activity and by 24 hours only the calpain activity associated fragment is detectable in our model (Figure 14). Thus the beneficial effect of protease inhibition may seem controversial, as the activation of these proteases degrade PARP and prevent the PARP mediated energy depletion, representing a favorable profile in ischemia-reperfusion injury.

PARP inhibition, which is also associated with the inhibition of necrosis in various diseases (118), was found to be beneficial in renal ischemia-reperfusion and radiocontrast injury models (35, 119, 120), but lacked any cytoprotective function in our model. The cytoprotection by PARP inhibition is primarily associated with the prevention of the rapid depletion of the cellular NAD^+ and ATP pools by PARP overactivation in response to (mitochondrial) reactive oxygen species (ROS) mediated DNA damage. We detected a gradual decrease in the amount of full-length PARP-1 during the reoxygenation period in our model. One hour following the OGD only half the amount of functional PARP-1 was present in the cells and by 8 hours the functional PARP-1 completely disappeared (Figure 14). The complete absence of PARP-1 might be attributed to the lack of novel PARP protein synthesis apart from the protease-mediated degradation. The loss of the mitochondrial membrane potential, the

suppression of mitochondrial oxygen consumption lead to low cellular NAD^+ and ATP levels and low level of mitochondrial oxidant production immediately after the OGD in our model. These processes might be accounted for the inefficacy of the PARP inhibitor PJ34 in our model in the early phase of the injury, while the lack of functional PARP is the major cause during the later phase.

Necroptosis is a distinct form of cell death, and the blockade of necroptosis is protective against hypoxic or ischemia-reperfusion injury. The inhibition of necroptosis by necrostatin did not possess a cytoprotective potential in our model (Figure 12), but it is plausible that any protective effect of necrostatin (and also PARP inhibition) is hindered by the fact that many parallel pathways are involved in the ischemia reperfusion injury.

During ischemia, a gradual acidification and a rapid increase in the pCO_2 occur in the kidney simultaneously with the development of hypoxia and the decrease of nutrients (120, 121). The major cause of hypercapnia might be the continuing tricarboxylic acid cycle. CO_2 can penetrate the cellular membranes and rapidly induce a drop in both intra- and extracellular pH, depleting the buffering capacity of the renal bicarbonate. During AKI, energy depletion and the loss of apical membrane transporters are responsible for the sustained acidosis and the bicarbonate reabsorption deficiency. The role of the acidification in renal failure is still controversial: early studies confirmed the protective function of acidosis (122), while bicarbonate treatment prevents metabolic acidosis. However, the evidence showing benefit of bicarbonate based fluids over saline in the prevention of AKI is limited (123). We also tested the effect of acidic environment via the application of 18% CO_2 in the gas mixture used to induce hypoxia (124) and found only little difference in cell survival in our model. As early correction of metabolic acidosis by bicarbonate supplementation is the currently accepted therapeutic approach, we performed our experiments using 5% CO_2 containing gas mixtures and culture medium containing 4.4 mM sodium bicarbonate to maintain stable pH and bicarbonate supply throughout the experiments.

5.2. Cell-based screening identifies adenosine as the most potent cytoprotective agent in OGD injury in LLC-PK cells

We screened a library of biologically active compounds for cytoprotective action in our cellular model of ATN. In the screens, we evaluated cell viability following the 24 hours of reoxygenation and glucose supplementation period in order to allow better discrimination of reversible dysfuntion and definitive cell death, and to exclude those effects that only attain a transient functional gain. We employed two distinct strategies in our approach. First, we simulated the usual clinical settings of the ischemic ATN by performing the OGD and then normalizing the oxygen level and the glucose concentration when we applied the compounds simultaneously following the OGD (post-OGD screen). This approach simulated the situation when the therapeutics reach the renal parenchyma only if after restored (or partially restored) renal blood flow. Second, we also used a model of ATN prevention by pre-treating the cells with the compounds immediately before the onset of the OGD (pre-OGD screen). This experimental setup resemble the preventive approach when hypoperfusion (or a nephrotoxic agent) increase the risk of renal injury but the drug delivery to the renal tissue is still possible by systemic application via the renal circulation (Figure 15). In our model, we screened the Sigma LOPAC library of compounds comprising of various pharmacological activators and inhibitors. In the post-OGD compound treatment screen the highest detected viability increase was around 15% for selected compounds, while the majority of the drugs did not possess any protective effect. On the other hand, in the pre-OGD treatment some of the compounds increased the viability by 40%, in good agreement with the general idea that it is easier to prevent the cellular injury than to attain complete recovery of the severely injured dysfunctional cells (Figure 16). Interestingly, those compounds that exerted cytoprotection in one setting were without effect in the other screen. The only notably exception was the purine nucleoside adenosine that showed the highest potency in the pre-treatment screen and was between the most protective compounds in the post-treatment assay (see Table 1). Disulfiram, inhibitor of acetaldehyde metabolism, was shown previously to exert protective effect against hypoxic injury (125-127). It interferes with xanthine oxidoreductase and possibly inhibits the endogenous purine breakdown, increases adenosine concentration and prevents the ischemia-induced depletion of the cellular adenine

nucleotide/nucleoside pool. Xanthine oxidoreductase represents an interconvertible enzyme that is mainly present in the cells as xanthine dehydrogenase and transfers electrons to NAD^+, however it is also converted to the more stable xanthine oxidase during hypoxia (128, 129). The NAD^+ depletion and the accumulation of hypoxanthine may also block the xanthine dehydrogenase to some extent, but the lack of oxygen certainly inhibits xanthine oxidase during hypoxia. Thus, the rapid conversion of the enzyme to xanthine oxidase induced by disulfiram protects the purine nucleoside pool from degradation. However, the resupply of oxygen and the accumulation of purine nucleosides reactivate xanthine oxidase and results in excessive reactive oxygen species production during the reoxygenation (130). In accordance with the above activities, disulfiram failed to exert any protective effect when applied after the OGD and lacked a potentiating effect when used in combination with exogenous adenosine.

Riluzole was protective in our pre-treatment screen. It increases the intracellular calcium level and trigger the unfold protein response, a mechanism that can exert some protective effect in renal ischemia-reperfusion injury (131-134).

In the post-treatment assay, among the most potent compounds next to adenosine there are some dopaminergic compounds (allylnorapomorphine, acethyldopamine) and aspartic acid. The dopaminergic compounds are also associated with renoprotective function, though this effect is mediated via their action on the renal vasculature *in vivo*, thus in this model a more probable explanation for their cytoprotective action is another mechanism similar to what we previously identified in an oxidant induced injury model on cardiomyoblasts (135). The amino acid aspartate exerts protection against hypoxia-reoxygenation injury by preserving the anerobic part of the mitochondrial ATP production. Aspartate, maleate and α-ketoglutarate are transferred through the mitochondrial inner membrane and metabolized via the citric acid cycle and respiratory complex I (136-139). Succinate, which is utilized downstream to the above molecules, is less effective during hypoxia, but also supports ATP production during the reoxygenation phase. Interestingly, maleate rather depletes the ATP and GSH content of proximal tubules and induces nephrotoxicity *in vivo* (140).

Adenosine and its metabolite inosine play a similar protective role in ischemia-reperfusion injury and inflammatory diseases in many tissues (86, 141), thus we also tested the effect of inosine on the hypoxic injury of LLC-PK cells. Both adenosine and

inosine pretreatment increased the viability of the cells in a dose-response manner with similar potency. Their cytoprotective effect was detectable from 10 µM and increased up to 1 mM, reaching complete protection against a severe OGD induced injury that caused more than 80% reduction in the cell viability, and similar decrease in the LDH release (Figure 17). In this respect, the cytoprotective potential of adenosine (and inosine) was mostly comparable to equal amount of glucose and was superior in the 30-100 µM concentration range. The cytoprotective effect of these purine nucleosides was also associated with a significant reduction in the OGD induced caspase activation, and in the partial preservation of the full length PARP (Figure 20). This scenario strongly suggested that the adenosine induced blockade of caspase activation prevented the apoptotic cell death and also reduced caspase mediated PARP cleavage. However, both the caspase inhibition and the protection of PARP were incomplete, still adenosine exerted a near complete restoration of the viability. Also, the caspase inhibitor Z-VAD-FMK increased the viability by only approximately 10% in this model, suggesting that adenosine's protective action is not mediated merely via the caspase inhibition. Similarly, adenosine was found to block autophagy in the liver (142, 143), exert protection in glial cell injury (144, 145), and the protective function of inosine in experimental renal injury was also described but the mechanism of action remained undiscovered (146-150).

Based on the protective action of adenosine in the pre- and post-OGD screens we also searched for compounds that potentiate its action if added simultaneously, prior to the OGD or applied later during the reoxygenation. Many of the protective compounds similarly enhanced the viability either added prior to or following the OGD. Adenosine preserves various functions of the cells after OGD and provides the cells with large amount of xanthine load that may promote ROS production by xanthine oxidoreductase. This enzyme is largely transformed to xanthine oxidase by hypoxia; therefore, it uses oxygen as electron acceptor leading to superoxide generation. The superoxide may react with NO and form peroxynitrite a highly toxic, short-lived molecule. The oxidative and nitrosative damage caused by superoxide and peroxynitrite, in particular DNA strand breaks activate PARP during the reoxygenation or reperfusion (151). Adenosine reduces the OGD-induced caspase activation and preserves functional PARP protein, thus it is not surprising that PARP inhibition confers an additional

benefit. In addition, compounds that reduce NO synthesis either by directly inhibiting NOS or by preventing the nuclear factor-κB mediated NOS expression showed similar effect.

L-aspartic acid represents the only compound that got into the “top five” in both post-hypoxia screens that clearly tells that the protective action of aspartate works in a parallel fashion to the adenosine-mediated viability increase. Aspartate, used for the proton transfer, feeds the respiratory chain and supports the energy production within the mitochondria. This non-overlapping function suggests that adenosine acts via different pathways and independently from the mitochondrial respiration.

These examples of protective pathways may also add to the cytoprotective action of adenosine and inosine in certain cases, however, the benefit of using such compounds in combination with the purine nucleosides over using higher concentration of the purines is questionable in the current model, as the purines can exert complete cytoprotection within a well tolerable concentration range.

5.3. Adenosine exerts cytoprotection via ATP replenishment in renal proximal tubule cells

Adenosine, inosine and hypoxanthine are postulated to reach high levels locally from endogenous sources in hypoxic tissues. Depending on the species and the length of the ischemia, 3-10 fold increase occurs in the interstitial levels of both adenosine and inosine, reaching the low micromolar range (152-158), but their level rapidly decreases after the ischemia as their urinary excretion peaks early during the post-ischemic reperfusion period (154, 155). The protective effect of adenosine and inosine is well documented in *in vivo* models of ATN. Inosine (146, 148-150), endogenous adenosine and selective A1, A2a and A2b adenosine receptor agonists (159-163) all ameliorate renal ischemic injury, while their protective action is inhibited by their respective receptor antagonists (159, 161, 164). LLC-PK cells express adenosine A1 and A2 receptors. The majority of the A1 receptors are localized to the basolateral membrane, whereas the A2 receptors are present in greater quantity on the apical membrane (165), similar to the distribution that was seen in freshly isolated proximal tubules that also express A3 receptors, mostly present on the apical membrane (166). Interestingly, none

of the adenosine receptor antagonists blocked the protective action of inosine and adenosine (Figure 21). Thus, the protection exerted by adenosine and inosine in our model was independent of the adenosine cell surface receptors, suggesting an intracellular mechanism or the indirect action via the P2 type purinergic receptors.

The P2 purinergic receptors have been implicated in the protective role of exogenous ATP in renal ischemia (167, 168). Exogenous ATP treatment enhances both the recovery of the tissue ATP content, prevents the morphological changes (tubular swelling and necrosis) and improves renal function (as measured by the inulin clearance) after renal ischemia (169-172). LLC-PK cells also express functional P2 receptors (173). Adenosine, unlike ADP and ATP, has a negligible effect on P2 purinergic receptors in the micromolar range; however, it may increase the concentration of AMP and ADP and thus exert an indirect action on P2 receptors. Though, the direct P2 purinergic agonists (UDP, methylthio-ATP, 2-chloro-ATP) did not possess a cytoprotective potential in our screens, thus it is unlikely that this mechanism plays a role in the adenosine and inosine mediated cytoprotection in our model.

Cells take up adenosine and inosine via nucleoside transporters that are present on both the apical and basolateral membrane of the proximal tubular epithelial cells. Nucleoside transporters are classified as equilibrative nucleoside transporters (ENT) that represent sodium-independent diffusion limited channels and concentrative nucleoside transporters (CNT) that are sodium dependent symporters (174-176). The sodium dependent CNTs are present in the brush border on the apical membrane of the cells and the ENTs are mainly on the basolateral membrane in the proximal tubules, thus supporting the tubular reabsorption and vectoral transfer of nucleosides (177, 178) that was also demonstrated for adenosine on human proximal tubule cells (179). The localization of the transporters is very similar on cultured LLC-PK cells: the CNT transporters are mainly localized to the apical membrane (180) and the ENT transporters are present mainly on the basolateral membranes (181). ENT1 and CNT3 are the two major isoforms of nucleoside transporters on human proximal tubular epithelium in vivo (182), and both of them are present in the apical membrane. A nucleoside transport system was also described in the LLC-PK cells that possessed a sodium dependent component sensitive to papaverine and a sodium independent component that is

inhibited by papaverine or adenine (183). In our model, adenosine and inosine exerted cytoprotection in a concentration dependent manner, with increased cell survival up to 1 mM adenosine or inosine, whereas 30 μM papaverine completely abolished the cytoprotective effect of adenosine in our screens. These data suggest that the cellular uptake of adenosine and inosine may also occur via the papaverine sensitive nucleoside transporters in the renal proximal tubule cells.

Adenosine deaminase (ADA) metabolizes adenosine to inosine. ADA and adenosine deaminase binding or complexing protein, a membrane bound protein that specifically binds ADA, are present in the proximal tubules in the brush border of the cells (184). The binding protein and ADA, as other brush border proteins, may detach from the proximal tubules and excreted in the urine during ATN, thus might be used as early urinary markers (109, 185). The similar efficacy of inosine and adenosine suggested that inosine is the active metabolite that exerts cytoprotection in this model and adenosine is merely a pre-drug converted to inosine by ADA. In fact, the pharmacological blockade of ADA with EHNA abolished most of the cytoprotective effects of adenosine, whereas EHNA had no effect on the protective potential of inosine or glucose (Figure 22). Inosine can be utilized to generate ATP in an anaerobic fashion via the pentose phosphate pathway by its further metabolization to ribose-phosphate. In our model, adenosine and inosine increased the viability comparable to equimolar amount of glucose, and the adenosine induced viability increase even surpassed the effect of glucose in the 30-100 μM range (Figure 17), thus it is conceivable that the utilization of adenosine (and inosine) may be favorable even to the glycolytic glucose utilization under severe long-term ischemia or hypoxia. In contrast to glucose phosphorylation by hexokinase that requires ATP, the conversion of inosine to ribose-phosphate (and hypoxanthine) does not need ATP but inorganic phosphate. LLC-PK cells uptake glucose by either the sodium-coupled glucose transporter (SGLT) or the sodium-independent facilitated glucose transporter (GLUT) (186, 187). The GLUT transporter is localized mainly to the basolateral membrane, while the SGLT is present on the apical membrane that reflects their physiological function: SGLT is involved in the glucose reabsorption from the tubule lumen and GLUT is implicated in the glucose uptake from the circulation (188). Only one isoform of each (SGLT1 and GLUT1) was identified in this cell line and their expression is shown to be regulated by the glucose

concentration: exposure to high glucose downregulates both transporters, complete deprivation or low levels of glucose upregulates GLUT1 while SGLT expression is highest between 5-10 mM glucose and it almost completely disappears after glucose deprivation (186). The sodium independent transport is also shown to be upregulated after glucose deprivation (188), showing that the GLUT mediated transport is dominant in glucose deprivation. Thus both glucose and the purine nucleoside uptake are partly connected to sodium transport that necessitates the active removal of sodium from the cell via the basolateral sodium-potassium ATPase. The sodium-potassium exchanger works with a 3:2 (or as low as 3:0) sodium:potassium stoichiometry per ATP hydrolyzed (189). Thus, the glucose utilization via glycolysis yields 2 ATP molecules and 2NADH and H^+ per glucose, if sodium transport is not calculated, while adenosine or inosine may yield 3 ATP molecules (10/3 ATP produced per ribose-phosphate minus 1/3 ATP required for transport at 1:1 sodium:nucleoside transfer ratio). Since the produced NADH and H^+ cannot be converted to ATP without oxygen, NADH generation can be detrimental in hypoxia if it completely exhausts the cellular NAD pool. In fact, adenosine or inosine supplementation during the OGD completely prevented the reduction of proton production, measured after we resupplied the cells with glucose and oxygen. This reflects an intact glycolysis that requires NAD to proceed, while we measured severe proton reduction in the OGD group. Furthermore, the cellular ATP content was higher after the hypoxia in the adenosine and inosine pretreated cells than in the cells that received equimolar amount of glucose pretreatment (Figure 23), supporting the higher ATP generating potential of these nucleosides.

The incomplete blockade of the adenosine-mediated cytoprotection by ADA inhibition strongly suggested the existence of other pathways participating in the cytoprotective action of adenosine and inosine. As adenosine can also be converted to adenosine monophosphate (AMP) by adenosine kinase (AK) that uses ATP to phosphorylate adenosine and generates ADP, we tested whether AK inhibition destroys the protective effect of adenosine. AK is highly expressed in the kidney (190) and it is present in the proximal tubule cells in the brush border vesicles (191). AK inhibition by ABT 702 significantly reduced the viability increase induced by adenosine, confirming the action of AK in the adenosine-mediated cytoprotection. The inhibition of AK reduced the protective effect of inosine as well, but had only negligible effect on the

glucose-mediated protection. AK inhibition reduced the protective effect of adenosine with a similar potency to that of ADA inhibition and had comparable effect on the inosine-mediated cytoprotection. However, adenosine and inosine retained some of their protective action in the presence of the AK inhibitor ABT 702 (Figure 22). AK also possesses other enzymatic function: it can mediate phosphotransfer between various nucleosides, thus can rapidly exchange GMP, IMP and dAMP to AMP in the presence of adenosine (191), explaining the similar effect of AK inhibition on adenosine and inosine in our model. This mechanism allows interconverting the various nucleosides according to the actual requirements, however, with the limitation of their availability and their near equal ratio within the cell. Similar to adenosine, guanosine exerts protection in renal ischemia (192) and increases GTP and to a lesser extent ATP levels, which suggest the interconversion of these nucleosides during renal ischemic injury. Similar to adenosine, guanosine was shown to exert protection in renal ischemia (193) and to increase GTP and to a lesser extent ATP levels, which also suggest the interconversion of these nucleosides during renal ischemic injury. We also tested the effect of nucleobases and various nucleosides, and found that none of the nucleobases (that lack the ribose-phosphate moiety) possessed a cytoprotective effect and the viability was only increased significantly by purine nucleosides (Figure 19). The inefficacy of pyrimidine nucleosides may be explained by higher affinity of the transporters present on the cells for purine nucleosides

The combined blockade of AK and ADA completely abolished the protective effect of both adenosine and inosine, which clearly underlines the coordinated actions of these enzymes in the protective function of inosine and adenosine (Figure 22). While the metabolism of these nucleosides via the pentose phosphate pathway can generate ATP, this process also requires ADP as phosphate acceptor. The reduction of cellular ADP content may decrease the ATP generation, especially if the majority of ADP is further metabolized to adenosine and overall to ribose-phosphate. Thus, adenosine (or inosine) supplementation can be simultaneously utilized for dual purposes: they provide the cells with energy in the form of their sugar part and they block the breakdown of ADP (or may be used directly to produce AMP and ADP). The combined inhibition of AK and ADA even reduced the glucose mediated viability increase, which may reflect the importance of the endogenous adenosine and inosine production induced by

hypoxia. The anaerobic glucose metabolism also requires ADP that may be the limiting factor of ATP production. Thus, the endogenous adenosine can supply AMP and ADP to convert the energy in the sugar to ATP, a readily available format for most purposes. Interestingly, AK inhibition by ABT 702 also had a mild cytoprotective effect in the absence of glucose and exogenous adenosine and inosine in our screens. In this case, the very low level of sugars represents the limiting factor of energy production thus the endogenous nucleosides might be of use merely as sugars in the pentose phosphate pathway, facilitated by the blockade of the AK pathway.

The cellular ATP content diminished severely after the OGD in the proximal tubule epithelial cells in our model, reaching values below 10% of the control ATP concentration. We detected a gradual increase in the ATP content, reaching 20% of the control values after 24 hours of reoxygenation and glucose re-supplementation. The OGD induced cell death was prevented by the presence of adenosine and inosine (at 300 μM) as determined by the various viability assays following the 24 hour-long recovery period, however, the ATP content of these cells was still approximately 20% of the control cells immediately after the OGD. Adenosine or inosine pretreatment significantly increased the rate of the cellular ATP pool regeneration that restored completely by 24 hours, while the presence of equimolar amount of glucose during the hypoxia supported the recovery of no more than 60% of ATP content by that time. In addition, adenosine had a protective effect in our screens when applied following the OGD, being one of the most potent compounds in that screen (Figure 23). These effects strongly suggested an active role for the adenosine and inosine in the post-hypoxic recovery processes. As the adenosine receptor antagonists were ineffective on the adenosine induced viability increase as measured after the recovery period, we hypothesized the contribution of either AK or ADA in the enhanced post-hypoxic regeneration. In this respect both ADA and AK appeared to cooperate with the cellular glucose metabolism and energy production, since the post-hypoxic ADA and AK inhibition both reduced the viability of both the adenosine and inosine pretreated, and the glucose-pretreated cells. Moreover, the viability decreasing effect of ADA and AK inhibition was summative in both the nucleoside- and the glucose-pretreated groups (Figure 24). Thus, it is conceivable that AK is implicated in the interconversion of nucleosides and the regeneration of the AMP and ADP content of the cells, while ADA

is still needed in the presence of glucose to promote the usage of nucleosides and their ribose part through the pentose-phosphate pathway.

We detected a severe blockade of the mitochondrial respiration after the OGD, and a near complete loss of the mitochondrial potential (reserve capacity) (Figure 25). The adenosine treated cells showed comparable level of anaerobic metabolism (proton production) to the control cells after OGD, but significantly reduced mitochondrial basal respiration and an even greater decrease in the mitochondrial reserve capacity. Cells undergoing OGD without adenosine pretreatment had severely damaged aerobic and anaerobic metabolism, and showed very little improvement during the recovery period in spite of the presence of glucose and oxygen. This is in agreement with the impaired ATP regeneration in these cells. In the adenosine-pretreated cells, the mitochondrial respiration increased steadily during the recovery period and the basal mitochondrial respiration of the cells reached 90% of the controls by 24 hours. In contrast, the mitochondrial potential, though also increased, remained approximately 30% lower than that of the controls. These data support the significance of the anaerobic metabolism in the cells after an extensive period of hypoxia. Thus, lactate, though widely used in intensive care, is an inferior energy source for the kidney after ischemia, as it requires mitochondrial metabolism to produce ATP. It should be noted, however, that the tissue content of nucleosides rapidly decrease after hypoxia in the kidney. These molecules are also excreted in the urine (152, 153, 155, 157, 158), if they are not taken up by the cells from the glomerular filtrate. The loss of the tubular barrier, cell shedding and the loss of the cellular polarity may destine the cells to perform the transport processes excessively, as the vectorial transport of many compounds are inefficient since they can re-enter the tubule lumen from the interstitial space via the intercellular leakage. Additionally, the dislocation of the transporters may induce reverse transport processes that counteract the physiological transfer direction and reduce the overall efficiency. These processes may further enhance the cellular ATP depletion after the hypoxia and contribute to cellular injury. ATN is characterized by detachment of the brush border with many of transporters in the apical membrane (194-196). This certainly reduces the ATP usage via the decrease in the transport processes, but may also lead to the loss of the brush border enzymes ADA and AK. Therefore, the reperfusion not only reduces the levels of nucleosides that possess a beneficial role in

the post-hypoxic regeneration, but the proximal tubules may lose their transport system required for extracellular nucleoside uptake and the enzymes necessary for conversion of nucleosides to ATP. These all advise for an early purine nucleoside therapy in ATN.

5.4. Sustained hyperosmolarity in the renal medulla might contribute to fibrosis via overexpression of profibrotic transcription factors

Our study on inner medullary collecting duct cells shows that IMCD cells exposed to chronic, sustained hypertonicity show upregulation of profibrotic factors, including TGF-ß and the transcription factors Egr-1 and AP-1. TGF-ß has a major impact on kidney fibrosis (60, 61); however, less is known about its role in tubular function depsite TGF-ß is present in the inner medulla. TGF-ß not only inhibits sodium transport by the inner medullary collecting duct (IMCD) cells (64) but it can induce the trascription of several genes, including collagens and the transcription factor Egr-1 (early growth response factor-1) which has been associated with upregulation of extracellular matrix production (197-199). As renal medullary cells are exposed to fluctuating but sustained hypertonicity (200, 201), we postulated that osmotic concentration might regulate TGF-ß and Egr-1 expression of IMCD cells. Acute hyperosmolar conditions lead to increased TGF-ß activity of rat kidney fibrobast cells *in vitro*, without affecting mRNA or protein expression (57). Our slightly different results could be explained by the distinct cell type (IMCD vs fibroblast) and hyperosmolar conditions (chronic vs acute) used.

Egr-1 overexpression of IMCD cells *in vitro* induced by acute changes in osmolarity has been previously observed, which implicates an important role of Egr-1 in cellular responses against osmolar stress. Short term (10 or 30 minutes) hyperosmotic urea treatment has been reported to upregulate Egr-1 in IMCD cells (72-74). On the other hand, acute hypotonic stress of IMCD cells for 6 hours also increased Egr-1 expression (202), Egr-1 is able to induce TGF-ß expression (68, 203) and can directly regulate the promoter of both type III and type IV collagens (68, 204). When we maintained the IMCD cells under normal osmolarity, treatment with recombinant TGF-ß increased the expression of Egr-1, as we previuosly expected, in parallel with a mild increase in type IV collagen mRNA expression. As both expression levels of Egr-1 and

type IV collagen were less marked in IMCD cells after TGF-ß treatment as compared to hyperosmolarity, and TGF-ß treatment failed to induce type III collagen expression, we postulate that the interplay between TGF-ß and Egr-1 overexpressions might be a key step promoting collagen synthesis in the renal medulla under hyperosmolar conditions.

Our *in vitro* treatment protocol tried to resemble the physiological environment of the renal medulla. We used the murine inner medullary collecting duct cell line (mIMCD-3), which has been reported to retain most of the characteristics of IMCD cells in vivo, including the ability to adapt and grow in hypertonic medium *in vitro* (205). Although medullary cells are exposed to high concentrations of both urea and NaCl, previous reports on IMCD cell culture in hyperosmolar or hypoosmolar environment used only urea as the osmotic stressor, since urea is membrane-permeant, therefore it is not considered a hypertonic stressor as compared to NaCl (201). We treated the cells with the combination of urea and NaCl for two reasons: first, we wished to model the *in vivo* milieu as IMCD cells in the renal papilla have contact with high concentration of both urea and NaCl; second, it has been reported that the combination of urea and NaCl significantly enhances IMCD cell survival as compared to urea alone at 900 mOsm (206). Additionally, our method of gradually increasing medium osmolarity for 6 days up to 900 mOsm allowed a slow accomodation of the cells to the hyperosmolar environment in contrast to previously reported acute hyperosmolar stress models, where the majority of the cells would have died within 24 hours (206, 207). Thus, we established a model where we were able to study the effects of sustained hyperosmolarity, which better resembles the *in vivo* environment.

Taken together, our *in vitro* study on IMCD cells shows that sustained hypertonicity induces the expression of TGF-ß, Egr-1 and AP-1 components in the renal medulla, facilitating the production of extracellular matrix components.

6. CONCLUSION

In a cellular model of ATN we screened a library of compounds possessing known biological function, searching for a novel function of these drugs, a renoprotective action in hypoxia. The purine nucleoside adenosine not only showed the highest cytoprotective potential in the pre-hypoxia setting, it represented the only compound in the tested collection that exerted a marked cytoprotective action both if applied after the hypoxic challenge or before the onset of the hypoxia. Inosine, the metabolite of adenosine, exerted similar protection and the viability increase these compounds achieved was comparable to the effect of equimolar glucose. The cell surface adenosine receptors that were implicated in the renoprotective action of adenosine in various *in vivo* models, did not play a part in adenosine- and inosine-mediated cytoprotection in this model. The protective action of these purine nucleosides was solely dependent of their intracellular metabolism by ADA and AK (as summarized on Figure 29). Both the ADA mediated conversion of adenosine to inosine and the AK mediated phosphorylation of adenosine or the phosphotransfer function of the enzyme were essential for the full protective effect of adenosine. These pathways complemented each other in supporting the ATP production of the cells during both the hypoxia and the following recovery period that yet again provided access to glucose and oxygen.

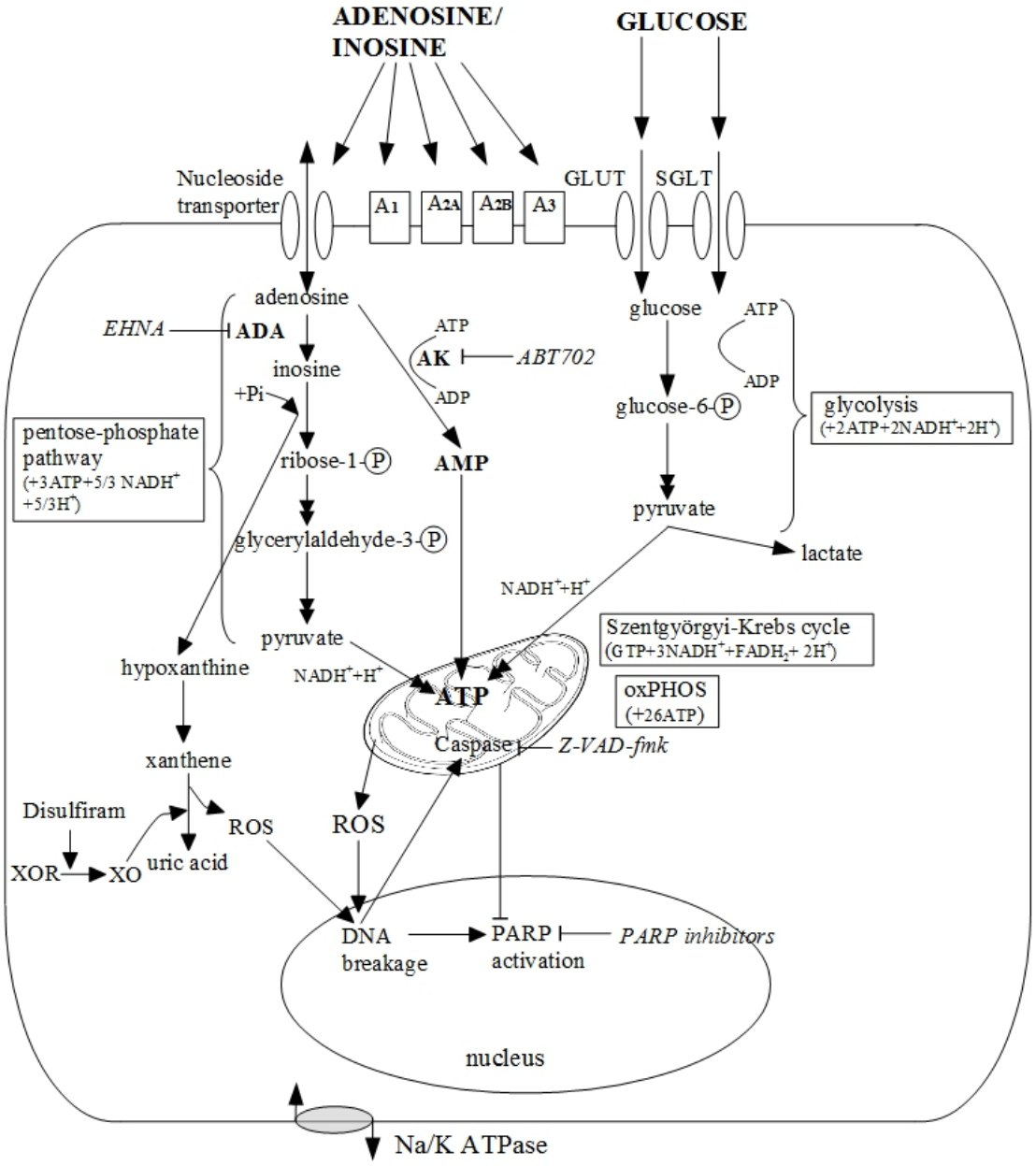

Figure 29. Possible pathway of adenosine and inosine cytoprotective effect. Scheme representing metabolic pathways for the conversion of glucose, adenosine and inosine to cells ATP/energy produce.

Surprisingly, in the proximal tubule cells these nucleosides were better sources of energy under the hypoxic condition than similar amount of glucose. Though, the ATP content of the cells also decreased in the adenosine treated cells, nucleoside supplementation accelerated the recovery of the cellular ATP pool and completely restored the cellular viability in an OGD induced injury that resulted in 80% decrease in

viability in non–treated cells. These results also underline the central role of the fluctuation of the cellular energy resources and the significance of the metabolic changes that occur in severe ischemia and give us an example how these processes may determine the cell fate in the subsequent reperfusion period. Also, the energetic basis of renal injury and the multiple downstream components involved in the tissue damage emphasize that need for novel pharmacological approaches for successful therapy in ATN. These interventions do not necessarily involve a classic agonist/antagonist or one drug-one target approach, and instead of confirming the short-term benefits of interventions rather focus on the overall outcome of the disease, and aim the better preservation and functional recovery of proximal tubules. The protective effect of direct ATP replenishment has long been discovered (169-171), though the penetration of ATP through the cell membrane is still questionable (208). However, no cell permeable alternatives or other methods were systematically searched to aim the rapid restoration of the ATP content in proximal tubule cells. Thus, the ATP restoring capacity of purine nucleosides may embody an essentially novel approach in which the control of the cellular metabolism represents the pharmacological target and a broadly functional substrate is the drug treatment. Also, the similar efficacy of other purine nucleosides and the additional benefits conferred by aspartic acid suggests that a combination therapy with various purine nucleosides and amino acids is a feasible alternative of a single nucleoside therapy that may be further supplemented with the blockade of various inhibitors of the high energy consumptive non-essential cellular pathways.

Moreover, we successfully established an *in vitro* model to study the effects of sustained hyperosmolarity on renal medullary cells, showing that chronic hyperosmolarity might facilitate interstitial fibrosis through the upregulation of profibrotic TGF-ß and the transcription factors Egr-1 and AP-1 in the inner medullary collecting duct cells.

7. SUMMARY

Acute tubular necrosis (ATN) is a mechanism of cellular dysfunction and cell death in proximal tubular cells, caused by ischemic injury, nephrotoxins or contrast dyes. As no effective therapies exist yet to treat an established acute kidney injury, it dramatically increases the mortality of hospitalized patients. Thus, there is a high clinical demand to nourish the endogenous repair processes and retard associated fibrosis.

In our experiments, we established a cell culture model of acute renal injury. We deprived proximal tubular cells of both oxygen and glucose (OGD) for an extended period to mimic the ischemic origin of acute tubular necrosis, then restored back oxygen and glucose to model reperfusion and screened a library of compounds possessing known biological function in order to search renoprotective action during and after the ischemia. The purine nucleoside adenosine had the highest cytoprotective effect both if applied before or after hypoxia. Inosine, the metabolite of adenosine, exerted similar protection. The cell surface adenosine receptors did not play a role in adenosine- and inosine-mediated cytoprotection in this model, but their protective action was dependent on their intracellular metabolism by ADA and AK. Both the ADA mediated conversion of adenosine to inosine and the AK mediated phosphorylation of adenosine or the phosphotransfer function of the enzyme were essential for the fully protective effect of adenosine. These pathways complemented each other in supporting the ATP production of the cells during both hypoxia and the following recovery period. The combination therapy with various purine nucleosides provided additional benefit with better energy preservation, and could effectively prevent injury and accelerate tissue repair during ATN.

Renal medullary cells are exposed to significant changes in osmolarity even under physiological conditions. To study its effects *in vitro*, we established a sustained hypertonicity model on inner medullary collecting duct (IMCD) cells. Our study demonstrated a hyperosmolarity dependent upregulation of early immediate genes such as profibrotic the TGF-ß and transcription factors Egr-1 and AP-1, facilitating the production of extracellular matrix components.

8. ÖSSZEFOGLALÓ

Az akut tubuláris nekrózis során a vese proximális tubulus sejtek különböző eltérő inzultust (pl. ischaemia, nefrotoxikus gyógyszerek, kontrasztanyag) követően károsodnak, ami a sejtek sérülését, majd pusztulását és a vesefunkció beszűkülését eredményezi. A kialakult akut veseelégtelenség specifikus kezelése jelenleg nem megoldott, jelentősen növelve a hospitalizált betegek mortalitását. Ezért nagy klinikai jelentőségű lenne olyan kezelést találni mely az endogén sejtgyógyulási mechanizmusokat támogatva lassítaná az asszociált fibrózist is.

Munkánk során létrehoztunk az akut tubuláris nekrózis in vitro modelljét proximális tubulus sejteken. A sejtek átmeneti oxigén és glükóz megvonása alatt illetve ezt követően vizsgáltuk különböző, ismert biológiai funkciójú molekulák lehetséges protektív hatását. A legerősebb, mind hypoxia előtti vagy utáni citoprotektív hatással egy, a természetben is előfurduló nukleozid, az adenozin rendelkezett. Modellünkben az adenozinnal analóg inozin is hasonló hatást mutatott. Az adenozin és inozin citoprotektív hatása a sejtfelszíni receptoroktól függetlenül, intracelluláris útvonalon keresztül alakult ki az adenozin kináz (AK) illetve az adenozin deamináz (ADA) révén. Az adenozinnak mind az ADA mediált átalakítása inozinná, mind az AK mediált foszforilációja illetve az enzim foszfotranszfer funkciója szükséges volt az adenosine teljes citoprotektív hatásához. Ezen útvonalak egymást kiegészítve biztosították a sejtek hypoxia alatti és utáni ATP termelését. A különféle purin nukleozidokkal történő kombinált kezelés erősebb hatása is rámutatott, hogy ezen molekulák a jobb energiaszint megtartás mellett hatékonyan csökkenthetik az ATN asszociált szöveti sérülést illetve fokozhatják a regenerációt.

A vesevelő sejtjeit élettani körülmények között is folyamatosan változó mértékű ozmotikus stressz éri, melynek főleg akut *in vitro* hatásai ismertek. A krónikus hatások *in vitro* vizsgálatára létrehoztunk egy fenntartott hipertonicitás modellt vesevelő belső gyűjtőcsatorna sejteken. Kísérleteinkben az ozmolaritás emelkedésével párhuzamosan fokozódott számos ún. “korai azonnali gén” expressziója , mint pl. a profibrotikus hatású TGF-ß és az Egr-1 valamint AP-1 transzkripciós faktorok. A krónikus hiperozmolaritás így elősegítheti az extracelluláris mátrix komponensek fokozott termelődését.

9. BIBLIOGRAPHY

1. Kumar S, Liu J, McMahon AP. (2014) Defining the acute kidney injury and repair transcriptome. Semin Nephrol, 34(4): 404-417.
2. Skarupskiene I, Balciuviene V, Ziginskiene E, Kuzminskis V, Vaiciuniene R, Bumblyte IA. (2016) Changes of etiology, incidence and outcomes of severe acute kidney injury during a 12-year period (2001-2012) in large university hospital. Nephrol Ther, 12(6): 448-453.
3. Schrier RW, Wang W, Poole B, Mitra A. (2004) Acute renal failure: definitions, diagnosis, pathogenesis, and therapy. J Clin Invest, 114(1): 5-14.
4. Kassahun WT, Schulz T, Richter O, Hauss J. (2008) Unchanged high mortality rates from acute occlusive intestinal ischemia: six year review. Langenbecks Arch Surg, 393(2): 163-171.
5. Stowe DF, Camara AK. (2009) Mitochondrial reactive oxygen species production in excitable cells: modulators of mitochondrial and cell function. Antioxid Redox Signal, 11(6): 1373-1414.
6. Snowdowne KW, Borle AB. (1985) Effects of low extracellular sodium on cytosolic ionized calcium. Na+-Ca2+ exchange as a major calcium influx pathway in kidney cells. J Biol Chem, 260(28): 14998-14507.
7. Devarajan P. (2005) Cellular and molecular derangements in acute tubular necrosis. Curr Opin Pediatr, 17(2): 193-199.
8. Paller MS, Hoidal JR, Ferris TF. (1984) Oxygen free radicals in ischemic acute renal failure in the rat. J Clin Invest, 74(4): 1156-1164.
9. Furuichi K, Wada T, Yokoyama H, Kobayashi KI. (2002) Role of Cytokines and Chemokines in Renal Ischemia-Reperfusion Injury. Drug News Perspect, 15(8): 477-482.
10. Patel NS, Chatterjee PK, Di Paola R, Mazzon E, Britti D, De Sarro A, Cuzzocrea S, Thiemermann C. (2005) Endogenous interleukin-6 enhances the renal injury, dysfunction, and inflammation caused by ischemia/reperfusion. J Pharmacol Exp Ther, 312(3): 1170-1178.
11. Donnahoo KK, Shames BD, Harken AH, Meldrum DR. (1999) Review article: the role of tumor necrosis factor in renal ischemia-reperfusion injury. J Urol, 162(1): 196-203.

12. Faubel S, Edelstein CL. (2005) Caspases as drug targets in ischemic organ injury. Curr Drug Targets Immune Endocr Metabol Disord, 5(3): 269-287.
13. McCord JM. (1985) Oxygen-derived free radicals in postischemic tissue injury. N Engl J Med, 312(3): 159-163.
14. Linas SL, Whittenburg D, Parsons PE, Repine JE. (1995) Ischemia increases neutrophil retention and worsens acute renal failure: role of oxygen metabolites and ICAM 1. Kidney Int, 48(5): 1584-1591.
15. Noiri E, Nakao A, Uchida K, Tsukahara H, Ohno M, Fujita T, Brodsky S, Goligorsky MS. (2001) Oxidative and nitrosative stress in acute renal ischemia. Am J Physiol Renal Physiol, 281(5): F948-957.
16. Li H, Zhu H, Xu CJ, Yuan J. (1998) Cleavage of BID by caspase 8 mediates the mitochondrial damage in the Fas pathway of apoptosis. Cell, 94(4): 491-501.
17. Riedl SJ, Shi Y. (2004) Molecular mechanisms of caspase regulation during apoptosis. Nat Rev Mol Cell Biol, 5(11): 897-907.
18. Tait SW, Oberst A, Quarato G, Milasta S, Haller M, Wang R, Karvela M, Ichim G, Yatim N, Albert ML, Kidd G, Wakefield R, Frase S, Krautwald S, Linkermann A, Green DR. (2013) Widespread mitochondrial depletion via mitophagy does not compromise necroptosis. Cell Rep, 5(4): 878-885.
19. Holler N, Zaru R, Micheau O, Thome M, Attinger A, Valitutti S, Bodmer JL, Schneider P, Seed B, Tschopp J. (2000) Fas triggers an alternative, caspase-8-independent cell death pathway using the kinase RIP as effector molecule. Nat Immunol, 1(6): 489-495.
20. Thapa RJ, Nogusa S, Chen P, Maki JL, Lerro A, Andrake M, Rall GF, Degterev A, Balachandran S. (2013) Interferon-induced RIP1/RIP3-mediated necrosis requires PKR and is licensed by FADD and caspases. Proc Natl Acad Sci U S A, 110(33): E3109-3118.
21. Tenev T, Bianchi K, Darding M, Broemer M, Langlais C, Wallberg F, Zachariou A, Lopez J, MacFarlane M, Cain K, Meier P. (2011) The Ripoptosome, a signaling platform that assembles in response to genotoxic stress and loss of IAPs. Mol Cell, 43(3): 432-448.
22. Kaiser WJ, Upton JW, Mocarski ES. (2013) Viral modulation of programmed necrosis. Curr Opin Virol, 3(3): 296-306.

23. Huang C, Luo Y, Zhao J, Yang F, Zhao H, Fan W, Ge P. (2013) Shikonin kills glioma cells through necroptosis mediated by RIP-1. PLoS One, 8(6): e66326.
24. Basit F, Cristofanon S, Fulda S. (2013) Obatoclax (GX15-070) triggers necroptosis by promoting the assembly of the necrosome on autophagosomal membranes. Cell Death Differ, 20(9): 1161-1173.
25. Kaczmarek A, Vandenabeele P, Krysko DV. (2013) Necroptosis: the release of damage-associated molecular patterns and its physiological relevance. Immunity, 38(2): 209-223.
26. Vanden Berghe T, Linkermann A, Jouan-Lanhouet S, Walczak H, Vandenabeele P. (2014) Regulated necrosis: the expanding network of non-apoptotic cell death pathways. Nat Rev Mol Cell Biol, 15(2): 135-147.
27. Javadov S, Kuznetsov A. (2013) Mitochondrial permeability transition and cell death: the role of cyclophilin d. Front Physiol, 4: 76.
28. Cookson BT, Brennan MA. (2001) Pro-inflammatory programmed cell death. Trends Microbiol, 9(3): 113-114.
29. Wang S, Miura M, Jung YK, Zhu H, Li E, Yuan J. (1998) Murine caspase-11, an ICE-interacting protease, is essential for the activation of ICE. Cell, 92(4): 501-509.
30. Yang JR, Yao FH, Zhang JG, Ji ZY, Li KL, Zhan J, Tong YN, Lin LR, He YN. (2014) Ischemia-reperfusion induces renal tubule pyroptosis via the CHOP-caspase-11 pathway. Am J Physiol Renal Physiol, 306(1): F75-84.
31. Ame JC, Spenlehauer C, de Murcia G. (2004) The PARP superfamily. Bioessays, 26(8): 882-893.
32. Hegedus C, Virag L. (2014) Inputs and outputs of poly(ADP-ribosyl)ation: Relevance to oxidative stress. Redox Biol, 2: 978-982.
33. Hassa PO, Hottiger MO. (2008) The diverse biological roles of mammalian PARPS, a small but powerful family of poly-ADP-ribose polymerases. Front Biosci, 13: 3046-3082.
34. Devalaraja-Narashimha K, Padanilam BJ. (2009) PARP-1 inhibits glycolysis in ischemic kidneys. J Am Soc Nephrol, 20(1): 95-103.

35. Martin DR, Lewington AJ, Hammerman MR, Padanilam BJ. (2000) Inhibition of poly(ADP-ribose) polymerase attenuates ischemic renal injury in rats. Am J Physiol Regul Integr Comp Physiol, 279(5): R1834-1840.
36. Gagne JP, Isabelle M, Lo KS, Bourassa S, Hendzel MJ, Dawson VL, Dawson TM, Poirier GG. (2008) Proteome-wide identification of poly(ADP-ribose) binding proteins and poly(ADP-ribose)-associated protein complexes. Nucleic Acids Res, 36(22): 6959-6976.
37. Wang Y, Kim NS, Haince JF, Kang HC, David KK, Andrabi SA, Poirier GG, Dawson VL, Dawson TM. (2011) Poly(ADP-ribose) (PAR) binding to apoptosis-inducing factor is critical for PAR polymerase-1-dependent cell death (parthanatos). Sci Signal, 4(167): ra20.
38. Yu SW, Wang H, Poitras MF, Coombs C, Bowers WJ, Federoff HJ, Poirier GG, Dawson TM, Dawson VL. (2002) Mediation of poly(ADP-ribose) polymerase-1-dependent cell death by apoptosis-inducing factor. Science, 297(5579): 259-263.
39. Yang WS, Stockwell BR. (2016) Ferroptosis: Death by Lipid Peroxidation. Trends Cell Biol, 26(3): 165-176.
40. Dixon Scott J, Lemberg Kathryn M, Lamprecht Michael R, Skouta R, Zaitsev Eleina M, Gleason Caroline E, Patel Darpan N, Bauer Andras J, Cantley Alexandra M, Yang Wan S, Morrison B, III, Stockwell Brent R. Ferroptosis: An Iron-Dependent Form of Nonapoptotic Cell Death. Cell, 149(5): 1060-1072.
41. Yang WS, SriRamaratnam R, Welsch ME, Shimada K, Skouta R, Viswanathan VS, Cheah JH, Clemons PA, Shamji AF, Clish CB, Brown LM, Girotti AW, Cornish VW, Schreiber SL, Stockwell BR. (2014) Regulation of ferroptotic cancer cell death by GPX4. Cell, 156(1-2): 317-331.
42. Dagher PC. (2000) Modeling ischemia in vitro: selective depletion of adenine and guanine nucleotide pools. Am J Physiol Cell Physiol, 279(4): C1270-1277.
43. Frokiaer J, Jensen FT, Djurhuus JC, Christiansen PM, Harving N, Mortensen J. (1990) The impact of unilateral ureteral obstruction on pelvic and parenchymal transit times in the pig kidney. Eur J Nucl Med, 16(4-6): 349-352.
44. Eickelberg O, Seebach F, Riordan M, Thulin G, Mann A, Reidy KH, Van Why SK, Kashgarian M, Siegel N. (2002) Functional activation of heat shock factor

and hypoxia-inducible factor in the kidney. J Am Soc Nephrol, 13(8): 2094-2101.

45. Allen CB, Schneider BK, White CW. (2001) Limitations to oxygen diffusion and equilibration in in vitro cell exposure systems in hyperoxia and hypoxia. Am J Physiol Lung Cell Mol Physiol, 281(4): L1021-1027.
46. Felder E, Jennings P, Seppi T, Pfaller W. (2002) LLC-PK(1) cells maintained in a new perfusion cell culture system exhibit an improved oxidative metabolism. Cell Physiol Biochem, 12(2-3): 153-162.
47. Gstraunthaler G, Seppi T, Pfaller W. (1999) Impact of culture conditions, culture media volumes, and glucose content on metabolic properties of renal epithelial cell cultures. Are renal cells in tissue culture hypoxic? Cell Physiol Biochem, 9(3): 150-172.
48. Xie LP, Zheng XY, Qin J, Tong YY. (2004) Amino acids protects against renal ischemia-reperfusion injury and attenuates renal endothelin-1 disorder in rats. Chin J Traumatol, 7(2): 87-90.
49. Dvoriantchikova G, Barakat DJ, Hernandez E, Shestopalov VI, Ivanov D. (2010) Liposome-delivered ATP effectively protects the retina against ischemia-reperfusion injury. Mol Vis, 16: 2882-2890.
50. Wei Q, Xiao X, Fogle P, Dong Z. (2014) Changes in metabolic profiles during acute kidney injury and recovery following ischemia/reperfusion. PLoS One, 9(9): e106647.
51. Luo J, Borgens R, Shi R. (2002) Polyethylene glycol immediately repairs neuronal membranes and inhibits free radical production after acute spinal cord injury. J Neurochem, 83(2): 471-480.
52. Maxwell P. (2003) HIF-1: an oxygen response system with special relevance to the kidney. J Am Soc Nephrol, 14(11): 2712-2722.
53. Nunn A, Linder K, Strauss HW. (1995) Nitroimidazoles and imaging hypoxia. Eur J Nucl Med, 22(3): 265-280.
54. Yonehana T, Gemba M. (1999) Ameliorative effect of adenosine on hypoxia-reoxygenation injury in LLC-PK1, a porcine kidney cell line. Jpn J Pharmacol, 80(2): 163-167.

55. Cai Q, Michea L, Andrews P, Zhang Z, Rocha G, Dmitrieva N, Burg MB. (2002) Rate of increase of osmolality determines osmotic tolerance of mouse inner medullary epithelial cells. Am J Physiol Renal Physiol, 283(4): F792-798.
56. Burg MB, Garcia-Perez A. (1992) How tonicity regulates gene expression. J Am Soc Nephrol, 3(2): 121-127.
57. Sugiura T, Yamauchi A, Kitamura H, Matusoka Y, Horio M, Imai E, Hori M. (1998) Effects of hypertonic stress on transforming growth factor-beta activity in normal rat kidney cells. Kidney Int, 53(6): 1654-1660.
58. Khan R. (2007) Examining potential therapies targeting myocardial fibrosis through the inhibition of transforming growth factor-beta 1. Cardiology, 108(4): 368-380.
59. Murray LA, Chen Q, Kramer MS, Hesson DP, Argentieri RL, Peng X, Gulati M, Homer RJ, Russell T, van Rooijen N, Elias JA, Hogaboam CM, Herzog EL. (2011) TGF-beta driven lung fibrosis is macrophage dependent and blocked by Serum amyloid P. Int J Biochem Cell Biol, 43(1): 154-162.
60. Floege J, Alpers CE, Burns MW, Pritzl P, Gordon K, Couser WG, Johnson RJ. (1992) Glomerular cells, extracellular matrix accumulation, and the development of glomerulosclerosis in the remnant kidney model. Lab Invest, 66(4): 485-497.
61. Ebihara I, Suzuki S, Nakamura T, Fukui M, Yaguchi Y, Tomino Y, Koide H. (1993) Extracellular matrix component mRNA expression in glomeruli in experimental focal glomerulosclerosis. J Am Soc Nephrol, 3(7): 1387-1397.
62. Husted RF, Matsushita K, Stokes JB. (1994) Induction of resistance to mineralocorticoid hormone in cultured inner medullary collecting duct cells by TGF-beta 1. Am J Physiol, 267(5 Pt 2): F767-775.
63. Husted RF, Sigmund RD, Stokes JB. (2000) Mechanisms of inactivation of the action of aldosterone on collecting duct by TGF-beta. Am J Physiol Renal Physiol, 278(3): F425-433.
64. Husted RF, Stokes JB. (1996) Separate regulation of Na+ and anion transport by IMCD: location, aldosterone, hypertonicity, TGF-beta 1, and cAMP. Am J Physiol, 271(2 Pt 2): F433-439.

65. Husted RF, Zhang C, Stokes JB. (1998) Concerted actions of IL-1beta inhibit Na+ absorption and stimulate anion secretion by IMCD cells. Am J Physiol, 275(6 Pt 2): F946-954.
66. Sugiura T, Yamauchi A, Kitamura H, Matsuoka Y, Horio M, Imai E, Hori M. (1999) High water intake ameliorates tubulointerstitial injury in rats with subtotal nephrectomy: possible role of TGF-beta. Kidney Int, 55(5): 1800-1810.
67. Ying WZ, Sanders PW. (1998) Dietary salt modulates renal production of transforming growth factor-beta in rats. Am J Physiol, 274(4 Pt 2): F635-641.
68. Guerquin MJ, Charvet B, Nourissat G, Havis E, Ronsin O, Bonnin MA, Ruggiu M, Olivera-Martinez I, Robert N, Lu Y, Kadler KE, Baumberger T, Doursounian L, Berenbaum F, Duprez D. (2013) Transcription factor EGR1 directs tendon differentiation and promotes tendon repair. J Clin Invest, 123(8): 3564-3576.
69. Lv ZM, Wang Q, Wan Q, Lin JG, Hu MS, Liu YX, Wang R. (2011) The role of the p38 MAPK signaling pathway in high glucose-induced epithelial-mesenchymal transition of cultured human renal tubular epithelial cells. PLoS One, 6(7): e22806.
70. Avouac J, Palumbo K, Tomcik M, Zerr P, Dees C, Horn A, Maurer B, Akhmetshina A, Beyer C, Sadowski A, Schneider H, Shiozawa S, Distler O, Schett G, Allanore Y, Distler JH. (2012) Inhibition of activator protein 1 signaling abrogates transforming growth factor beta-mediated activation of fibroblasts and prevents experimental fibrosis. Arthritis Rheum, 64(5): 1642-1652.
71. Jochum W, Passegue E, Wagner EF. (2001) AP-1 in mouse development and tumorigenesis. Oncogene, 20(19): 2401-2412.
72. Cohen DM. (1996) Urea-inducible Egr-1 transcription in renal inner medullary collecting duct (mIMCD3) cells is mediated by extracellular signal-regulated kinase activation. Proc Natl Acad Sci U S A, 93(20): 11242-11247.
73. Cohen DM, Chin WW, Gullans SR. (1994) Hyperosmotic urea increases transcription and synthesis of Egr-1 in murine inner medullary collecting duct (mIMCD3) cells. J Biol Chem, 269(41): 25865-25870.

74. Tian W, Cohen DM. (2002) Urea stress is more akin to EGF exposure than to hypertonic stress in renal medullary cells. Am J Physiol Renal Physiol, 283(3): F388-398.
75. Kotz J. (2012) Phenotypic screening, take two. SciBX.
76. Wilkinson GF, Pritchard K. (2015) In vitro screening for drug repositioning. J Biomol Screen, 20(2): 167-179.
77. Mayr LM, Fuerst P. (2008) The future of high-throughput screening. J Biomol Screen, 13(6): 443-448.
78. Meng J, Lai MT, Munshi V, Grobler J, McCauley J, Zuck P, Johnson EN, Uebele VN, Hermes JD, Adam GC. (2015) Screening of HIV-1 Protease Using a Combination of an Ultra-High-Throughput Fluorescent-Based Assay and RapidFire Mass Spectrometry. J Biomol Screen, 20(5): 606-615.
79. Sink R, Gobec S, Pecar S, Zega A. (2010) False positives in the early stages of drug discovery. Curr Med Chem, 17(34): 4231-4255.
80. Malo N, Hanley JA, Cerquozzi S, Pelletier J, Nadon R. (2006) Statistical practice in high-throughput screening data analysis. Nat Biotechnol, 24(2): 167-175.
81. Hughes JP, Rees S, Kalindjian SB, Philpott KL. (2011) Principles of early drug discovery. Br J Pharmacol, 162(6): 1239-1249.
82. Sertkaya A, Wong HH, Jessup A, Beleche T. (2016) Key cost drivers of pharmaceutical clinical trials in the United States. Clin Trials, 13(2): 117-126.
83. Modis K, Gero D, Nagy N, Szoleczky P, Toth ZD, Szabo C. (2009) Cytoprotective effects of adenosine and inosine in an in vitro model of acute tubular necrosis. Br J Pharmacol, 158(6): 1565-1578.
84. Modis K, Gero D, Stangl R, Rosero O, Szijarto A, Lotz G, Mohacsik P, Szoleczky P, Coletta C, Szabo C. (2013) Adenosine and inosine exert cytoprotective effects in an in vitro model of liver ischemia-reperfusion injury. Int J Mol Med, 31(2): 437-446.
85. Chan L LJ, Clarke J, Ross BD. Acute Renal Failure: Pathophysiology, Prevention, and Treatment. The importance of pH in acute renal failure, in Acute Renal Failure, ed. Eliahou. Libbey. London.

86. Hasko G, Linden J, Cronstein B, Pacher P. (2008) Adenosine receptors: therapeutic aspects for inflammatory and immune diseases. Nat Rev Drug Discov, 7(9): 759-770.
87. Sharfuddin AA, Molitoris BA. (2011) Pathophysiology of ischemic acute kidney injury. Nature reviews. Nephrology, 7(4): 189-200.
88. Tait SW, Ichim G, Green DR. (2014) Die another way--non-apoptotic mechanisms of cell death. J Cell Sci, 127(Pt 10): 2135-2144.
89. Liang X, Chen Y, Zhang L, Jiang F, Wang W, Ye Z, Liu S, Yu C, Shi W. (2014) Necroptosis, a novel form of caspase-independent cell death, contributes to renal epithelial cell damage in an ATP-depleted renal ischemia model. Mol Med Rep, 10(2): 719-724.
90. Ma Z, Wei Q, Dong G, Huo Y, Dong Z. (2014) DNA damage response in renal ischemia-reperfusion and ATP-depletion injury of renal tubular cells. Biochim Biophys Acta, 1842(7): 1088-1096.
91. Yang RL, Wang XT, Liu DW, Liu SB. (2014) Energy and oxygen metabolism disorder during septic acute kidney injury. Kidney Blood Press Res, 39(4): 240-251.
92. Jain S, Keys D, Ljubanovic D, Edelstein CL, Jani A. (2015) Protection Against Cold Storage-Induced Renal Tubular Cell Apoptosis. Transplantation, 99(11): 2311-2316.
93. Shi Y, Melnikov VY, Schrier RW, Edelstein CL. (2000) Downregulation of the calpain inhibitor protein calpastatin by caspases during renal ischemia-reperfusion. Am J Physiol Renal Physiol, 279(3): F509-517.
94. Jani A, Ljubanovic D, Faubel S, Kim J, Mischak R, Edelstein CL. (2004) Caspase inhibition prevents the increase in caspase-3, -2, -8 and -9 activity and apoptosis in the cold ischemic mouse kidney. Am J Transplant, 4(8): 1246-1254.
95. Chatterjee PK, Todorovic Z, Sivarajah A, Mota-Filipe H, Brown PA, Stewart KN, Cuzzocrea S, Thiemermann C. (2004) Differential effects of caspase inhibitors on the renal dysfunction and injury caused by ischemia-reperfusion of the rat kidney. Eur J Pharmacol, 503(1-3): 173-183.
96. Rheaume E, Cohen LY, Uhlmann F, Lazure C, Alam A, Hurwitz J, Sekaly RP, Denis F. (1997) The large subunit of replication factor C is a substrate for

caspase-3 in vitro and is cleaved by a caspase-3-like protease during Fas-mediated apoptosis. The EMBO journal, 16(21): 6346-6354.

97. Benitez-Bribiesca L, Gomez-Camarillo M, Castellanos-Juarez E, Mravko E, Sanchez-Suarez P. (2000) Morphologic, biochemical and molecular mitochondrial changes during reperfusion phase following brief renal ischemia. Ann N Y Acad Sci, 926: 165-179.

98. Halestrap AP. (2006) Calcium, mitochondria and reperfusion injury: a pore way to die. Biochem Soc Trans, 34(Pt 2): 232-237.

99. Arany I, Faisal A, Clark JS, Vera T, Baliga R, Nagamine Y. (2010) p66SHC-mediated mitochondrial dysfunction in renal proximal tubule cells during oxidative injury. Am J Physiol Renal Physiol, 298(5): F1214-1221.

100. Szeto HH, Liu S, Soong Y, Wu D, Darrah SF, Cheng FY, Zhao Z, Ganger M, Tow CY, Seshan SV. (2011) Mitochondria-targeted peptide accelerates ATP recovery and reduces ischemic kidney injury. J Am Soc Nephrol, 22(6): 1041-1052.

101. Takaoka M, Itoh M, Kohyama S, Shibata A, Ohkita M, Matsumura Y. (2000) Proteasome inhibition attenuates renal endothelin-1 production and the development of ischemic acute renal failure in rats. Journal of cardiovascular pharmacology, 36(5 Suppl 1): S225-227.

102. Itoh M, Takaoka M, Shibata A, Ohkita M, Matsumura Y. (2001) Preventive effect of lactacystin, a selective proteasome inhibitor, on ischemic acute renal failure in rats. The Journal of pharmacology and experimental therapeutics, 298(2): 501-507.

103. Takaoka M, Itoh M, Hayashi S, Kuro T, Matsumura Y. (1999) Proteasome participates in the pathogenesis of ischemic acute renal failure in rats. European journal of pharmacology, 384(1): 43-46.

104. Chatterjee PK, Brown PA, Cuzzocrea S, Zacharowski K, Stewart KN, Mota-Filipe H, McDonald MC, Thiemermann C. (2001) Calpain inhibitor-1 reduces renal ischemia/reperfusion injury in the rat. Kidney international, 59(6): 2073-2083.

105. Chatterjee PK, Todorovic Z, Sivarajah A, Mota-Filipe H, Brown PA, Stewart KN, Mazzon E, Cuzzocrea S, Thiemermann C. (2005) Inhibitors of calpain

activation (PD150606 and E-64) and renal ischemia-reperfusion injury. Biochemical pharmacology, 69(7): 1121-1131.

106. Shimoda N, Fukazawa N, Nonomura K, Fairchild RL. (2007) Cathepsin g is required for sustained inflammation and tissue injury after reperfusion of ischemic kidneys. The American journal of pathology, 170(3): 930-940.

107. Cocchiaro P, Fox C, Tregidgo NW, Howarth R, Wood KM, Situmorang GR, Pavone LM, Sheerin NS, Moles A. (2016) Lysosomal protease cathepsin D; a new driver of apoptosis during acute kidney injury. Sci Rep, 6: 27112.

108. Pinheiro HS, Camara NO, Noronha IL, Maugeri IL, Franco MF, Medina JO, Pacheco-Silva A. (2007) Contribution of CD4+ T cells to the early mechanisms of ischemia- reperfusion injury in a mouse model of acute renal failure. Brazilian journal of medical and biological research = Revista brasileira de pesquisas medicas e biologicas / Sociedade Brasileira de Biofisica ... [et al.], 40(4): 557-568.

109. Trof RJ, Di Maggio F, Leemreis J, Groeneveld AB. (2006) Biomarkers of acute renal injury and renal failure. Shock, 26(3): 245-253.

110. Aiello S, Cassis P, Mister M, Solini S, Rocchetta F, Abbate M, Gagliardini E, Benigni A, Remuzzi G, Noris M. (2011) Rabbit anti-rat thymocyte immunoglobulin preserves renal function during ischemia/reperfusion injury in rat kidney transplantation. Transplant international : official journal of the European Society for Organ Transplantation.

111. Trapani JA, Jans DA, Jans PJ, Smyth MJ, Browne KA, Sutton VR. (1998) Efficient nuclear targeting of granzyme B and the nuclear consequences of apoptosis induced by granzyme B and perforin are caspase-dependent, but cell death is caspase-independent. The Journal of biological chemistry, 273(43): 27934-27938.

112. Gobeil S, Boucher CC, Nadeau D, Poirier GG. (2001) Characterization of the necrotic cleavage of poly(ADP-ribose) polymerase (PARP-1): implication of lysosomal proteases. Cell Death Differ, 8(6): 588-594.

113. Ferrer I, Planas AM. (2003) Signaling of cell death and cell survival following focal cerebral ischemia: life and death struggle in the penumbra. J Neuropathol Exp Neurol, 62(4): 329-339.

114. Chaitanya GV, Babu PP. (2009) Differential PARP cleavage: an indication of heterogeneous forms of cell death and involvement of multiple proteases in the infarct of focal cerebral ischemia in rat. Cell Mol Neurobiol, 29(4): 563-573.
115. Yang H, Zhou P, Huang H, Chen D, Ma N, Cui QC, Shen S, Dong W, Zhang X, Lian W, Wang X, Dou QP, Liu J. (2009) Shikonin exerts antitumor activity via proteasome inhibition and cell death induction in vitro and in vivo. Int J Cancer, 124(10): 2450-2459.
116. Aikin R, Rosenberg L, Paraskevas S, Maysinger D. (2004) Inhibition of caspase-mediated PARP-1 cleavage results in increased necrosis in isolated islets of Langerhans. J Mol Med (Berl), 82(6): 389-397.
117. Castri P, Lee Y-j, Ponzio T, Maric D, Spatz M, Bembry J, Hallenbeck J. (2014) Poly(ADP-ribose) polymerase-1 and its cleavage products differentially modulate cellular protection through NF-kB-dependent signaling. Biochimica et Biophysica Acta (BBA) - Molecular Cell Research, 1843(3): 640-651.
118. Gero D, Szabo C. (2008) Poly(ADP-ribose) polymerase: a new therapeutic target? Current opinion in anaesthesiology, 21(2): 111-121.
119. del Moral RM, Gomez-Morales M, Hernandez-Cortes P, Aguilar D, Caballero T, Aneiros-Fernandez J, Caba-Molina M, Rodriguez-Martinez MD, Peralta A, Galindo-Moreno P, Osuna A, Oliver FJ, del Moral RG, O'Valle F. (2013) PARP inhibition attenuates histopathological lesion in ischemia/reperfusion renal mouse model after cold prolonged ischemia. ScientificWorldJournal, 2013: 486574.
120. Zheng J, Devalaraja-Narashimha K, Singaravelu K, Padanilam BJ. (2005) Poly(ADP-ribose) polymerase-1 gene ablation protects mice from ischemic renal injury. Am J Physiol Renal Physiol, 288(2): F387-398.
121. Russ AL, Haberstroh KM, Rundell AE. (2007) Experimental strategies to improve in vitro models of renal ischemia. Exp Mol Pathol, 83(2): 143-159.
122. Bonventre JV, Cheung JY. (1985) Effects of metabolic acidosis on viability of cells exposed to anoxia. The American journal of physiology, 249(1 Pt 1): C149-159.
123. Kellum JA, Leblanc M, Venkataraman R. (2008) Acute renal failure. Clinical evidence, 2008.

124. Hotter G, Palacios L, Sola A. (2004) Low O2 and high CO2 in LLC-PK1 cells culture mimics renal ischemia-induced apoptosis. Laboratory investigation; a journal of technical methods and pathology, 84(2): 213-220.
125. Jennische E, Hansson HA. (1984) Disulfiram is protective against postischemic cell death in the liver. Acta physiologica Scandinavica, 122(2): 199-201.
126. Masukawa T, Nakanishi K. (1993) Protection by disulfiram and diethyldithiocarbamate against hypoxia-induced lethality in mice. Japanese journal of pharmacology, 63(3): 279-284.
127. Isaoglu U, Yilmaz M, Calik M, Polat B, Bakan E, Kurt A, Albayrak Y, Suleyman H. (2012) Biochemical and histopathological investigation of the protective effect of disulfiram in ischemia-induced ovary damage. Gynecol Endocrinol, 28(2): 143-147.
128. Kaminski ZW, Pohorecki R, Ballast CL, Domino EF. (1986) Three forms of xanthine: acceptor oxidoreductase in rat heart. Circulation research, 59(6): 628-632.
129. Linder N, Martelin E, Lapatto R, Raivio KO. (2003) Posttranslational inactivation of human xanthine oxidoreductase by oxygen under standard cell culture conditions. American journal of physiology. Cell physiology, 285(1): C48-55.
130. Greene EL, Paller MS. (1992) Xanthine oxidase produces O2-. in posthypoxic injury of renal epithelial cells. The American journal of physiology, 263(2 Pt 2): F251-255.
131. Prachasilchai W, Sonoda H, Yokota-Ikeda N, Oshikawa S, Aikawa C, Uchida K, Ito K, Kudo T, Imaizumi K, Ikeda M. (2008) A protective role of unfolded protein response in mouse ischemic acute kidney injury. European journal of pharmacology, 592(1-3): 138-145.
132. Chen WC, Cheng HH, Huang CJ, Chou CT, Liu SI, Chen IS, Hsu SS, Chang HT, Huang JK, Jan CR. (2006) Effect of riluzole on Ca2+ movement and cytotoxicity in Madin-Darby canine kidney cells. Human & experimental toxicology, 25(8): 461-469.

133. Weiss S, Benoist D, White E, Teng W, Saint DA. (2010) Riluzole protects against cardiac ischaemia and reperfusion damage via block of the persistent sodium current. British journal of pharmacology, 160(5): 1072-1082.
134. Fougeray S, Bouvier N, Beaune P, Legendre C, Anglicheau D, Thervet E, Pallet N. (2011) Metabolic stress promotes renal tubular inflammation by triggering the unfolded protein response. Cell death & disease, 2: e143.
135. Gero D, Modis K, Nagy N, Szoleczky P, Toth ZD, Dorman G, Szabo C. (2007) Oxidant-induced cardiomyocyte injury: identification of the cytoprotective effect of a dopamine 1 receptor agonist using a cell-based high-throughput assay. International journal of molecular medicine, 20(5): 749-761.
136. Feldkamp T, Kribben A, Weinberg JM. (2005) Assessment of mitochondrial membrane potential in proximal tubules after hypoxia-reoxygenation. American journal of physiology. Renal physiology, 288(6): F1092-1102.
137. Feldkamp T, Kribben A, Roeser NF, Senter RA, Kemner S, Venkatachalam MA, Nissim I, Weinberg JM. (2004) Preservation of complex I function during hypoxia-reoxygenation-induced mitochondrial injury in proximal tubules. American journal of physiology. Renal physiology, 286(4): F749-759.
138. Weinberg JM, Venkatachalam MA, Roeser NF, Nissim I. (2000) Mitochondrial dysfunction during hypoxia/reoxygenation and its correction by anaerobic metabolism of citric acid cycle intermediates. Proceedings of the National Academy of Sciences of the United States of America, 97(6): 2826-2831.
139. Weinberg JM, Venkatachalam MA, Roeser NF, Saikumar P, Dong Z, Senter RA, Nissim I. (2000) Anaerobic and aerobic pathways for salvage of proximal tubules from hypoxia-induced mitochondrial injury. American journal of physiology. Renal physiology, 279(5): F927-943.
140. Zager RA, Johnson AC, Naito M, Bomsztyk K. (2008) Maleate nephrotoxicity: mechanisms of injury and correlates with ischemic/hypoxic tubular cell death. American journal of physiology. Renal physiology, 294(1): F187-197.
141. Szabo G, Stumpf N, Radovits T, Sonnenberg K, Gero D, Hagl S, Szabo C, Bahrle S. (2006) Effects of inosine on reperfusion injury after heart transplantation. Eur J Cardiothorac Surg, 30(1): 96-102.

142. Kovacs AL, Gordon PB, Grotterod EM, Seglen PO. (1998) Inhibition of hepatocytic autophagy by adenosine, adenosine analogs and AMP. Biological chemistry, 379(11): 1341-1347.
143. Samari HR, Seglen PO. (1998) Inhibition of hepatocytic autophagy by adenosine, aminoimidazole-4-carboxamide riboside, and N6-mercaptopurine riboside. Evidence for involvement of amp-activated protein kinase. The Journal of biological chemistry, 273(37): 23758-23763.
144. Jurkowitz MS, Litsky ML, Browning MJ, Hohl CM. (1998) Adenosine, inosine, and guanosine protect glial cells during glucose deprivation and mitochondrial inhibition: correlation between protection and ATP preservation. Journal of neurochemistry, 71(2): 535-548.
145. Litsky ML, Hohl CM, Lucas JH, Jurkowitz MS. (1999) Inosine and guanosine preserve neuronal and glial cell viability in mouse spinal cord cultures during chemical hypoxia. Brain research, 821(2): 426-432.
146. Rothwell D, Bartley J, James M. (1981) Preservation of the ischaemic canine kidney with inosine. Urological research, 9(2): 75-78.
147. Kaufman JJ, Woo YC. (1977) Further studies of renal preservation: protection of the ischemic kidney with inosine. Transactions of the American Association of Genito-Urinary Surgeons, 69: 131-133.
148. Casali RE, Gibbs W, Barbour G, Straub D, Baker G. (1979) Effect of inosine on warm renal ischemia in monkeys and dogs. Surgical forum, 30: 315-317.
149. Fernando AR, Gunter PA, Hendry WF, Smith AF, Watkinson LE, Wickham JE. (1979) An ultrastructural study on the effects of warm ischaemia on the inosine-protected kidney. British journal of urology, 51(3): 167-172.
150. Fernando AR, Armstrong DM, Griffiths JR, Hendry WF, Watkinson LE, Whitfield HN, Wickham JE. (1979) Use of inosine to prevent renal ischaemic injury. Transplantation, 28(4): 357-358.
151. Gero D, Szabo C. (2006) Role of the peroxynitrite-poly (ADP-ribose) polymerase pathway in the pathogenesis of liver injury. Current pharmaceutical design, 12(23): 2903-2910.

152. Baranowski RL, Westenfelder C. (1994) Estimation of renal interstitial adenosine and purine metabolites by microdialysis. The American journal of physiology, 267(1 Pt 2): F174-182.
153. Yamamoto T, Moriwaki Y, Takahashi S, Tsutsumi Z, Hada T. (2000) Effect of furosemide on the plasma concentration and urinary excretion of purine bases, adenosine, and uridine. Metabolism: clinical and experimental, 49(7): 886-889.
154. Miller WL, Thomas RA, Berne RM, Rubio R. (1978) Adenosine production in the ischemic kidney. Circulation research, 43(3): 390-397.
155. Nishiyama A, Kimura S, He H, Miura K, Rahman M, Fujisawa Y, Fukui T, Abe Y. (2001) Renal interstitial adenosine metabolism during ischemia in dogs. American journal of physiology. Renal physiology, 280(2): F231-238.
156. Nishiyama A, Miura K, Miyatake A, Fujisawa Y, Yue W, Fukui T, Kimura S, Abe Y. (1999) Renal interstitial concentration of adenosine during endotoxin shock. European journal of pharmacology, 385(2-3): 209-216.
157. Grenz A, Zhang H, Hermes M, Eckle T, Klingel K, Huang DY, Muller CE, Robson SC, Osswald H, Eltzschig HK. (2007) Contribution of E-NTPDase1 (CD39) to renal protection from ischemia-reperfusion injury. The FASEB journal : official publication of the Federation of American Societies for Experimental Biology, 21(11): 2863-2873.
158. Grenz A, Zhang H, Eckle T, Mittelbronn M, Wehrmann M, Kohle C, Kloor D, Thompson LF, Osswald H, Eltzschig HK. (2007) Protective role of ecto-5'-nucleotidase (CD73) in renal ischemia. Journal of the American Society of Nephrology : JASN, 18(3): 833-845.
159. Lee HT, Gallos G, Nasr SH, Emala CW. (2004) A1 adenosine receptor activation inhibits inflammation, necrosis, and apoptosis after renal ischemia-reperfusion injury in mice. Journal of the American Society of Nephrology : JASN, 15(1): 102-111.
160. Lee HT, Emala CW. (2001) Systemic adenosine given after ischemia protects renal function via A(2a) adenosine receptor activation. American journal of kidney diseases : the official journal of the National Kidney Foundation, 38(3): 610-618.

161. Okusa MD, Linden J, Macdonald T, Huang L. (1999) Selective A2A adenosine receptor activation reduces ischemia-reperfusion injury in rat kidney. The American journal of physiology, 277(3 Pt 2): F404-412.
162. Okusa MD, Linden J, Huang L, Rosin DL, Smith DF, Sullivan G. (2001) Enhanced protection from renal ischemia-reperfusion [correction of ischemia:reperfusion] injury with A(2A)-adenosine receptor activation and PDE 4 inhibition. Kidney international, 59(6): 2114-2125.
163. Grenz A, Osswald H, Eckle T, Yang D, Zhang H, Tran ZV, Klingel K, Ravid K, Eltzschig HK. (2008) The reno-vascular A2B adenosine receptor protects the kidney from ischemia. PLoS medicine, 5(6): e137.
164. Lee HT, Emala CW. (2000) Protective effects of renal ischemic preconditioning and adenosine pretreatment: role of A(1) and A(3) receptors. American journal of physiology. Renal physiology, 278(3): F380-387.
165. LeVier DG, McCoy DE, Spielman WS. (1992) Functional localization of adenosine receptor-mediated pathways in the LLC-PK1 renal cell line. The American journal of physiology, 263(4 Pt 1): C729-735.
166. Jackson EK, Zacharia LC, Zhang M, Gillespie DG, Zhu C, Dubey RK. (2006) cAMP-adenosine pathway in the proximal tubule. The Journal of pharmacology and experimental therapeutics, 317(3): 1219-1229.
167. Paller MS, Schnaith EJ, Rosenberg ME. (1998) Purinergic receptors mediate cell proliferation and enhanced recovery from renal ischemia by adenosine triphosphate. The Journal of laboratory and clinical medicine, 131(2): 174-183.
168. Kribben A, Feldkamp T, Horbelt M, Lange B, Pietruck F, Herget-Rosenthal S, Heemann U, Philipp T. (2003) ATP protects, by way of receptor-mediated mechanisms, against hypoxia-induced injury in renal proximal tubules. The Journal of laboratory and clinical medicine, 141(1): 67-73.
169. Gaudio KM, Taylor MR, Chaudry IH, Kashgarian M, Siegel NJ. (1982) Accelerated recovery of single nephron function by the postischemic infusion of ATP-MgCl2. Kidney international, 22(1): 13-20.
170. Gaudio KM, Ardito TA, Reilly HF, Kashgarian M, Siegel NJ. (1983) Accelerated cellular recovery after an ischemic renal injury. The American journal of pathology, 112(3): 338-346.

171. Gaudio KM, Stromski M, Thulin G, Ardito T, Kashgarian M, Siegel NJ. (1986) Postischemic hemodynamics and recovery of renal adenosine triphosphate. The American journal of physiology, 251(4 Pt 2): F603-609.
172. Andrews PM, Coffey AK. (1983) Protection of kidneys from acute renal failure resulting from normothermic ischemia. Laboratory investigation; a journal of technical methods and pathology, 49(1): 87-98.
173. Filipovic DM, Adebanjo OA, Zaidi M, Reeves WB. (1998) Functional and molecular evidence for P2X receptors in LLC-PK1 cells. The American journal of physiology, 274(6 Pt 2): F1070-1077.
174. Rose JB, Coe IR. (2008) Physiology of nucleoside transporters: back to the future. Physiology, 23: 41-48.
175. Molina-Arcas M, Casado FJ, Pastor-Anglada M. (2009) Nucleoside transporter proteins. Current vascular pharmacology, 7(4): 426-434.
176. Thorn JA, Jarvis SM. (1996) Adenosine transporters. General pharmacology, 27(4): 613-620.
177. Lai Y, Bakken AH, Unadkat JD. (2002) Simultaneous expression of hCNT1-CFP and hENT1-YFP in Madin-Darby canine kidney cells. Localization and vectorial transport studies. The Journal of biological chemistry, 277(40): 37711-37717.
178. Williams TC, Doherty AJ, Griffith DA, Jarvis SM. (1989) Characterization of sodium-dependent and sodium-independent nucleoside transport systems in rabbit brush-border and basolateral plasma-membrane vesicles from the renal outer cortex. The Biochemical journal, 264(1): 223-231.
179. Elwi AN, Damaraju VL, Kuzma ML, Mowles DA, Baldwin SA, Young JD, Sawyer MB, Cass CE. (2009) Transepithelial fluxes of adenosine and 2'-deoxyadenosine across human renal proximal tubule cells: roles of nucleoside transporters hENT1, hENT2, and hCNT3. American journal of physiology. Renal physiology, 296(6): F1439-1451.
180. Mangravite LM, Lipschutz JH, Mostov KE, Giacomini KM. (2001) Localization of GFP-tagged concentrative nucleoside transporters in a renal polarized epithelial cell line. American journal of physiology. Renal physiology, 280(5): F879-885.

181. Mangravite LM, Xiao G, Giacomini KM. (2003) Localization of human equilibrative nucleoside transporters, hENT1 and hENT2, in renal epithelial cells. American journal of physiology. Renal physiology, 284(5): F902-910.
182. Damaraju VL, Elwi AN, Hunter C, Carpenter P, Santos C, Barron GM, Sun X, Baldwin SA, Young JD, Mackey JR, Sawyer MB, Cass CE. (2007) Localization of broadly selective equilibrative and concentrative nucleoside transporters, hENT1 and hCNT3, in human kidney. American journal of physiology. Renal physiology, 293(1): F200-211.
183. Griffith DA, Jarvis SM. (1993) High affinity sodium-dependent nucleobase transport in cultured renal epithelial cells (LLC-PK1). The Journal of biological chemistry, 268(27): 20085-20090.
184. Schrader WP, West CA, Rudofsky UH, Samsonoff WA. (1994) Subcellular distribution of adenosine deaminase and adenosine deaminase-complexing protein in rabbit kidney: implications for adenosine metabolism. The journal of histochemistry and cytochemistry : official journal of the Histochemistry Society, 42(6): 775-782.
185. Bagshaw SM, Langenberg C, Haase M, Wan L, May CN, Bellomo R. (2007) Urinary biomarkers in septic acute kidney injury. Intensive care medicine, 33(7): 1285-1296.
186. Ohta T, Isselbacher KJ, Rhoads DB. (1990) Regulation of glucose transporters in LLC-PK1 cells: effects of D-glucose and monosaccharides. Molecular and cellular biology, 10(12): 6491-6499.
187. Suketa Y. (2008) [Expression and regulation of renal sodium-cotransporters and -antiporters, and related-transport proteins]. Yakugaku Zasshi, 128(6): 901-917.
188. Mullin JM, McGinn MT, Snock KV, Kofeldt LM. (1989) Na+-independent sugar transport by cultured renal (LLC-PK1) epithelial cells. The American journal of physiology, 257(1 Pt 2): F11-17.
189. Cox TC, Helman SI. (1986) Na+ and K+ transport at basolateral membranes of epithelial cells. I. Stoichiometry of the Na,K-ATPase. The Journal of general physiology, 87(3): 467-483.

190. Sakowicz M, Grden M, Pawelczyk T. (2001) Expression level of adenosine kinase in rat tissues. Lack of phosphate effect on the enzyme activity. Acta biochimica Polonica, 48(3): 745-754.
191. Sayos J, Solsona C, Mallol J, Lluis C, Franco R. (1994) Phosphorylation of adenosine in renal brush-border membrane vesicles by an exchange reaction catalysed by adenosine kinase. The Biochemical journal, 297 (Pt 3): 491-496.
192. Kelly KJ, Plotkin Z, Dagher PC. (2001) Guanosine supplementation reduces apoptosis and protects renal function in the setting of ischemic injury. The Journal of clinical investigation, 108(9): 1291-1298.
193. Kelly KJ, Plotkin Z, Dagher PC. (2001) Guanosine supplementation reduces apoptosis and protects renal function in the setting of ischemic injury. The Journal of Clinical Investigation, 108(9): 1291-1298.
194. Racusen LC. (1998) Epithelial cell shedding in acute renal injury. Clinical and experimental pharmacology & physiology, 25(3-4): 273-275.
195. Racusen LC, Fivush BA, Li YL, Slatnik I, Solez K. (1991) Dissociation of tubular cell detachment and tubular cell death in clinical and experimental "acute tubular necrosis". Laboratory investigation; a journal of technical methods and pathology, 64(4): 546-556.
196. Solez K, Morel-Maroger L, Sraer JD. (1979) The morphology of "acute tubular necrosis" in man: analysis of 57 renal biopsies and a comparison with the glycerol model. Medicine, 58(5): 362-376.
197. Nakamura H, Isaka Y, Tsujie M, Rupprecht HD, Akagi Y, Ueda N, Imai E, Hori M. (2002) Introduction of DNA enzyme for Egr-1 into tubulointerstitial fibroblasts by electroporation reduced interstitial alpha-smooth muscle actin expression and fibrosis in unilateral ureteral obstruction (UUO) rats. Gene Ther, 9(8): 495-502.
198. Chen SJ, Ning H, Ishida W, Sodin-Semrl S, Takagawa S, Mori Y, Varga J. (2006) The early-immediate gene EGR-1 is induced by transforming growth factor-beta and mediates stimulation of collagen gene expression. J Biol Chem, 281(30): 21183-21197.

199. Friedrich B, Janessa A, Artunc F, Aicher WK, Muller GA, Lang F, Risler T, Alexander D. (2008) DOCA and TGF-beta induce early growth response gene-1 (Egr-1) expression. Cell Physiol Biochem, 22(5-6): 465-474.
200. Handler JS, Kwon HM. (1993) Regulation of renal cell organic osmolyte transport by tonicity. Am J Physiol, 265(6 Pt 1): C1449-1455.
201. Garcia-Perez A, Burg MB. (1991) Renal medullary organic osmolytes. Physiol Rev, 71(4): 1081-1115.
202. Zhang Z, Cohen DM. (1997) Hypotonicity increases transcription, expression, and action of Egr-1 in murine renal medullary mIMCD3 cells. Am J Physiol, 273(5 Pt 2): F837-842.
203. Liu C, Adamson E, Mercola D. (1996) Transcription factor EGR-1 suppresses the growth and transformation of human HT-1080 fibrosarcoma cells by induction of transforming growth factor beta 1. Proc Natl Acad Sci U S A, 93(21): 11831-11836.
204. Wang D, Guan MP, Zheng ZJ, Li WQ, Lyv FP, Pang RY, Xue YM. (2015) Transcription Factor Egr1 is Involved in High Glucose-Induced Proliferation and Fibrosis in Rat Glomerular Mesangial Cells. Cell Physiol Biochem, 36(6): 2093-2107.
205. Rauchman MI, Nigam SK, Delpire E, Gullans SR. (1993) An osmotically tolerant inner medullary collecting duct cell line from an SV40 transgenic mouse. Am J Physiol, 265(3 Pt 2): F416-424.
206. Santos BC, Chevaile A, Hebert MJ, Zagajeski J, Gullans SR. (1998) A combination of NaCl and urea enhances survival of IMCD cells to hyperosmolality. Am J Physiol, 274(6 Pt 2): F1167-1173.
207. Michea L, Ferguson DR, Peters EM, Andrews PM, Kirby MR, Burg MB. (2000) Cell cycle delay and apoptosis are induced by high salt and urea in renal medullary cells. Am J Physiol Renal Physiol, 278(2): F209-218.
208. Chaudry IH. (1982) Does ATP cross the cell plasma membrane. The Yale journal of biology and medicine, 55(1): 1-10.

10. BIBLIOGRAPHY OF THE CANDIDATE'S PUBLICATIONS

Publications related to present thesis:

1) Mózes MM*, **Szoleczky P***, Rosivall L, Kökény G. Sustained hyperosmolarity increses TGF-ß1 and Egr-1 expression in the rat renal medulla. *BMC Nephrology* 2017 July DOI: 10.1186/s12882-017-0626-2 *(* equal contribution)*
   IF: 2.289 (2016)

2) **Szoleczky P**, Módis K, Nagy N, Dóri Tóth Z, DeWitt D, Szabó C, Gero D. Identification of agents that reduce renal hypoxia-reoxygenation injury using cell-based screening: purine nucleosides are alternative energy sources in LLC-PK1 cells during hypoxia. *Arch Biochem Biophys.* 2012 Jan 1;517(1):53-70.
   IF: 3.370

3) Módis K, Gero D, Nagy N, **Szoleczky P**, Tóth ZD, Szabó C. Cytoprotective effects of adenosine and inosine in an in vitro model of acute tubular necrosis. *Br J Pharmacol.* 2009 Nov;158(6):1565-1578.
   IF: 5.204

Other publications in peer-reviewed journals:

1) Druzhyna N, Szczesny B, Olah G, Módis K, Asimakopoulou A, Pavlidou A, **Szoleczky P**, Gerö D, Yanagi K, Törö G, López-García I, Myrianthopoulos V, Mikros E, Zatarain JR, Chao C, Papapetropoulos A, Hellmich MR, Szabo C. Screening of a composite library of clinically used drugs and well-characterized pharmacological compounds for cystathionine β-synthase inhibition identifies benserazide as a drug potentially suitable for repurposing for the experimental therapy of colon cancer. *Pharmacol Res*. 2016 Nov;113(Pt A):18-37.
   IF: 4.480

2) López-García I, Gerő D, Szczesny B, **Szoleczky P**, Olah G, Módis K, Zhang K, Gao J, Wu P, Sowers LC, DeWitt D, Prough DS, Szabo C. Development of a stretch-induced neurotrauma model for medium-throughput screening in vitro: identification of rifampicin as a neuroprotectant. *Br J Pharmacol*. 2016 Oct 9.
   IF: 5.491

3) Chao C, Zatarain JR, Ding Y, Coletta C, Mrazek AA, Druzhyna N, Johnson P, Chen H, Hellmich JL, Asimakopoulou A, Yanagi K, Olah G, **Szoleczky P**, Törö G, Bohanon FJ, Cheema M, Lewis R, Eckelbarger D, Ahmad A, Módis K, Untereiner A, Szczesny B, Papapetropoulos A, Zhou J, Hellmich MR, Szabo C. Cystathionine-beta-synthase inhibition for colon cancer: Enhancement of the efficacy of aminooxyacetic acid via the prodrug approach. *Mol Med.* 2016 May 16;22.

IF: 3.457

4) Pribis JP, Al-Abed Y, Yang H, Gero D, Xu H, Montenegro MF, Bauer EM, Kim S, Chavan SS, Cai C, Li T, **Szoleczky P**, Szabo C, Tracey KJ, Billiar TR. The HIV protease inhibitor saquinavir inhibits HMGB1 driven inflammation by targeting the interaction of cathepsin V with TLR4/MyD88. *Mol Med.* 2015 Sep 2.

IF: 3.530

5) Gerö D, **Szoleczky P**, Chatzianastasiou A, Papapetropoulos A, Szabo C. Modulation of poly(ADP-ribose) polymerase-1 (PARP-1)-mediated oxidative cell injury by ring finger protein 146 (RNF146) in cardiac myocytes. *Mol Med.* 2014 Jul 31;20:313-328.

IF: 4.508

6) Gerö D, **Szoleczky P**, Módis K, Pribis JP, Al-Abed Y, Yang H, Chevan S, Billiar TR, Tracey KJ, Szabo C. Identification of pharmacological modulators of HMGB1-induced inflammatory response by cell-based screening. *PLoS One.* 2013 Jun 14;8(6):e65994

IF: 3.534

7) Gerö D, **Szoleczky P**, Suzuki K, Módis K, Oláh G, Coletta C, Szabo C. Cell-based screening identifies paroxetine as an inhibitor of diabetic endothelial dysfunction. *Diabetes.* 2013 Mar;62(3):698-700

IF: 8.474

8) Módis K, Gerő D, Stangl R, Rosero O, Szijártó A, Lotz G, Mohácsik P, **Szoleczky P**, Coletta C, Szabó C. Adenosine and inosine exert cytoprotective effects in an in vitro model of liver ischemia-reperfusion injury. *Int J Mol Med.* 2013 Feb;31(2):
IF: 1.880

9) Módis K, Gerő D, Erdélyi K, **Szoleczky P**, Dewitt D, Szabo C. Cellular bioenergetics is regulated by PARP1 under resting conditions and during oxidative stress. *Biochem Pharmacol.* 2012 Mar 1;83(5):633-643
IF: 4.889

10) Suzuki K, Olah G, Modis K, Coletta C, Kulp G, Gerö D, **Szoleczky P**, Chang T, Zhou Z, Wu L, Wang R, Papapetropoulos A, Szabo C. Hydrogen sulfide replacement therapy protects the vascular endothelium in hyperglycemia by preserving mitochondrial function. *Proc Natl Acad Sci U S A.* 2011 Aug 16;108(33):13829-34. Cited:5
IF: 9.771

11) Gerö D, Módis K, Nagy N, **Szoleczky P**, Tóth ZD, Dormán G, Szabó C. Oxidant-induced cardiomyocyte injury: identification of the cytoprotective effect of a dopamine 1 receptor agonist using a cell-based high-throughput assay. *Int J Mol Med.* 2007, 20(5):749-61. Cited:9
IF: 1.847

11. ACKNOWLEDGEMENT

First, I would like to thank my supervisor Dr. Gábor Kökény for giving me the opportunity to write this thesis and I am very grateful for his guidance and support during the whole process. I would also like to thank Prof. Csaba Szabó for providing me an opportunity to work in his laboratory. Furthermore, I would like to express my gratitude to Dr. Domokos Gerő who shared his experience and knowledge with me, without his help and guidance I would not be where I am today. A special thank goes to my colleagues of CellScreen Applied Research Center, Semmelweis University, especially to Nóra Nagy, and Katalin Módis for their assistance.